UiT
THE ARCTIC UNIVERSITY OF NORWAY

Faculty of Engineering Science and Technology
Department of Computer Science and Computational Engineering

Working Chair for Physically Disabled Children

A Product Development Project

—

Ludvig Larsson

Master's thesis in Engineering Design 3 June 2019

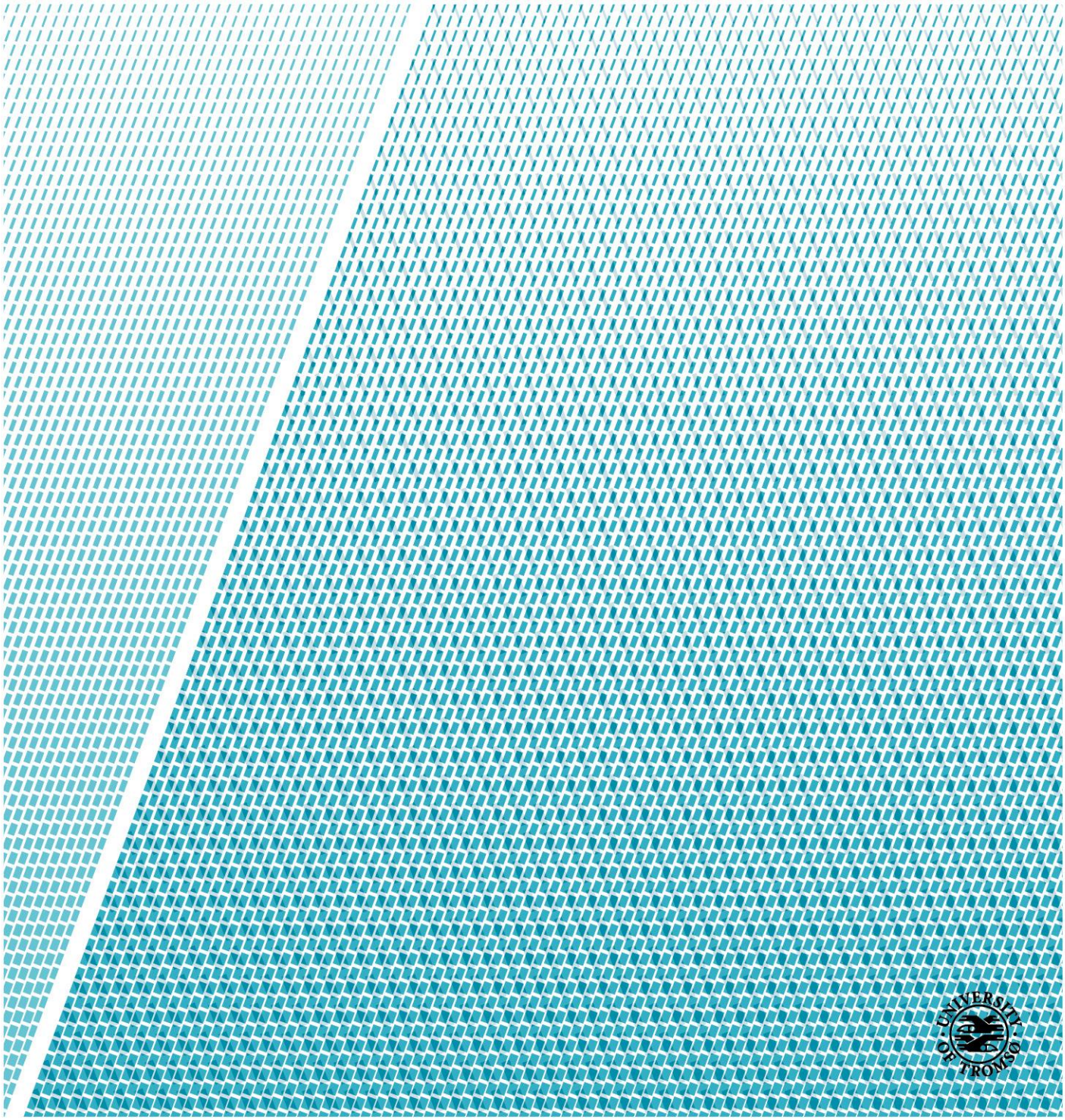

Abstract

A product development process was initiated with the purpose of designing a saddle seat working chair for physically disabled children on behalf of Fysionord AB. An objectives tree diagram was made using Mindomo.com. Sub-functions in existing solutions were listed, leading to the discovery of four modules, constituting the working chair: footrest, seat, backrest and undercarriage with wheels. The latter was defined as outside of the system boundary of the project. A requirement specification was compiled, stating demands and wishes regarding the future product. Concepts were generated for each module. This resulted in an adjustable footrest fastened by levers to the rear part of a non-adjustable seat based on mean anthropometrical dimensions of the intended target group. As well as a double curved hexagonal backrest fastened on a sheet metal post, enabling height adjustment. The three module concepts were assembled into a final working chair concept, which was modeled in Autodesk Inventor 2018. Using Ansys Workbench, numerical and analytical strength analysis was implemented on two sheet metal components: the backrest post and the “hub” for fastening all modules. Based on the analysis, the components were iteratively redesigned to reduce stress prior to selecting material, carbon steel AISI 1095, using CES Edupak.

Table of Contents

List of Tables

List of Figures

Thanks to

Prof. Annette Meidell, Supervisor

Charlotte Wemmenborn

Anders Larsson

1 Introduction

Chapter 1.1 to 1.5 present theory needed to understand the task, background to the project, its purpose and delimitations, followed by a time plan for the spring of 2019.

1.1 Theory

Chapter 1.1.1-1.1.6 presents a method of assessing sitting ability, followed by theory within children anthropometry, hip joints and posture, the concept of saddle seats, geometries and proportions in design, as well as a summary of Swedish laws and regulations regarding medical devices for physically disabled people.

1.1.1 Assessment of Sitting Ability

The sitting ability of an individual can be assessed according to PPAS (Posture and Postural Ability Scale):

1. Cannot be placed in sitting position.
2. Can be placed in sitting position but needs support.
3. Can sit without support but not move.
4. Can lean the torso forward and backward within the area of support.
5. Can transfer weight laterally and return to the initial position
6. Can exit sitting position (for example transfer weight to feet in order to change position).
7. Can enter and exit sitting position. [1]

1.1.2 Anthropometry

Anthropometry refers to measurements and proportions of the human body. Anthropometrical differences exist between different demographics. When developing a new product, it is therefore important to use anthropometrical data that represents the intended user target group.

Both underweight and obesity is common among physically disabled people, creating two anthropometrical extremes in the same target group. [2]

Anthropometrical data regarding height and lengths was gathered from United States Centers for Disease Control and Prevention (cdc.gov) and correlates to Scandinavian data while including more measures, such as femur length. However, American data regarding weight was discovered not to be relevant for Scandinavian users. Therefore, such data was gathered from nettdoktor.no. [3] [4]

1.1.3 Hip Joints and Pelvis related to Sitting Posture

Since the hip is a ball joint, the 6 medical terms for movements in the joint corresponds to 3 rotational degrees of freedom and no translation:

- Flexion and extension: forward/backward kicking motion.
- Abduction and adduction: spreading the legs and pinching them together.
- Lateral and medial rotation: rotating the foot (assuming a straight leg) outwards and inwards. [5]

When seated, the positioning of the pelvis effects the curvature of the back, which in turn effects neck and shoulder position. A posterior pelvic tilt often leads to exaggerated kyphosis, rounded shoulders and bent neck, creating stress in neck and back. A neutral or slight anterior pelvic tilt creates a neutral back position and reduces mentioned stress [6] [7]. This is visualized in Figure 1. The two uppermost, "wing-like", parts of the pelvis are called *iliac crests* [8].

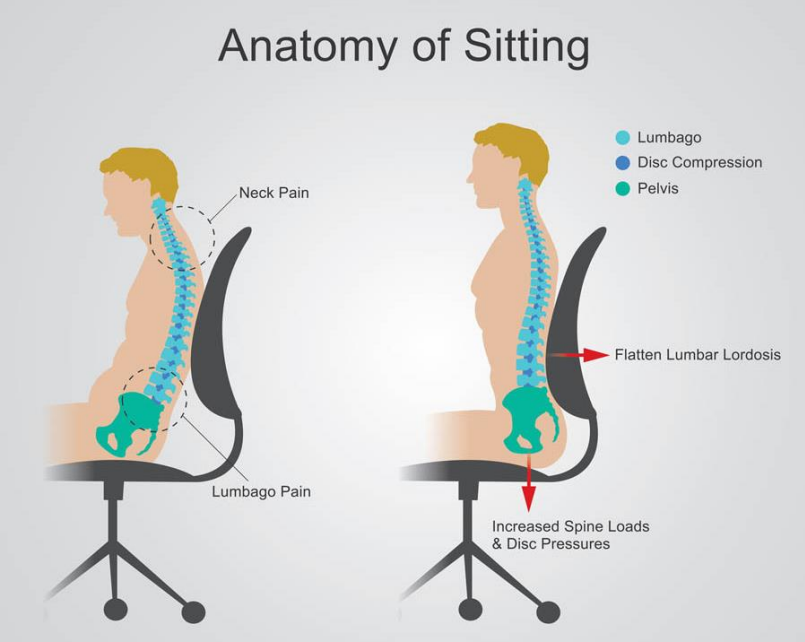

Figure 1 Consequences of posterior pelvic tilt (left) compared to a neutral pelvic position (right) [6].

1.1.4 Saddle Seat Ergonomics

The use of a seat shaped as a traditional horse saddle is proven facilitate an upright, ergonomically correct back position due to slight anterior pelvic tilt. An example of such seat can be seen in Figure 2.

Figure 2 Saddle seat chair [9].

Ideal joint angles for saddle sitting are visualized in Figure 3 and sums up as follows:

1. Circa 120° between upper body and thigh (flexion/extension direction of hip joint).
2. 15°-25° hip abduction.
3. 90° in knees and ankles. [10]

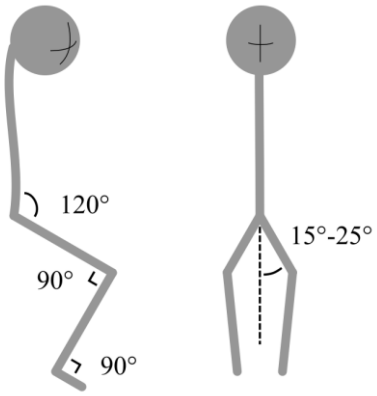

Figure 3 Profile (left) and front view (right) of appropriate joint angles when seated on a saddle seat.

1.1.5 Geometries and Proportions of Design

The visual appeal of a product largely depends on its geometries and proportions. The book "Geometry of Design-Studies in Proportions and Composition" was used as a guide during the project in the strive towards creating an aesthetically pleasing product. [11]

1.1.6 Swedish and European Laws and Regulations regarding Medical Devices

A product is considered a medical device if it "[…]proves, monitors, treats, relieves or compensates an injury or a disability[…]", according to §2 in law (1993:584) regarding medical devices. [12]

Within the European Union, new medical devices must be CE marked prior to introduction to the market. The CE marking is an assurance from the manufacturer that the construction and

documentation of the product fulfills regulatory requirements stated by the European Union. It is also an assurance that the manufacturer practices systematic risk assessment. [13] By following the harmonizing standards of the European Union, manufacturers can make sure that these demands are being met. [14]

Essential requirements regarding construction of medical devices can be found in European Directive 93/42/EEC Annex I. Annex X in the same directive describes clinical assessment of usage, including risk assessment. [15]

According to Swedish medical products agency regulation LVFS 2003:11 regarding medical devices, all medical devices can be divided into following classes:

- Class I
- Class Is
- Class Im
- Class IIa
- Class IIb
- Class III

Non-invasive products that are not connected to a device of a higher class, store or change the composition of blood or other body fluids are within the boundaries of class I devices. Only products in class I can be CE marked without involving a third party. [16]

All class I medical devices must be registered at the Swedish medical products agency (*Läkemedelsverket*) prior to launch in Sweden [17]. ISO 7176 specifies requirements on wheelchairs as well as testing methods [18].

1.2 Background

Chapter 1.2.1 gives a short introduction to the company Fysionord AB, existing working chairs for disabled children are discussed in chapter 1.2.2, followed by the recognition of problems to solve in chapter 1.2.3.

1.2.1 Fysionord AB

Fysionord AB was founded in 2011 with the business idea to make functional, aesthetic and innovative aids available to physically disabled children in Sweden. The company is run by Charlotte Wemmenborn and Anders Larsson, who together have about 50 years of experience of working with aids for physically disabled people. Within the company there are both expert knowledge in ergonomic sitting, as well as experience in product development through the

Eurovema SitRite system. Currently, the company wants to develop a working chair for children with PPAS sitting ability 3-7 (Chapter 1.1.1). The future product is intended to be used indoors when seated at a table or desk and engaging in activities such as schoolwork, using a computer or eating.

1.2.2 Existing Solutions

Following working chairs, listed with their weight for comparison, were identified as existing solutions for children with PPAS sitting ability 3-7:

- Krabat Jockey Lite Size 2, 10 kg [19]
- Leckey PAL Size 4, 10 kg [20]
- Euroflex ABC SitRite, 28 kg [21]
- Mercado Real 9000 Plus, 28 kg [22]
- Vela Hip Hop 100, 19 kg [23]

Both mean and median weight of these products is 19 kg. Following non-medical products were studied as inspiration:

- Bambach
- Salli
- Stokke Balans

Observed advantages and disadvantages for each product can be seen in Appendix A.

1.2.3 Problem Recognition

Fysionord AB has identified one or multiple of the following problems with all known existing solutions:

- Safety: the user is exposed to immediate danger due to the design of some of the current solutions.
- Ergonomics: A common issue in existing solutions is posterior pelvic tilt. No known existing saddle seat solution enables the leg position explained in chapter 1.1.4.
- Aesthetics: the majority of existing solutions lack visual appeal.

1.3 Purpose

The purpose of this project has been to, on behalf of Fysionord AB, develop a working chair to serve as an indoor aid for disabled children in Sweden within the age group 6 to 11 years old, with level 3-7 sitting ability according to PPAS.

1.4 Delimitations

By the request of Fysionord AB, two limitations were made in the process of generating a new product:

- The new solution must use a pre-manufactured undercarriage that provides 5 wheels and adjustment of tilt and sitting height, as on a conventional office chair. The height adjustment component and gas spring must be the same as on the existing product Krabat Jockey Lite. Undercarriage from such chair can be seen in Appendix B.
- Due to the ergonomic advantages of saddle seats (chapter 1.1.4), experience within the field and positive feedback from users, the new product should have a saddle shaped seat.

The product is eventually intended to be used by both children, adolescents and young adults. However, due to the time constraints of the project, the age demographic to target initially was determined as children of age 6 to 11 years old. The lower age limit was justified by the sudden increase of sedentary indoor activity associated with starting school. The upper age limit was intended to not include growth spurts related to puberty, and therefore reduce variations in length and weight of the intended users. To simplify future adaptations for both younger and older users than the initial target group it was deemed important to generate a module based solution.

The project was limited to the development of 3 main modules. However, possibilities of creating an interface for adding more modules were investigated in order to promote future development of additional products. This is explained further in chapter 3.

Due to time constraints, the choice of textile and foam materials for possible cushioning was excluded from the project.

The product should not be confused with a wheelchair. It is not intended for transporting the user, but is to be used as a conventional office chair.

CE marking and ensuring that the product fulfills all requirements found in European directives was not included in the project due to the limited timeframe.

1.5 Time Plan

The project was limited to the spring of 2019, starting January 7 and ending June 11. A Gantt chart time plan was created using Teamweek.com and can be seen online:

https://app.teamweek.com/#timeline/387094/groups/349126?zoom=month

Please note that an invitation is needed to access the online time plan. A simplified version of the time plan can be seen in Appendix C.

The project followed the steps illustrated in Figure 4. The structure of this report follows the same steps.

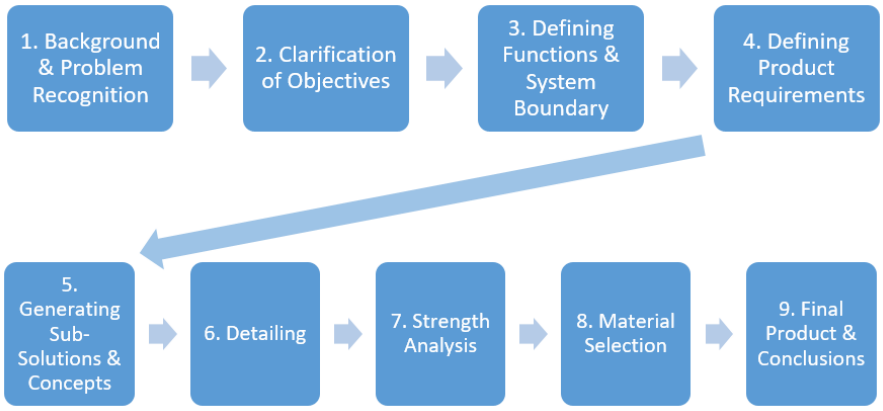

Figure 4 The 9 steps of the product development project.

2 Clarification of Objectives

An Objectives Tree Diagram for the future product can be seen in Appendix D. Each main objective and associated sub-objectives are color coded for visual clarity. The three main objectives were defined as:

- Safe (red): the design must not expose the user to immediate danger.
- Positive user experience (blue): convenient everyday use.
- Positive product image (green): creating a sense of "want" just by seeing or hearing about the product.

Looking from top to bottom in the diagram provides answers to how the different objectives can be fulfilled. Similarly, looking from bottom to top in the diagram motivates why each sub objective is necessary. Some sub-objectives answer to multiple objectives.

The problem areas in current solutions (listed in chapter 1.2.3) can be found in the diagram. However, excelling in these areas (besides safety) are not main objectives, but rather means of fulfilling the main objectives.

3 Functions and System Boundary

The basic idea of the product is to improve the posture of its user and enabling them of engaging in sedentary activity. The main functions found in the majority of existing working chairs for disabled children can be summed up as follows:

1. Support legs or feet.
2. Support weight of user.
3. Support back.
4. Move around on floor.
5. Adjustment of sitting height and tilt.

Adjustment of sitting height and tilt are differentiated from other adjustments since they are intended to answer to external factors, such as varying heights of tables, rather than the variation of physical needs between different users. Adjustments for personalization are explained in chapter 3.1 to 3.3.

Due to the time constraints of the project it was decided to not include functions observed in only a few of the existing solutions. However, after discussions with Fysionord AB, it was concluded that it should be possible to add following functions in eventual further development of the working chair:

- Support for arms.
- Automatic sitting height adjustment.
- Grip for guardian or caretaker to help user move around while seated.
- Possibly fastening of the user at waist if the target group is to be expanded in the future towards children with PPAS sitting ability 2.
- Fastening of feet or legs after eventual fastening at the waist.

Using a pre-manufactured undercarriage, including height and tilt adjustment functions as well as wheels as requested, puts the functions “move around on floor” and “adjustment of sitting height and tilt” outside of the system boundary. This is illustrated in Figure 5.

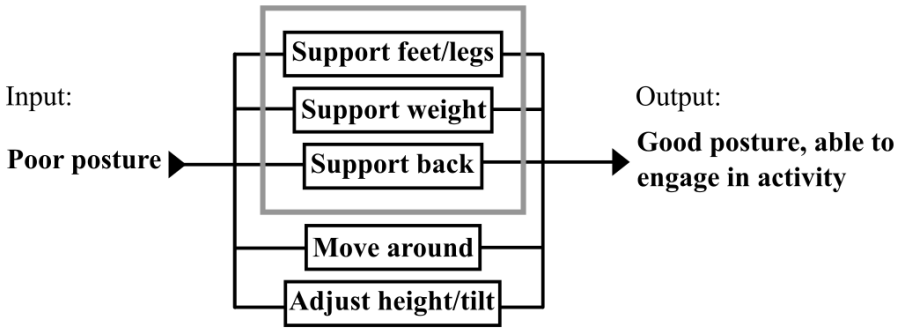

Figure 5 The main idea of the working chair and its 5 main functions, of which 3 were included within the system boundary of the project. The boundary is illustrated by the grey rectangle.

These main functions can be summed up in a schematic image of the product (Figure 6), consisting of four main modules, each answering to one or more main functions:

1. Foot- or legrest
2. Seat
3. Backrest
4. Undercarriage with height/tilt adjustment and wheels

Again, undercarriage and wheels were placed outside of the system boundary, which is emphasized by their grey color in Figure 6.

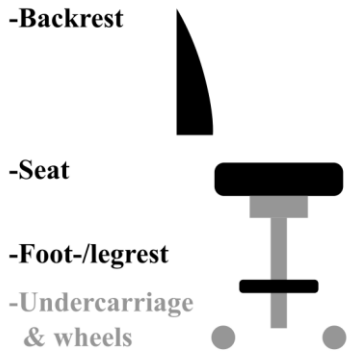

Figure 6 Schematic visualization of a working chair.

In turn, each module must possess a number of functions and sub-parts for the product to be adaptable for different users and overall functional.

3.1 Functions of Foot- or Legrest

Five functions and sub-parts were identified for creating an individually adaptable foot- or legrest:

- Attachment to chair; the foot- or legrest must be attached to the rest of the chair.
- Support area; the part that supports the weight of legs and feet.

- Adjustable knee angle. Ideally, the knee should be bent 90°. However, this might not be achievable for some users due to impaired mobility.
- Adjustable for users with different femur length.
- Adjustable for users with different knee height.

3.2 Functions of Seat

Other than supporting the weight of the user, the seat must enable the saddle seat position described in 1.1.4.for users with varying

- Femur length
- Hip breadth

while leaving room for the user to find their own individual sitting position.

3.3 Functions of Backrest

The backrest must

- Offer support in backward direction.
- Offer some support in lateral direction.
- Fit the sitting height of differently sized users.
- Fit the back width of differently sized users.

According to Fysionord AB, there is no need for a tilting function of the backrest.

4 Product Requirements

A requirement specification was compiled, differentiating compulsory “Demands” (D) and desired but not necessary “Wishes” (W).

Linking back to the 3 of the 4 main modules of the product that were defined as inside the system boundary in chapter 3, the requirement specification was divided into one section for each module. An additional section was added for requirements that are relevant for the entire product, making it 4 sections in total:

- General requirements
- Foot- /legrest requirements
- Seat requirements
- Backrest requirements

4.1 General Requirements

Based on Norwegian data regarding weight of 6-11 year old children [4], user weight was set to 15-50 kg. A minimum weight is relevant due to the height adjustment system.

For the working chair to be convenient to handle, it must not be heavier than the mean weight of current solutions listed in chapter 1.2.2. Ideally, it should be more light weight than any of these products.

To ensure the safety of the user, it was decided that all adjustments of the chair should be done by a supervising adult, while it should not be possible for the user the make any accidental or intentional adjustments other than sitting height.

The entire construction must be module based to promote future development of specific parts and enable replacement of broken parts. An interface should be included for attaching armrests and a module such as handlebars for guardians to help maneuver the chair. The chair must fit through a standard door opening without being disassembled.

To make potential users interested simply by seeing the product, its visual appearance should have more resemblance with high end, modern furniture than wheelchairs. Therefore, the aesthetic vision of this project has been to make sure that the chair does not look like a medical device.

The retail price of the product should be comparable to its competitors. A price that is too high is an argument for customers to keep using other products. Meanwhile, customers might associate a price that is “too low” with cheap materials and bad products. Therefore, materials and manufacturing costs should be kept as small as possible in order to increase profit margin rather than providing a low retail price. Partly, this can be achieved by using standardized pre-manufactured components.

Center of gravity (CoG) should be equal or lower than competing solutions for reduced risk of tipping over. However, data regarding CoG of existing solutions was not available.

As seen in Table 1, in which all general requirements are found, the same color-coding was used as in the Objectives Tree Diagram:

- Red: Safety
- Blue: User experience
- Green: Product image

Table 1 General requirement specification.

#	D/W	Requirement	Description/quantity
1	D	Min user weight	15 kg
2	D	Max user weight	50 kg
3	D	Max product weight	Mean weight of competitors, 19 kg
4	W	Goal product weight	Lighter than all competitors, 10 kg
5	D	No sharp edges close to user	
6	D	Avoid adjustments by user	Accidental and intentional except height
7	D	Easy adjustments by guardian	
8	W	One hand adjustments by guardian	
9	D	Modular construction	
10	D	Design space	Standard door width circa 900 mm.
11	W	Grip for guardian interface	Place on most suitable module
12	W	Interface for armrests	Place on most suitable module
13	D	Fulfill aesthetic vision	“Not look like a medical device”
14	D	Price comparable to competitors	
15	W	Standard components	Where applicable
16	W	Low CoG	Compared to competitors

4.2 Foot- or Legrest Requirements

Including the 5 to 95 percentiles of 8 to 11 year old American children, femur length was found to be between 271 mm and 390 mm [3]. However, since the product is intended to be used by children from the age of 6 the femur length span was set to 200-400 mm.

“Knee height” is the vertical distance from the foot sole to the top of the thigh when seated with 90° knee angle. The 5-95 percentile of American children of age 6-11 are within the knee height span 315 to 498 mm. [24]

Hip, knee and ankle joint angles should correspond to the ideal positioning described in chapter 1.1.4, but must be adjustable for individual needs.

Interface for a future solution of fastening the feet of the user should be included in the foot- or legrest.

Saddle seat chairs are commonly used with unconventionally high tables. The legs of the user must fit under such table when using the product. Ideally, the legs should fit under an ordinary table.

When adjusting sitting height, the foot- or legrest should follow the adjustment automatically.

Table 2 Foot- or legrest requirement specification.

#	D/W	Requirement	Description/quantity
1	D	Min femur length	200 mm
2	D	Max femur length	400 mm
3	D	Min knee height	300 mm
4	D	Max knee height	500 mm
5	D	Hip flexion angle adjustable	Aiming at 120° + individual differences
6	D	Knee angle adjustable	Aiming at 90° + individual differences
7	D	Ankle joint angle adjustable	Aiming at 90° + individual differences
8	D	Legs fitting under raised table	
9	W	Interface for fastening of feet	Simplifying future further development
10	W	Legs fitting under standard table	Standard table height: 720-750 mm
11	W	Follow height adjustment of seat	Eliminating one operation of adjustment

4.3 Seat Requirements

The minimum and maximum femur lengths affect the design of the seat as well as the foot- or legrest.

Hip breadth is measured between the outsides of the hips of a sitting person. The hip breadth of 6 to 11 year-old children are typically within the span 215 to 290 mm. [25]

Hip abduction angles must correspond to the ideal positioning described in chapter 1.1.4. As for the foot- or legrest, the seat must be compatible with a raised table, while it also should fit under a conventional table.

The seat must be adapted for fastening to an office chair undercarriage, while not interfering with its height and tilt mechanisms. There should be an interface for adding a waist belt.

Table 3 Seat requirement specification.

#	D/W	Requirement	Description/quantity
1	D	Min femur length	200 mm
2	D	Max femur length	400 mm
3	D	Min hip breadth	215 mm
4	D	Max hip breadth	290 mm
5	D	Max hip abduction	25°
6	D	Min hip abduction	15°
7	D	Seat fitting under raised table	
8	W	Seat fitting under standard table	
9	D	Interface to undercarriage	
10	D	Not interfere with height/tilt levers.	
11	W	Interface for waist belt	Simplifying future further development

4.4 Backrest Requirements

"Sitting height" is measured on a person sitting on a flat surface such as a chair. It refers to the distance from the surface to the top of the head of the subject. The 5-95 percentile of American children of age 6-11 are within the sitting height span 581 to 807 mm. [24] Therefore, the backrest must be adjustable in height for children with sitting height 550 to 850 mm.

Some users might be prone to asserting large forces backwards, which the backrest must support. It must also provide lateral stability. However, exaggerated fixation of the user may increase the risk of tipping over. All backrest requirements are compiled in Table 4.

Table 4 Backrest requirement specification.

#	D/W	Requirement	Description/quantity
1	D	Min sitting height	550 mm
2	D	Max sitting height	850 mm
3	D	Stepless height adjustment	Adjust for 550-850 mm sitting height.
4	D	Posterior support	Support force asserted by user.
5	D	Lateral support	
6	D	Not too much lateral support	Reduce risk of tipping to the side.
7	W	Adjustable back width	

5 Generating Concepts

The recognition of the three main modules led to a “middle out” approach, where concepts for each module were generated and later assembled before detailing. In chapter 5.1 to 5.3 the concept generation phase is presented for the three modules:

1. Foot- or legrest
2. Seat
3. Backrest

It was regarded likely that the foot- or legrest would be fastened to the seat. In order to avoid the risk of having to redesign the seat, it was deemed suitable to create a concept for the foot- or legrest before the seat.

5.1 Foot-/Legrest Concept Generation

Chapter 5.1.1 to 5.1.5 present sub-solutions, fulfilling the required functions for any foot- or legrest explained in chapter 3.1. The sub-solutions were compiled in a morphological matrix (chapter 5.1.6) and combined into seven different concepts (chapter 5.1.7), out of which two were prototyped and one was chosen for further development (chapter 5.1.8).

5.1.1 Attachment to Chair

The foot- or legrest can be fastened to the rest of the chair as follows:

- At the very front or back part of the seat.
- Underneath the seat.
- Around the gas spring on the undercarriage.

5.1.2 Support Area

The weight of the legs and feet can be supported by

- A simple straight bar for the feet.
- A flat foot pad.
- A curved foot pad, giving the same ankle joint angle for different knee angles.
- Shin pads similar to *Stokke Balans*, supporting the lower legs of the user rather than the feet.

5.1.3 Knee Angle

Adjustable knee angle can be achieved through:

- A hinge at fastening of the foot- or legrest, changing its position and therefore also the angle in the knee joints. The angle of the hinge is fixed by attaching the footrest to the seat above it with a strap.

- Horizontal translation of the foot- or legrest.
- The same curved foot pad mentioned in chapter 5.1.2 enables the user to choose knee angle without adjusting the chair.
- Vertical translation of the foot- or legrest.

5.1.4 Femur Length

To be able to adapt for different femur lengths, the foot-/ or legrest should be able to translate back and forth horizontally.

5.1.5 Knee Height

In order to adapt to different knee heights, the distance from the knee to the lowest part of the foot- or legrest could be prolonged along the tibia. Another solution could be to divide this adjustment into a vertical and horizontal component. This is illustrated in Figure 7.

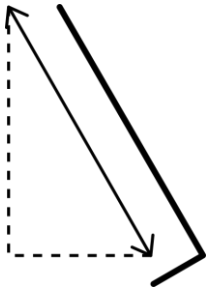

Figure 7 Visualization of dividing knee height adjustment into vertical and horizontal components (dashed lines).

5.1.6 Morphological matrix

The sub-solutions explained in chapter 5.1.1 to 5.1.5 were compiled in a morphological matrix (Table 5) and combined into seven concepts, visualized by the colored lines.

Table 5 Morphological matrix combining sub-solutions into foot- or legrest concepts.

	Fastening	Support Area	Knee Angle	Femur Length	Knee height
Concept 1 Concept 2	Front of seat	Bar	Hinge at fastening		Translation along shin
Concept 5	Under seat	Flat foot pad	↔ translation	↔ translation	↕+↔ translation
Concept 3 Concept 4	Back of seat	Curved foot pad	Curved foot pad		
Concept 6 Concept 7	Undercarriage	Shin pad	↕ translation		

The matrix can be seen without lines in Appendix E.

5.1.7 Concepts

Five concepts for foot-/legrests intended to be fastened to the seat, as well as two concepts intended to be fastened to the undercarriage were generated. Sketches of all concepts can be seen in Appendix F.

Concept 1. Fastened in the front of the seat on an extruded beam with the possibility to be pushed into or pulled out of the seat for femur length adaption. Knee height is adjusted similarly while knee angle is given by a hinge at the front of the chair. Support for the feet are given by a conventional foot pad. A solution for adjusting the ankle joint angle was yet to be defined at this point.

Concept 2. Similar to the first concept but replacing the footrest with leg pads. In this way, support is offered to the shins instead of the feet.

Concept 3. Similar to the first concept but with fastening at the rear part of the seat.

Concept 4. Similar to the third concept but simplified foot support given by a bent bar instead of a foot pad.

Concept 5. An additional gas spring connects a curved footrest to a surface that can move horizontally back and forth underneath the seat.

Concept 6. A curved footrest (similar to concept 5) is fastened to the height adjustment gas spring and fixated by bolts. As seen in the morphological matrix (Table 5), this concept cannot be adjusted horizontally.

Concept 7. Fastened similarly as concept 6 but with a flat foot pad and adjustable tilt angle in anterior/posterior direction. The (green) foot pad can translate along the foot sole by fastening in the slot of the orange component for angle adjustment.

5.1.8 Choice of Concept and Prototyping

Advantages and disadvantages were identified for fastening the foot- or legrest to the seat as well as to the undercarriage:

- The undercarriage will naturally be close to the feet of the user. Therefore, a solution fastened to this part of the chair will likely be relatively minimalistic while eliminating torque associated with long levers.

- Fastening to the undercarriage would likely give a lower center of gravity than fastening to the seat.
- It will likely be hard to avoid rotation of the foot- or legrest if it is mounted around the cylindrical gas spring of the undercarriage.
- The undercarriage is to be delivered as pre-manufactured components by an external manufacturer. Creating an interface to the seat rather than the undercarriage means that the exact geometries of the undercarriage must not be known at this point. It might also simplify any eventual change of undercarriage supplier in the future.
- Clamping the gas spring of the undercarriage might impair its height adjustment function.
- Fastening to the seat will likely simplify automatic height adjustment of the foot- or legrest in the sense that it follows the adjustment of sitting height.

Based on this, a solution for fastening the foot- or legrest to the seat was deemed favorable.

Fastening the foot- or legrest at the rear part of the seat was considered to likely interfere with the development of the backrest. Also, the pressure on the foot soles given by the bar in concept 4 might trigger spasticity for some users [10].

Comparing remaining concept 1, 2 and 5, the latter stands out as significantly more complex than the first two.

Even though concept 1 and 2 are similar, the construction of concept 2 is simpler, while likely allowing slightly taller children to use the product than concept 1. Also, concept 2 is the less conventional choice of the two, differentiating itself both functionally and visually from competitors as new and innovative. However, it would likely be easier for a user to independently enter and exit a chair using footrest concept 1. Therefore, after dialog with Fysionord AB, concept 1 was chosen for further development.

Additional sketches and a draft full scale prototype of concept 1 were created and lead to the discovery of two new issues:

- The center of gravity might be located too far forward when the footrest is adapted to tall users.
- The chair might still be hard to enter or exit due to the protruding hinge in front of the seat.

Based on this, the fastening of the footrest was moved to the rear of the seat, creating a prototype of concept 3. When doing so it was discovered that the footrest could reach any desired position underneath the seat without using the horizontal translation at its fastening, making that function redundant. The changes from concept 1 to the modified concept 3 can be seen in both the prototype and sketches in Appendix G. The modified concept 3 can also be seen in Figure 8.

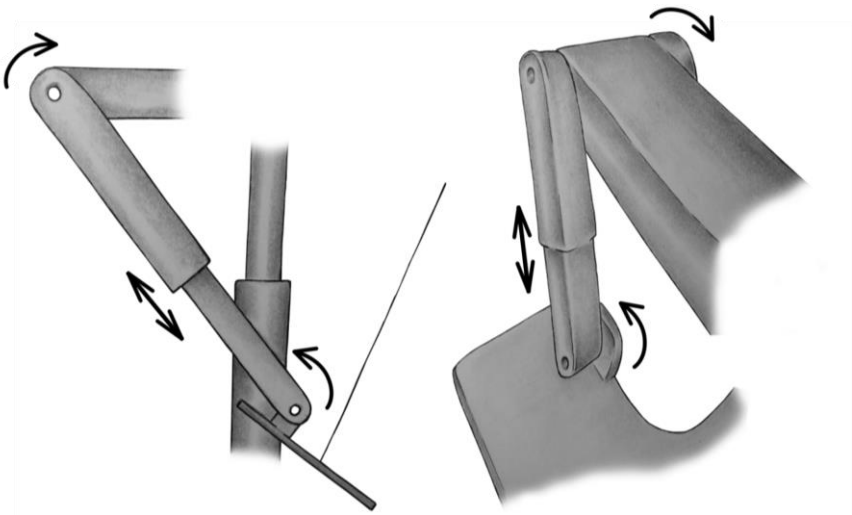

Figure 8 The final footrest concept seen from the side (left) in context with the gas spring of the chair while showing the strap for knee angle fixation, as well as seen in perspective (right).

As mentioned, this solution was suspected to likely interfere with the development of the backrest. A solution for adjusting the angle of the ankle joint was not yet defined at this point.

In order to simplify the construction as well as manufacturing process, it was decided to redesign the elongation mechanism of the footrest levers. The upper hollow parts of the levers were replaced with short loops, possible to manufacture through extrusion and some minor subtracting operations such as cutting and drilling. Levers with rectangular cross section offer a relatively high second moment of area, counteracting bending. Such levers can be based on pre-manufactured bars formed into rounded hinges in their interface to the footpad.

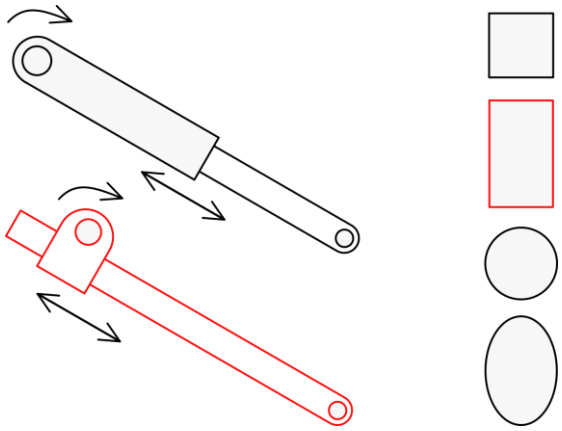

Figure 9 Two possible elongation mechanisms for the footrest levers (left) and lever cross sections (right). Chosen solutions are marked in red.

5.2 Seat Concept Generation

In addition to the demands listed in the requirement specification, the seat must also have be compatible with the chosen footrest concept described in chapter 5.1.8.

Chapter 5.2.1 to 5.2.3 present the creation of draft initial seat shapes, concepts partly based on feedback on these initial shapes, followed by the selection and modification of a final seat concept.

5.2.1 Draft Seat Shapes

Before creating concepts of seats, it was decided to sketch draft shapes in the context of a user and the undercarriage of the chair. This was done mainly to establish visual communication with Fysionord AB and receive feedback early.

A .stp-model of a child intended for anthropometrical validation was used in order to create a basic idea of possible geometries and proportions of seats. It was downloaded from 3dcontentcenter.com [26]. The model was modified from a conventional sitting position into the saddle seat position described in chapter 1.1.4 using Rhinoceros 5. The model was also slightly scaled up in order to represent the largest intended user of the chair. In addition, models of wheels and the bottom part of an undercarriage was downloaded from GrabCAD.com [27] [28]. A simplified gas spring (in extended position) was recreated in Inventor 2018 based on measurements on a Krabat Jockey Lite chair. All parts were assembled in Inventor, a screenshot was taken of the assembly and printed to function as a foundation for sketching draft shapes for seats.

Figure 10 Assembly of model for anthropometrical validation and working chair undercarriage.

The process of creating an initial shape of the seat can be seen in Figure 11 and Figure 12.

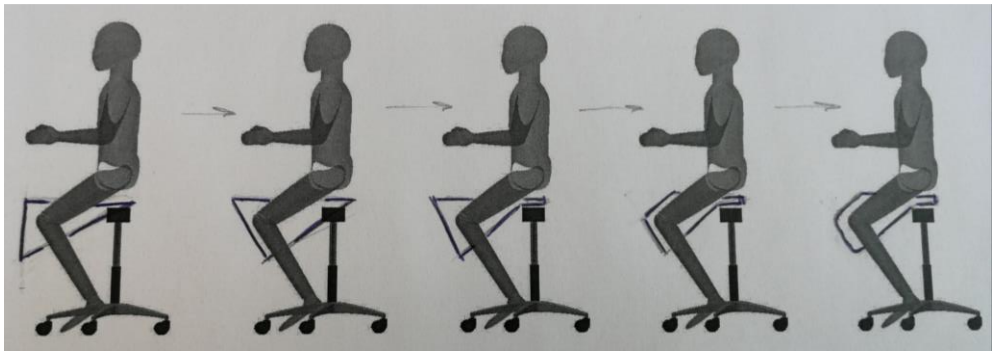

Figure 11 Sketches of seat shapes using printed screenshot of 3D model as reference.

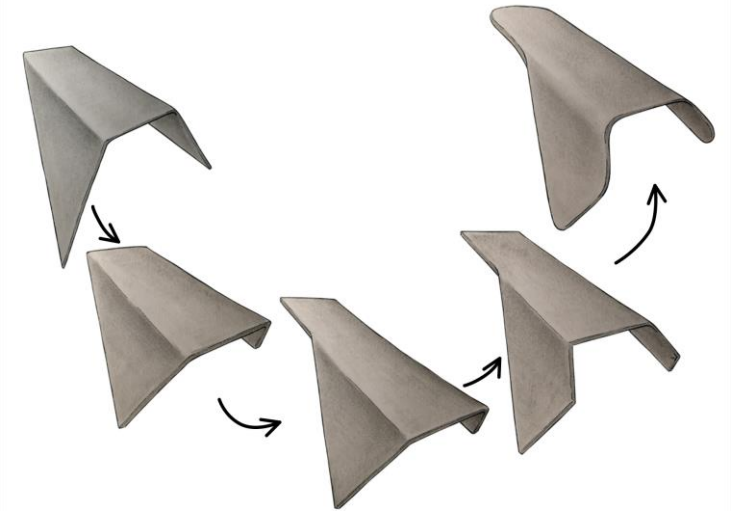

Figure 12 Sketches of the same iterative process of developing seat shapes as shown in Figure 11.

Following the process step by step (from left to right in Figure 11 and Figure 12) it can be described as follows:

1. An initial shape was created intended to match the forward tilting angle of the thighs.
2. Excess material was removed following the angle of the shins.

3. A sitting pad was added at the rear part of the seat to avoid interference with the height adjustment component of the undercarriage.
4. Excess material was removed close to the knees of the user.
5. Fillets were added for rounded geometries.

The final iteration (furthest to the right in Figure 11 and Figure 12) was presented to Fysionord AB. Feedback was given on four points:

- The rear part of the seat, supporting the weight of the user, should be wider than the front part in order to efficiently distribute weight while maintaining desired hip angles.
- To promote neutrally positioned knees and ankles, the wing-like geometries intended to support the thighs should be vertical.
- With the same motivation, the seat should not be extended below the knees of the user in such a way that the lower legs are pushed outwards.
- The seat should always protrude in front of the knees for maximum support of the thighs.

5.2.2 Seat Concepts

The main challenge prior to designing the seat was identified as maintaining given hip flexion and hip abduction for users with varying hip breadth and femur length.

This process was geometrically challenging rather than a matter of combining independent sub-solutions as in the case with the footrest. Therefore, concepts were generated through unorganized sketching with the CAD-model in Figure 10 as a reference. Following five concepts were generated:

"The Wedge" (Figure 13): The seat is mounted on the undercarriage depending on the size of the user in such a way that taller users with greater hip breadth use the wider front part of the seat while small users are positioned on the narrower rear part of the seat.

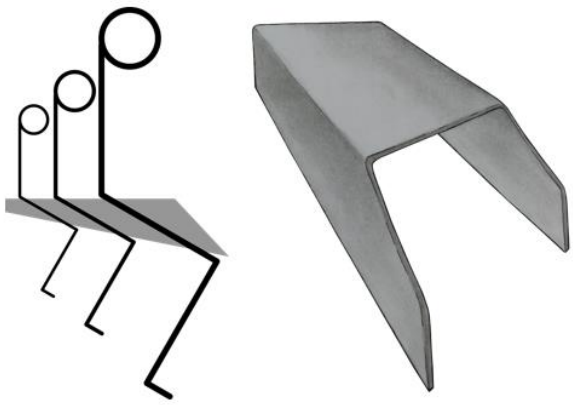

Figure 13 Visualization of how differently sized users sit on different parts of the chair (left) and "the Wedge" seen in 2-point perspective (right). Please note that the seat is not intended to be used by several individuals simultaneously.

"The Fish" (Figure 14): Seen from above, the seat has an hourglass-like shape. Users with greater hip breadth are placed at the rear part of the seat while smaller users sit closer to the narrowest point of the seat. By matching data for hip breadth and femur length, the idea is to give similar hip abduction angle for differently sized users.

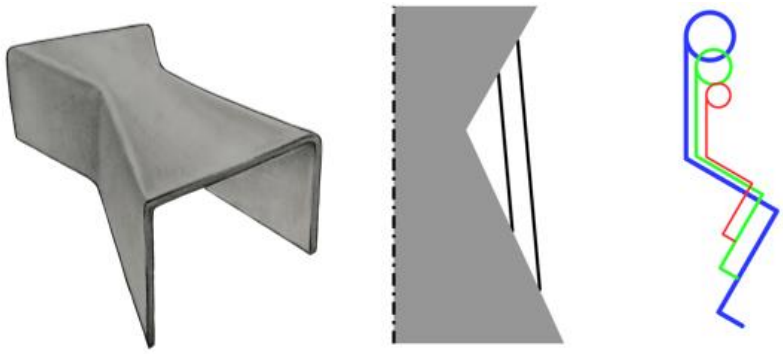

Figure 14 To the right "the Fish" is seen in isometric view. In the middle, half of "the Fish" is seen from above. The two parallel lines represent two differently sized thighs. To the right, three differently sized users are lined up with the tallest in the back and the smallest in front.

"The Hinge" (Figure 15): By attaching the parts of the seat intended to support the thighs of the user with a hinge, it would be possible to adjust the angle of these parts in such a way that they would fit users with different femur lengths without protruding downwards below the knees.

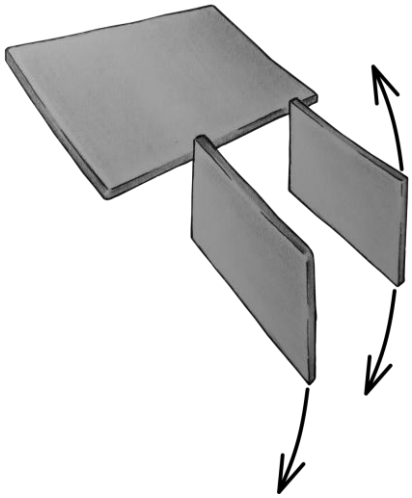

Figure 15 Sketch of "the Hinge"

"The Slider" (Figure 16): With the same motivation as for "the Hinge", the parts supporting the thighs of the user can translate horizontally back and forth.

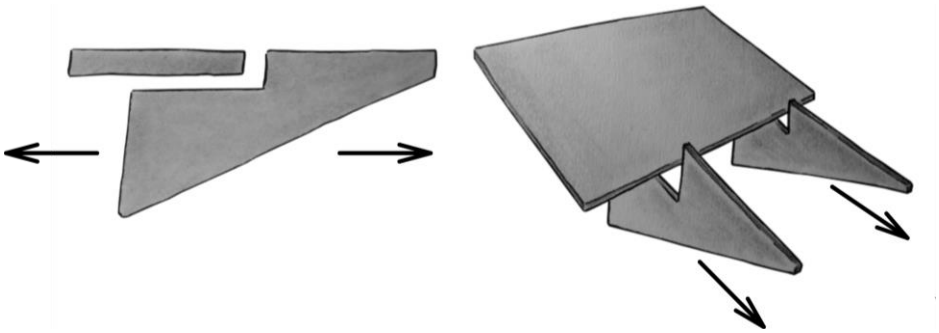

Figure 16 Sketches of "the Slider", seen from the side (left) and in perspective from above (right).

"The Average" (Figure 17): By calculating mean values of necessary anthropometrical data, a seat can be created that is likely to fit few individuals perfectly, while fitting most individuals good enough. Besides *Salli*, this seems to be how most saddle seats are created.

Figure 17 Sketch of "the Average".

5.2.3 Choice and Further Development of Seat Concept

All concepts were presented to and discussed with Fysionord AB.

While “the Wedge” may fit many users ergonomically as they grow taller, the seat will be inconveniently long for indoor use, especially for small users when seated at a table.

“The Fish” has the ability to “grow” with its user as well. However, creating appropriate support for the thighs was found to be harder when placing bigger users further back and smaller users in the front. This challenge can be understood more easily by looking at the right part of Figure 14 and comparing it to the left part of Figure 13. Also, the gap between the seat and the legs of the user will likely require individually adapted padding.

Both “the Hinge” and “the Slider” could likely be combined with other concepts to increase the seats ability to be adapted more efficiently for each user. However, moving parts might introduce weak links in the construction.

As stated, “the Average” is not a perfect solution. However, since the concept is intended to be seated on in the same way by any user and does not require any adjustments, there is little room for misunderstandings on how to use the product. It is relatively minimalistic with few excessive features that can lead to failure. Due to this simplicity it was also regarded as a plausible choice when considering the timeframe of the project. Based on this, “the Average” was chosen for further development.

For further increased support of the thighs, the seat was changed to protrude upwards in front of the area supporting the weight of the user. A sketch of the final concept can be seen in Figure 18 while the process of creating its shape is described in Appendix H.

Figure 18 Final seat concept.

Fysionord AB approved of the concept but pointed out that the bowl shape in the rear part of the seat shown in Figure 18 would be unnecessary.

5.3 Backrest Concept Generation

Considering the four functions of the backrest described in chapter 3.3, it was decided to start close to the user by deciding on a shape for the backrest as well as investigating eventual width adjustment. As a second step of the development, solutions for height adjustment and interface to the chair were examined.

5.3.1 Backrest Shape

No solutions supporting the chest of the user rather than the back was examined since such a solution was deemed likely to impair breathing.

As stated in chapter 4.4, "[…]exaggerated fixation of the user may increase the risk of tipping over." If the width of the backrest is adjustable, there is a risk that it will be adjusted too tightly around the upper body of the user, creating such fixation. Therefore, it was decided to create a backrest without any width adjustment function.

Through dialog with Fysionord AB, following guidelines for designing the backrest shape were established:

- The bottom part of the backrest should end at the top of the iliac crests of the user.
- The top of the backrest should end at the bottom of the shoulder blades to not interfere with arm and shoulder movements.
- The backrest should follow the lumbar curve of the lower back.
- Existing backrest of the Krabat Jockey Lite chair is a good example of appropriate curvature for lateral support.

Together, these four points create a double curved surface with defined ideal top and bottom edges with respect to the back of the user. Since the users will vary in sitting height, this raised the question whether the height of the backrest itself (and not only its position) should be adjustable. However, this idea was dismissed since it was already decided to create a backrest with fixed width. This resulted in a similar approach as with the seat; creating a backrest with a fixed geometry that fits as many users as possible.

A .3dm-model of a human skeleton was downloaded from grabcad.com and opened in Rhinoceros 5 [29]. Its arms (and legs) were removed for increased visibility of the spine. Rendered images of the remaining model were printed to function as a basis for sketching

backrest shapes. An iterative sketching process was then conducted based on above mentioned guidelines. The iterative process is explained in Appendix I and the final result can be seen in Figure 19 and Figure 20.

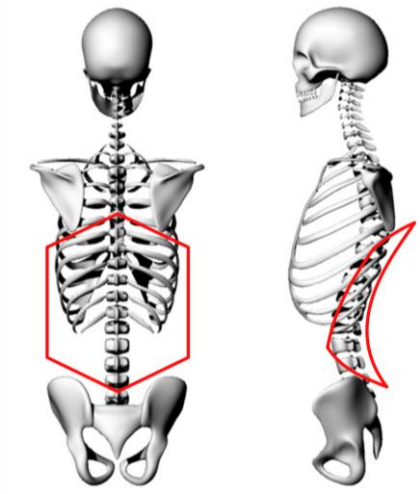

Figure 19 Fifth and final iteration of the sketch process creating the shape of the backrest.

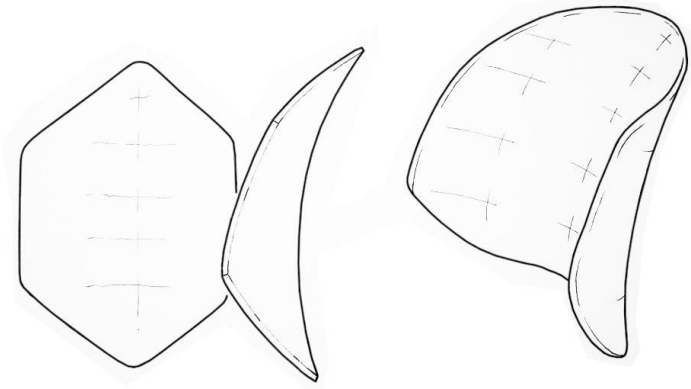

Figure 20 Sketches of the backrest seen from the front (left), from the side (middle) and in perspective (right).

At this point, exact curvatures and dimensions were not defined.

5.3.2 Backrest Height Adjustment and Interface to Chair

Ideas of different backrest post geometries and location of the backrest height adjustment mechanism were generated and can be summed up as follows (from left to right in Figure 21):

- Post geometries:
    1. Pipe with circular cross section.
    2. Pipe with elliptic cross section.
    3. Hollow rectangular bar.
    4. Single sheet metal slab.
    5. Extruded U-shaped beam.

6 Bent or welded sheet metal creating a U-shaped cross section and a triangular side profile for increased second moment of area close to the seat.

- Location of backrest height adjustment mechanism:
  - A In interface between post and backrest.
  - B In the middle of the post.
  - C Close to the seat.

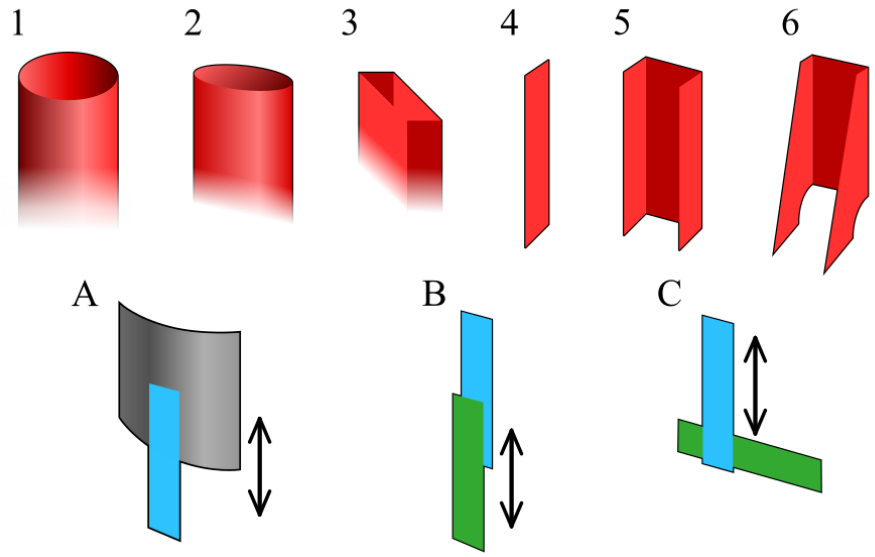

Figure 21 Backrest post geometries (top) and different locations for height adjustment (bottom).

Placing the height adjustment mechanism close to the seat would probably provide the most geometrically simple solution since the relatively complex double-curved surface of the backrest would not be involved with any moving parts. However, as a result of forces asserted by the user, great moments might occur in the area and interfere with moving parts.

Post geometries and height adjustment locations were combined into seven concepts for backrest posts, which can be seen in Appendix J.

The concept 4A was chosen for further development, this was based on following:

- Due to its intended fastening under the seat, rather than close to the hinge of the footrest, it was deemed unlikely to interfere with the footrest.
- The simplicity is likely to make this solution relatively visually appealing.

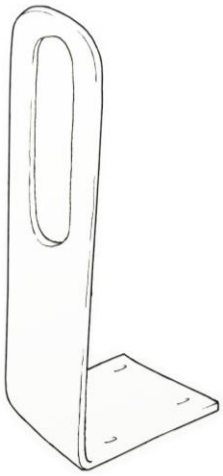

Figure 22 Ink sketch of backrest post concept 4A.

However, it was also decided that it should be tested whether the 4A solution can be made rigid enough without exaggerated material thickness.

5.4 Working Chair Concept

The three main modules were assembled into a complete concept for the working chair, which can be seen in Figure 23.

Figure 23 Watercolor sketch of the working chair. The strap fixating the position of the footrest and the lower part of the undercarriage, including wheels, are not included in the sketch.

The following points were left to be defined or evaluated during the detailing phase:

1. Dimensions of the “ideal user” of the working chair and of the product itself
2. A solution for fixating the angle of the footpad
3. Shape of the footpad
4. Reinforcement of the seat to enable it of supporting the weight of the user
5. Interface between the seat and surrounding modules
6. Interface between backrest and backrest post

6 Detailing

Chapter 6.1 provides clarity to the six points of uncertainties regarding the final concept in the end of chapter 5.4, while chapter 6.2 presents an initial model of the working chair.

6.1 Further Definition of the Final Concept

Linking back to the list in chapter 5.4, chapter 6.1.1 to 6.1.5 present:

- Anthropometrical dimensions used for the detailing of the chair
- A mechanical solution for fixating the angle of the footpad
- The shape of the footpad itself
- A solution for reinforcing the seat and connecting all modules
- The interface between the backrest and the backrest post

6.1.1 Anthropometrical Dimensions of the “Ideal User”

Body measurements of the “ideal user” were defined as the mean values of minimum and maximum anthropometric data listed in the requirement specification in chapter 4. If the size distribution of the users would have been considered, this might have led to an “offset”, making the biggest or smallest users unable of using the product.

Table 6 Anthropometrical dimensions of an ideal user of the working chair.

Measurement	**Mean value of min and max**
Hip breadth	252.5 mm
Femur length	300 mm
Knee height	400 mm
Sitting height	700 mm
Hip abduction	20°

6.1.2 Angle Fixation of the Footpad

The angle of the footpad is fixated by an existing solution often referred to as “Lasse-led” among Swedish medical technicians, later referred to as “Friction joint” in this report. It consists of two identical components, each fastened at opposing sides of a hinge and producing friction against each other when fixated with a M8 bolt. Images and dimensions of such components can be seen in Appendix K.

6.1.3 Shape of Footpad

A curved footpad (Figure 24) was generated to avoid interference with the undercarriage. The front slots (1) are intended for fastening of straps for fixating the feet of the user. The rear slot (2) functions as fasting for the footrest height adjustment strap. The four holes at the rear part of the footpad (3) are intended for fastening friction joints while keeping the feet of the user away from sharp components. The process of generating the shape of the footpad is described in Appendix L a).

Figure 24 Footpad, front of the component facing the viewer.

6.1.4 Reinforcement of Seat and Interface between Modules

In conjunction with modeling of the seat (Appendix L b)), a sheet metal frame (Figure 25) was developed to reinforce the seat, as well as to function as a “hub” for fastening surrounding modules.

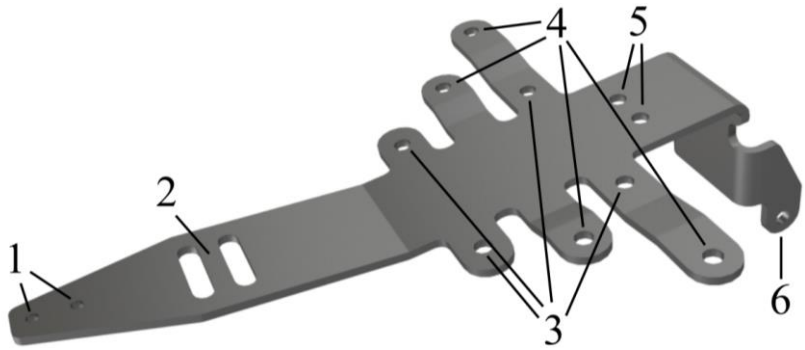

Figure 25 Sheet metal “hub” to be fastened under the seat, seen from above with its front to the left and its rear to the right in the figure.

The numbers in Figure 25 explain how the different modules are to be fastened to the hub:

1. Fastening of the front part of the seat.
2. Fastening of the strap for adjustment of the footrest position.
3. Fastening of the undercarriage.
4. Fastening of the rear part of the seat. Also intended for future fastening of waist belt.
5. Fastening of the backrest.
6. Fastening of the hinges connecting the footrest.

The process of generating the hub is described in Appendix L d).

6.1.5 Interface between Backrest and Post

To create an interface between the backrest and the backrest post, a flat area on the backside of the backrest was generated, leading to a cavity in the backrest itself. A metal component containing a threaded M14 hole for fastening to the post was added in the cavity. The component was also intended to prevent rotation of the backrest. This is visualized in Figure 26. A solution for covering the cavity must be developed at a later stage.

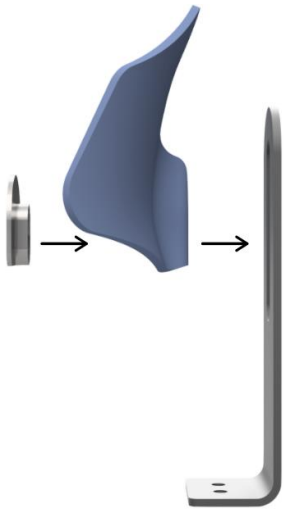

Figure 26 Exploded view of the backrest.

The iterative processes of developing the shape of the backrest is explained in Appendix L c).

6.2 Initial Model of the Working Chair

An initial 3D model of the working chair, created in Inventor 2018, can be seen in Figure 27 and Figure 28. No padding or fastening elements, such as bolts, were included in the model.

Figure 27 Initial CAD-model of the working chair. The front of the chair facing the viewer.

The three blue components are intended to be manufactured through vacuum forming thermoplastic due to their relatively complex geometries. Manufacturing process was defined during detailing since it affects the choice of geometries.

The height adjustment component was modeled according to measurements on a Krabat Jockey Lite chair, its main dimensions can be seen in Appendix M.

The originally independent hinges for fastening the footrest to the hub were joined into a single hinge component for increased stability.

Length adjustment of the footrest levers are made stepwise and secured by bolts to the hinge. The angle of the footrest is to be adjusted in small steps due to the design of the pre-manufactures friction joint angle adjustment mechanism. All other adjustments are stepless.

The main dimensions of the working chair are illustrated in Figure 28. As with the length, the maximum width of the chair, 675 mm, is given by the undercarriage.

Figure 28 Main dimensions of the working chair seen from the side with the backrest set to its highest position.

7 Finite Element Calculations

To enable work while attending project related activities away from UiT Campus Narvik, two different versions of *Ansys* were used:

- *Ansys R19.2 Academic*, installed at UiT Campus Narvik with unknown maximum amount of nodes. Models with up to 240 000 nodes tested successfully.
- *Ansys 2019 R1 Academic*, installed on personal computer, allowing mesh with up to 32 000 nodes.

The two sheet metal components of the working chair were chosen for investigation through finite element analysis:

- Hub: since all modules are fastened to this component, it is subject to multiple loads. It was therefore deemed to likely be the part of the chair with the greatest concentrations of stress.
- Backrest post: due to the relatively simple geometries of the component, it was deemed suitable for analysis while being limited to creating mesh with up to 32 000 nodes.

Structural steel, pre-defined by Ansys, was chosen as material in all simulations. Material data can be seen in Appendix N.

7.1 Analysis of the Hub

To enable decreased element size, the model of the hub was split along its symmetry line in Inventor and exported in .stp format to be opened in a “Static Structural” analysis in Ansys Workbench.

Rather than using safety factors for the applied loads, all forces were set to 250 N.

$$250\ N \approx (\underbrace{50\ kg}_{\max body\ mass} \cdot \underbrace{9.82}_{g}) / \underbrace{2}_{symmetry}$$

Creating exaggerated extreme cases where the entire body weight of the user is applied at multiple parts of the component simultaneously. Loads and supports are shown in Figure 29 and explained in the list below. All loads are simplified in the sense that they only act on the holes for fastening corresponding modules rather than entire contact surfaces.

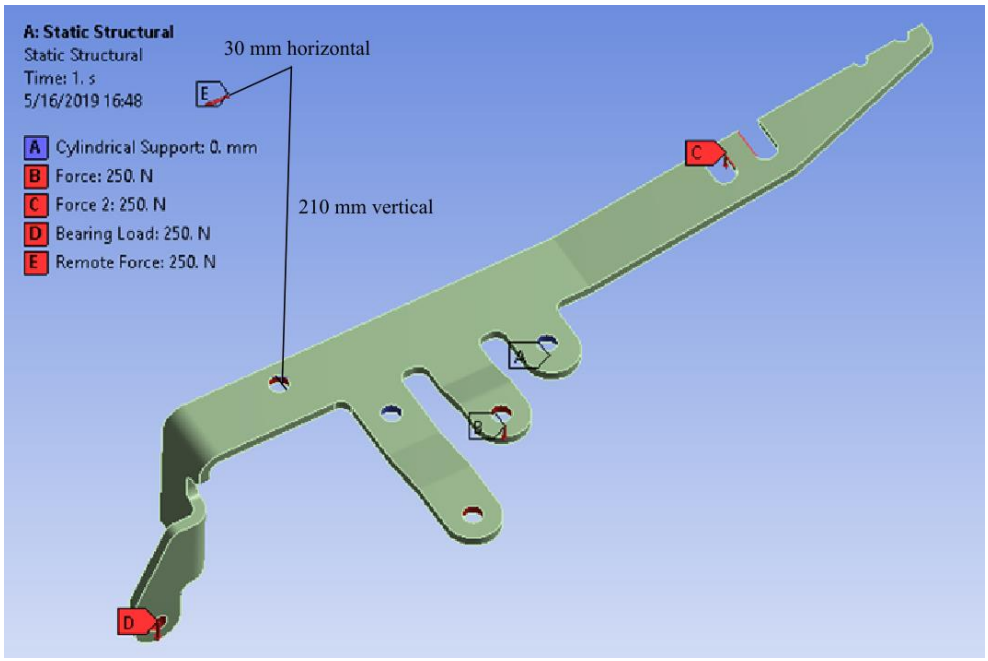

Figure 29 Loads and supports for initial analysis of the hub.

A. The hub was fixed through cylindrical supports in the holes connecting it to the undercarriage.
B. A vertical, downward force was applied in the holes connecting the seat to the hub, emulating the weight of a user.
C. A vertical, downward force was applied on the edges of the fastening point for the strap connecting to the footrest.
D. A vertical, downward bearing load was applied on the hinges at the rear part of the hub.

E. A horizontal, backward remote force creating moment around the fastening points for the backrest post, while being offset as if acting on the backrest when adjusted to its highest position, 210 mm above the fastening holes and 30 mm behind their center.

Regarding E, no data was found linking user weight and ability to assert large forces backwards towards the backrest. Such data could likely be gathered at a later prototyping stage through measuring pressure between the back of an actual user and the backrest. However, if the entire body weight of a 50 kg user would be thrusted backward against the backrest, it is reasonable to believe that the chair would fall over due to its relatively small wheel base. This is a problem on its own, but it means that the hub and backrest post only have to support such loads that are not great enough to make the chair fall over. No force was applied on the front mounting points of the seat since such a load was deemed to make the chair fall over forward rather than producing great stresses in the hub.

7.1.1 Hub Analysis Iteration 1

Non-straight sided tetrahedral elements were used to maintain smooth curvatures. Element size was set to 3 mm to leave margin for later refinement, producing 50 800 nodes. "Virtual cells" were used to facilitate meshing, defining a top, a bottom and a side face rather than the original multiple faces given by each bend. The mesh is shown in the four first images in Appendix O a).

Initially, each load was applied separately by creating a multistep analysis, in which only one load was active during each step. When doing so, it became apparent that the remote force (E in Figure 29) mimicking force asserted backwards on the backrest, created significantly larger stresses in the hub than any of the other loads. Maximum stresses for the different load cases are compared in the graph in Figure 30. while the stress distribution from remote force E is shown above in the same figure.

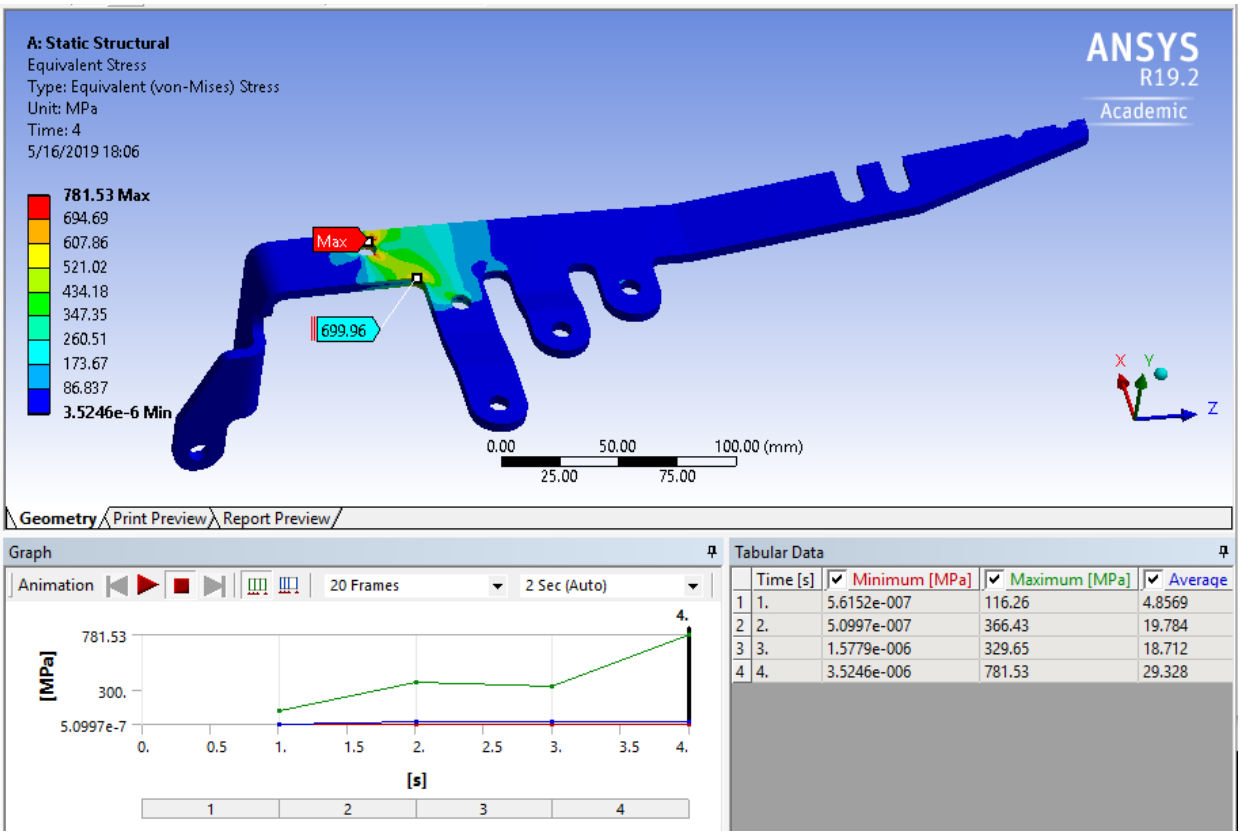

Figure 30 Stress distribution from remote force E and comparison of stress from different loads. force B active in step 1, force C active in step 2, bearing load D active in step 3 and remote force E active in step 4.

Because of this, redesigning the hub and backrest post to reduce the stress originating from force applied on the backrest was made a priority.

Prior to redesigning the hub, it was decided to make sure that the results of the first simulation were relevant. To validate the use of a remote force to mimic a force acting on the backrest, an additional simulation was made using an assembly consisting of the hub and the backrest post. 3 mm element size produced mesh containing 136 993 nodes without using symmetry. Contact between the parts was defined as "frictionless", allowing separation and translation between the parts, but no penetration, while the two bolts fixating the parts were simplified into "revolute joints". The assembly can be seen in Figure 31.

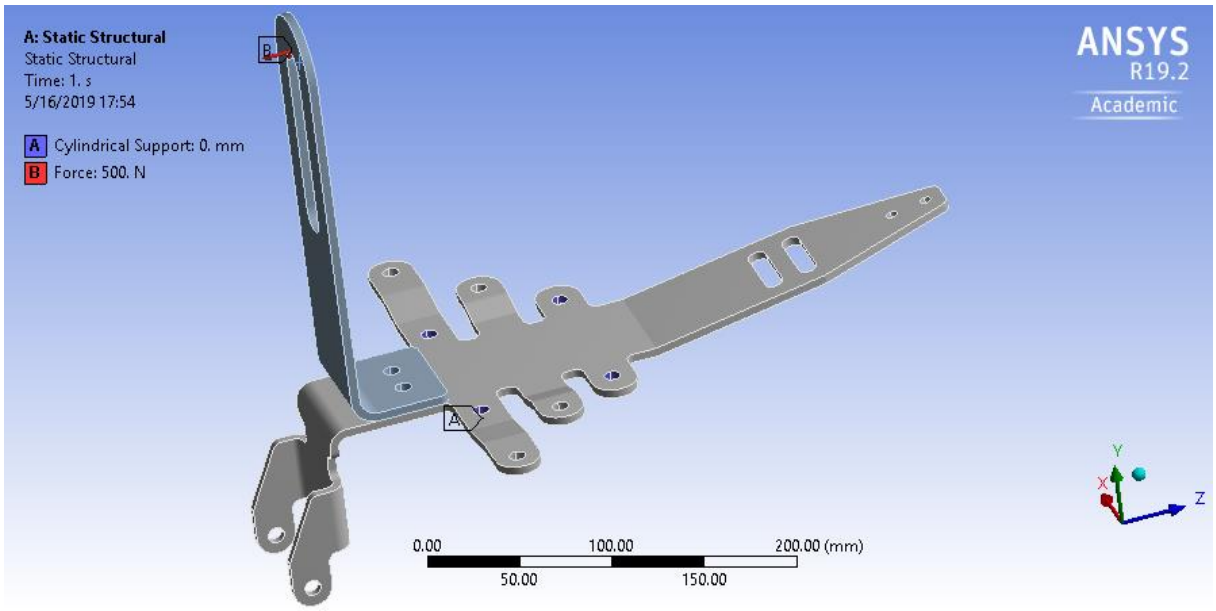

Figure 31 Assembly used for validating the use of a remote force to mimic force applied on the backrest.

A stress plot from the analysis of the assembly can be seen in Appendix Oa). After comparing the stress distributions generated by the two methods, it was concluded that the simplified method of using a remote force seemed to produce similar stress in the rear fillets of the hub (likely due to notch effect) as applying a force on an actual part. However, differences in stress magnitude were observed in the backrest fastening points, in which the remote force and corresponding joints were applied. Neglecting this area, the remote force was used in remaining iterations.

To further investigate the results of iteration 1, the mesh was refined stepwise in the area subject to notch effect. This was done using the "sphere of influence" function, refining all elements within a 10 mm radius from the center of the fillet. Location of the refinement can be seen in Figure 32.

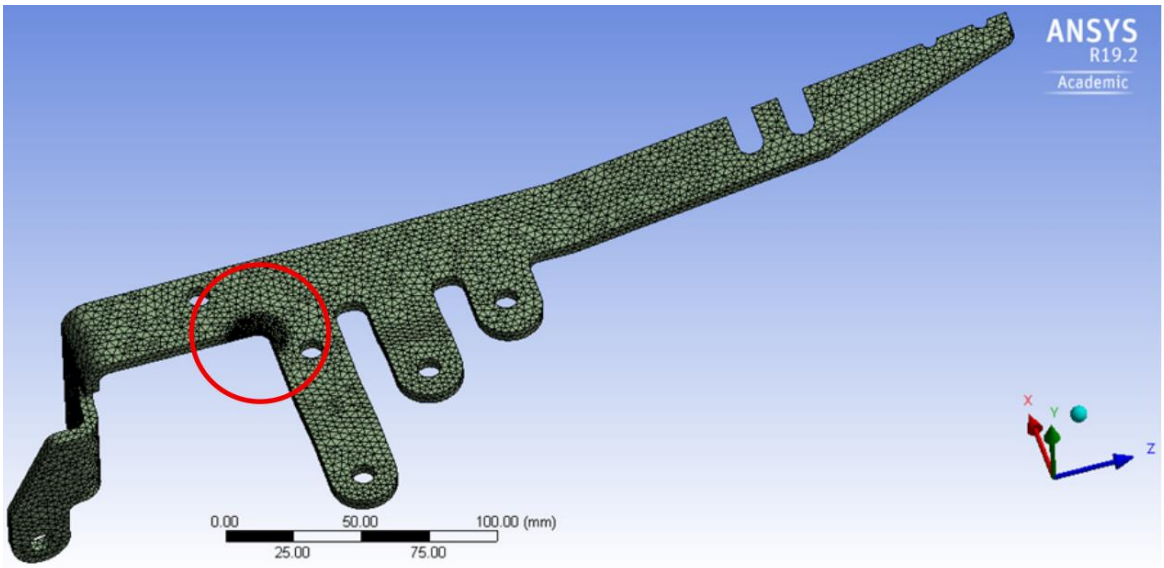

Figure 32 Meshed model of the initial hub with refinement within the red circle.

Maximum equivalent stresses in the refined area for different element sizes are presented in Table 7. Stress plots of the fillet included in the refined area can be seen in Appendix O a).

Table 7 Maximum equivalent stresses for stepwise refined mesh. Surrounding element size was fixed at 3 mm.

Refined element size	**Max von-Mises stress in refined area**	**Nodes**
3 mm	699.96 MPa	50 800
2 mm	715.13 MPa	52 183
1 mm	729.42 MPa	60 928
0.7 mm	739.14 MPa	77 812
0.4 mm	748.90 MPa	173 531
0.37 mm	751.08 MPa	203 334

When using element size smaller than 0.37 mm, following error message appeared: “Your product license has numerical size limits, you have exceeded these problem size limits and the solver cannot proceed.” The warning refers to exceeding the maximum amount of nodes. According to online forum threads, it could also be a side effect from using remote forces [30].

As seen in Table 7, the maximum stress increased when the mesh was refined, without seeming to converge toward a finite number. This could be due to the edge causing a singularity, in which the theoretical, numerically computed stress goes to infinity. It is also

possible that the increased stress depicts reality. However, it was decided to increase the fillet radius in an attempt to avoid the problem entirely.

7.1.2 Hub Analysis Iteration 2

In addition to enlarging the fillet investigated in iteration 1, the cutouts between the arm-like geometries on the sides of the hub were removed. The orientation of the two holes for fastening of the backrest post was changed to create a lever, while allowing place for nuts on the underside of the hub without interfering with the height adjustment mechanism of the undercarriage.

The same loads as previously were applied to the hub in a second iteration of simulations. Due to the changes in the backrest post fastening, the remote force mimicking load on the backrest was defined as 25 mm behind the rear of the two fastening holes to maintain its original position.

In addition, another remote force was added to emulate the footrest being pushed to the side by the feet of the user, creating moment around the hinges in the rear part of the hub. To create an extreme case, the load was located 440 mm below the hinges and 450 mm in front of them, corresponding to the position of the front part of the footpad when located as far away from the hinges as possible. It was deemed unlikely that a force corresponding to the entire weight of the user would be asserted laterally on the footpad. In combination with the long levers, redesigning the hub for such loads would likely lead to making it excessively large and heavy. Therefore, in lack of real life data, the added remote force was arbitrarily scaled down to 250 N. To enable investigation of such load, no symmetry was used. Loads and supports for analysis of the second iteration of the hub can be seen in Figure 33.

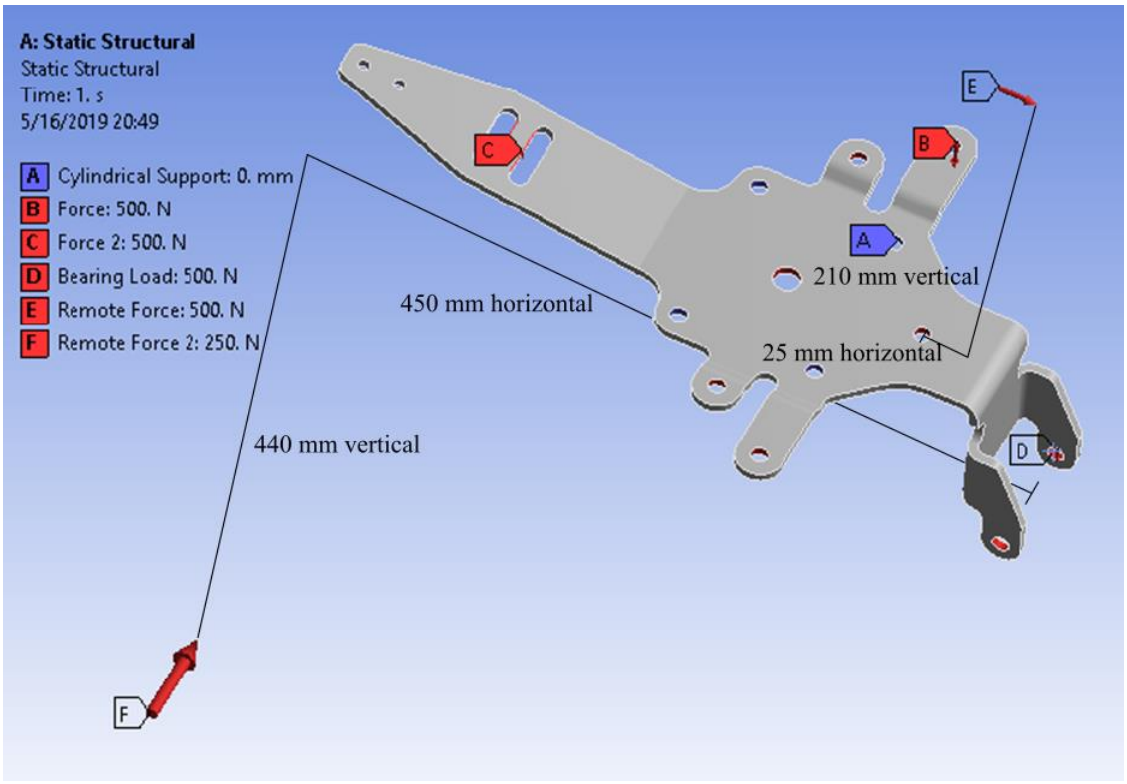

Figure 33 Loads and supports for analysis of the second iteration of the hub.

As in iteration 1, element size was set to 3 mm and tetrahedral elements were used, producing 102 964 nodes.

The redesigning of the hub led to reduced stress from the force acting on the backrest. However, the newly added lateral remote force F produced stresses with magnitude up to 1014 MPa. A stress plot and comparison of maximum stresses can be seen in Appendix Ob).

7.1.3 Hub Analysis Iteration 3

The rear part of the hub was widened to reduce stress from lateral load on the footrest. The hinges were made into a separate part from the hub, to be fastened with two M14 bolts or rivets. Contact between the two parts was defined as “frictionless” and the two fastening bolts or rivets were simplified to “revolute joints”. To further simplify the shape of the hub, the arm-like geometries for mounting the seat were redesigned as well.

Using tetrahedral elements with side length 3 mm produced mesh with 80 355 nodes. As seen in Figure 34, applying the same remote force F from the footrest as previously produced stresses with magnitude up to circa 616 MPa close to the fastening of the new hinge. Stresses with magnitude of circa 455 MPa were observed in the area close to the rear fastening points to the undercarriage. It was deemed to likely be a combination of the fixed geometry and notch effect.

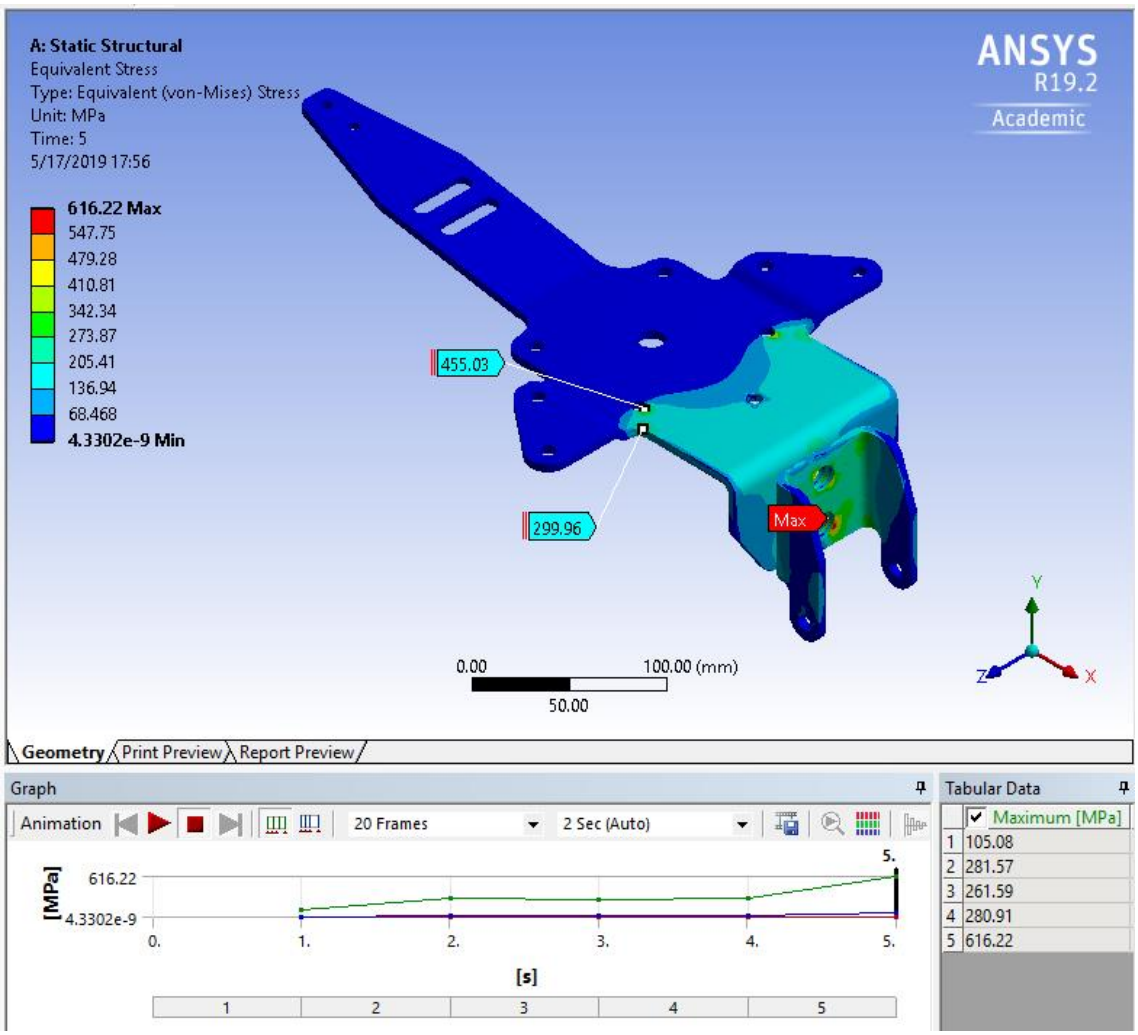

Figure 34 Stress distribution from lateral remote force on the rear hinges in the third iteration of the hub. Comparison of maximum stresses for different loads.

The mesh was refined at one of the undercarriage fastening points and the nearby notch, as well as in the lower of the two fastening points for the hinge. Maximum equivalent stresses for the refined areas for different element sizes are gathered in Table 8. Areas of refined mesh and stress plots can be seen in Appendix O c).

Table 8 Maximum equivalent stresses for stepwise refined mesh. Surrounding element size was fixed at 3 mm.

Refined element size	**Notch max stress**	**Undercarriage fastening max stress**	**Hinge fastening max stress**	**Nodes**
3 mm	299.96 MPa	455.03 MPa	616.22 MPa	80 355
2 mm	290.08 MPa	435.16 MPa	665.59 MPa	145 768
1 mm	298.10 MPa	507.10 MPa	835.29 MPa	210 622

Further attempts at refining the mesh produced the same error message regarding problem size limits as during iteration 1. Based on the limited data available in Table 8, following was concluded:

- The maximum stress in the notch seems to converge at circa 290-300 MPa.
- The data provides no clarity regarding the stress at the undercarriage fastening point, but the magnitude is likely increased due to the close proximity to the notch.
- The maximum stress in the hinge fastening point seems to go to infinity. However, without further validation it cannot be ignored as a singularity.

7.1.4 Hub Analysis Iteration 4

Sheet metal thickness was increased to 6 mm. To prevent notch effect from increasing the stress at the rear undercarriage fastening points, the bends connecting to the seat were redesigned to once again enable larger fillets in the rear part of the hub. To reduce stresses at the fastening points of the hinge, the contact area between the two parts was redefined as "bonded" in Ansys in order to emulate them being welded together in addition to the bolts or rivets. Element size was set to 3 mm, producing 168 217 nodes. The stress distribution from applying the same lateral remote force (F) as in previous iterations, mimicking force from the footrest, can be seen in Figure 35.

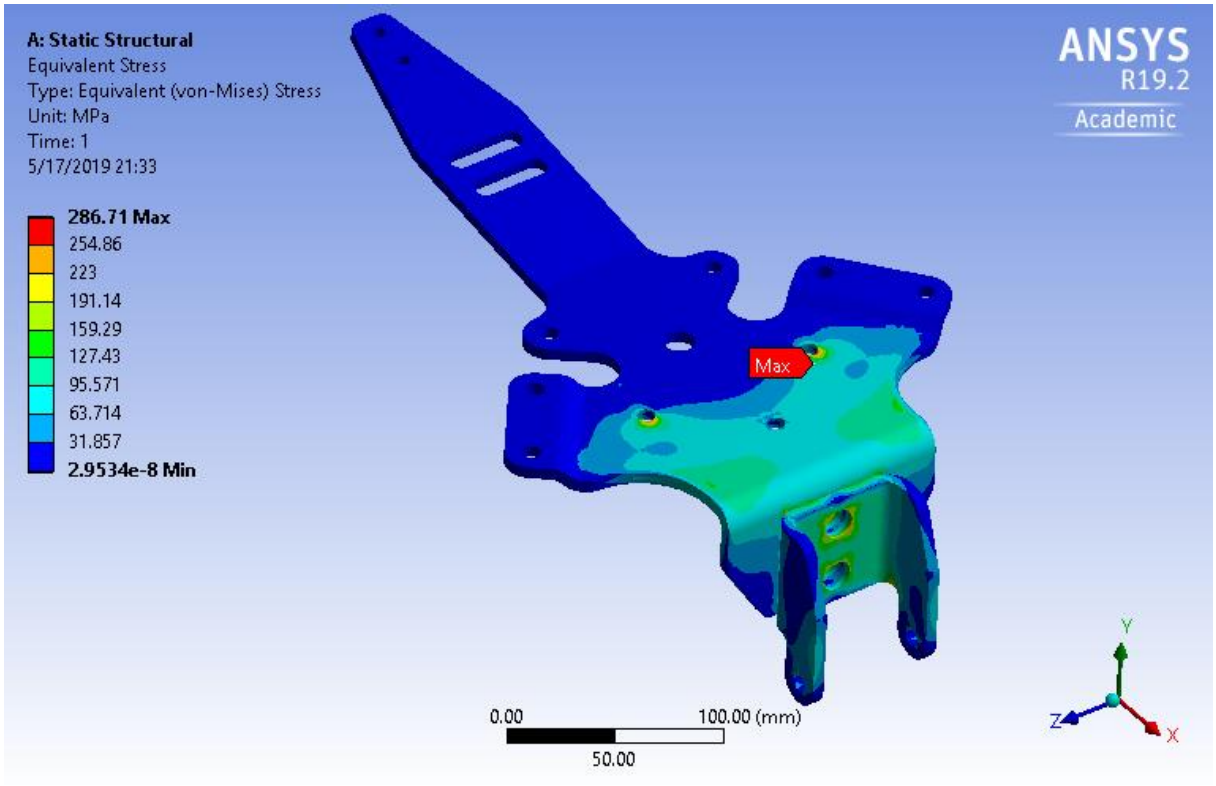

Figure 35 Stress distribution from lateral remote force on the rear hinges in the fourth iteration of the hub.

An additional stress plot, only including the hinge, can be seen in Figure 36. It shows how the maximum stress in the component no longer was found near the fastening points, and that it was reduced to circa 240 MPa.

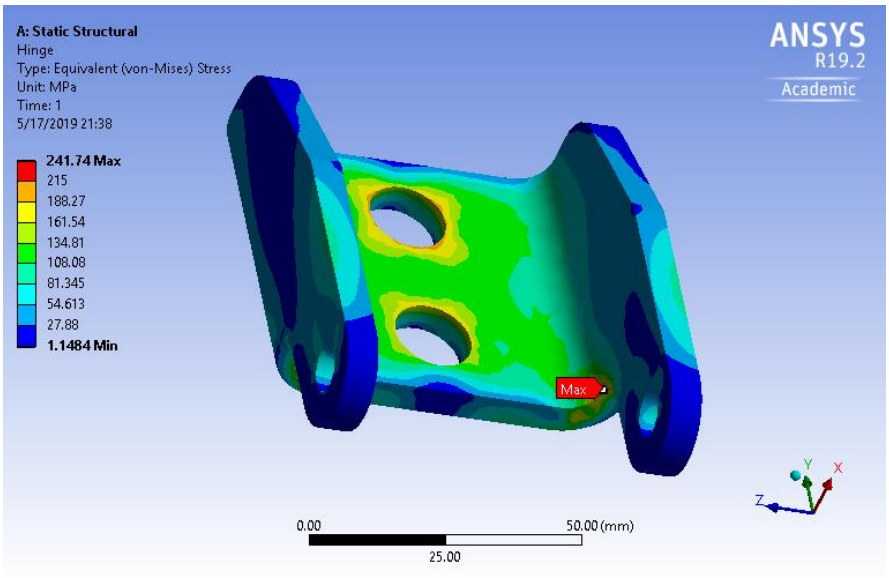

Figure 36 Stress distribution in hinge from lateral remote force.

To test the hub for multiple simultaneous loads, the two loads acting on the hinge (vertical bearing load D and lateral remote force F) were alternated while all other loads shown in Figure 37 were applied to the hub.

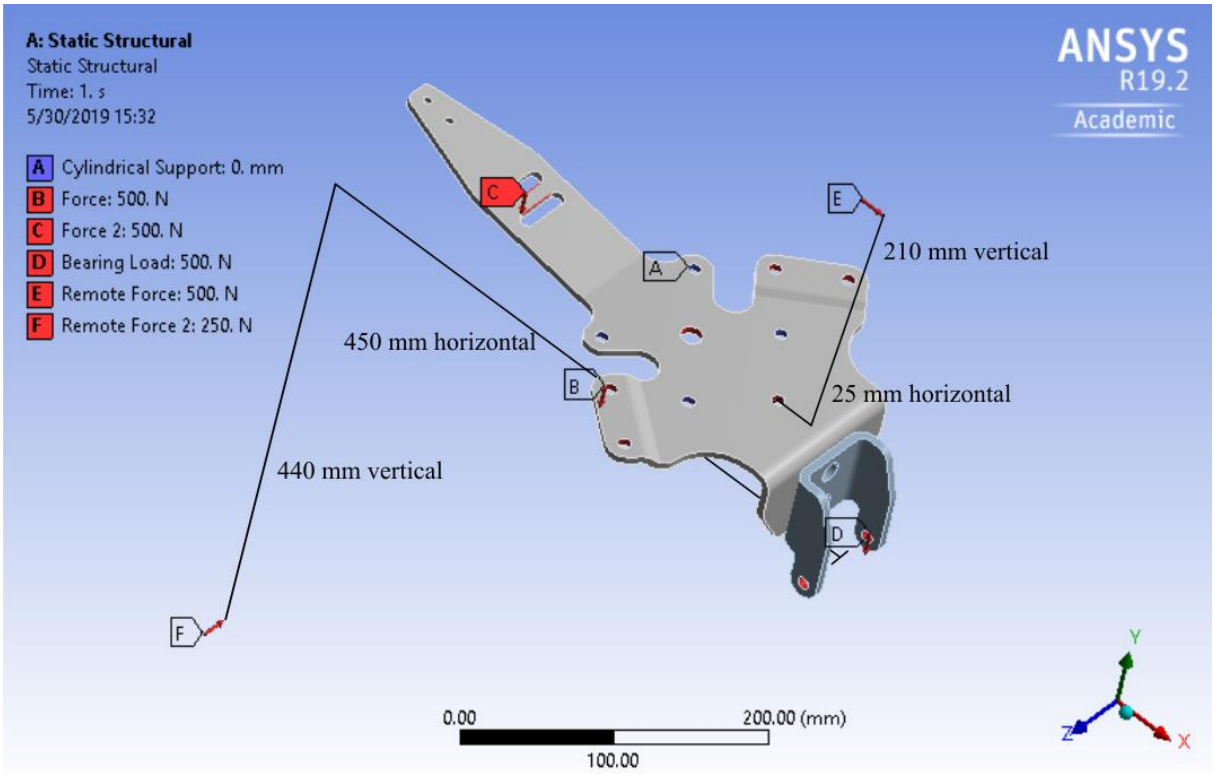

Figure 37 Loads and supports for analysis of the fourth iteration of the hub.

The idea was to emulate two scenarios, only differing in magnitude and direction of the force applied on the footrest. This led to maximum stresses of circa 427 MPa from lateral remote force (F) in combination with other loads, and circa 300 MPa for the corresponding vertical load case. Stress plots for both scenarios can be seen in Appendix O d). Due to time limitations, only the lateral load case (stress distribution shown in Figure 38) was investigated further through refined mesh.

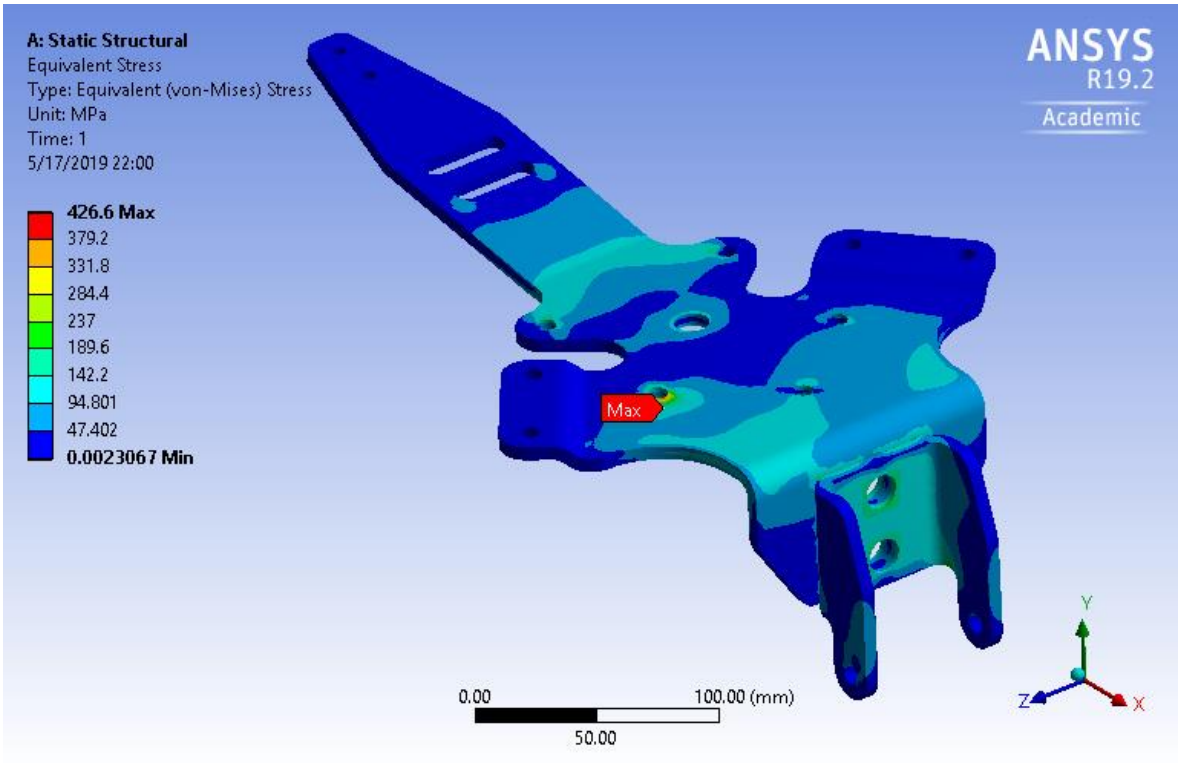

Figure 38 Stress distribution from multiple simultaneous loads with lateral remote force F active.

The area containing the maximum stress was refined using the "sphere of influence" function. The area of refined mesh and stress plots can be seen in Appendix Od) while maximum stresses for different element sizes are summed up in Table 9.

Table 9 Maximum equivalent stresses for stepwise refined mesh. Surrounding element size was fixed at 3 mm.

Refined element size	**Max von-Mises stress in refined area**	**Nodes**
3 mm	426.60 MPa	168 217
2 mm	470.02 MPa	176 118
1 mm	584.89 MPa	223 816
0.9 mm	601.62 MPa	242 216

As seen in Table 9, no convergence towards a finite magnitude of stress was found. Fillets and chamfers were added in unsuccessful attempts to avoid the issue. Increasing the radius was not an option since the size of the holes must match the undercarriage.

To create a case more similar to reality, the uppermost sheet metal parts of the height adjustment mechanism were added to the assembly, replacing the cylindrical support. This can be seen in Appendix O d). Contact between the undercarriage and the hub was set to "frictionless" and the fastening holes were defined as revolute joints. Element size 3 mm resulted in 177 336 nodes. As seen in Figure 39, this method eliminated the problems with large stress concentrations in the rear undercarriage fastening points. Comparing Figure 36 and Figure 39 it appears as if the stress was slightly increased in the area of the new maximum. This could be due to increased stiffness in the area of the newly added parts.

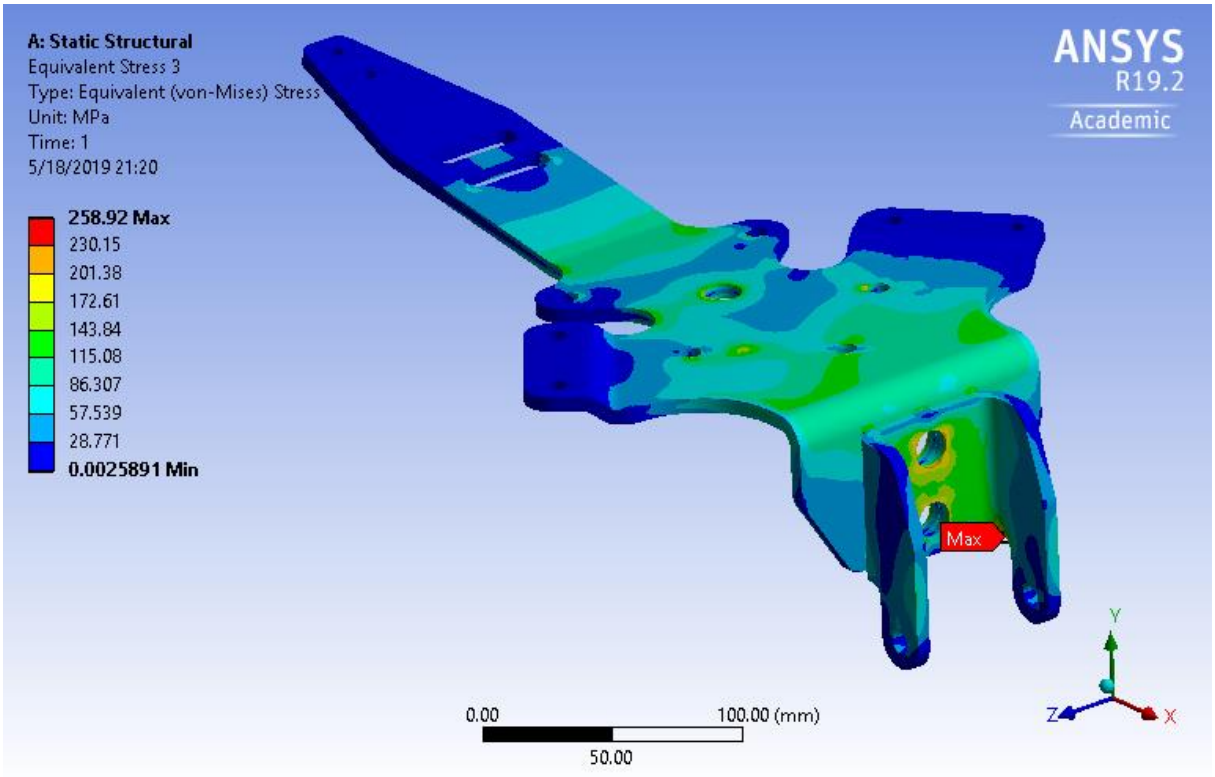

Figure 39 Stress distribution from multiple loads and lateral remote force active on the rear hinges. Cylindrical supports replaced with sheet metal parts from undercarriage.

No further refinements were made at this point due to the limited time devoted to numerical analysis. The area containing the new maximum stress should be investigated further and possibly redesigned prior to manufacturing. Also, manufacturing could likely be made more efficient if the component was redesigned in such a way that welding would no longer be necessary.

7.2 Analysis of the Backrest Post

Following the changes to the hub, the backrest post was redesigned and the sheet metal thickness was increased to 6 mm to match the thickness of the hub.

The backrest post was tested for the same horizontal 500 N force as the hub (remote force E in Figure 29) based on the same reasoning as in chapter 7.1. Initially, contact with the hub was substituted with a "compression only" support. However, due to convergence issues, this method was abandoned for the use of an assembly consisting of the backrest post and a simplified model of the hub, as seen in Figure 40. No symmetry was used since this would require splitting contact areas, which may affect the results of the analysis.

Figure 40 Loads and supports for initial analysis of the backrest post.

7.2.1 Backrest Post Analysis Iteration 1

When investigating extreme values in the backrest post, maximum deflection (circa 12 mm) was found at the top of the post, while maximum stress (close to 360 MPa) was found in the bend. Plots of displacement and stress can be seen in Appendix P a).

To validate the results, normal stress in vertical direction was plotted (Figure 41) and compared to analytically computed bending stress along two lines, A and B. The analytical computations, which can be seen in Appendix Q, resulted in 190 MPa bending stress in point A and 270 MPa bending stress in point B. More detailed descriptions of the locations of A and B are also found in Appendix Q.

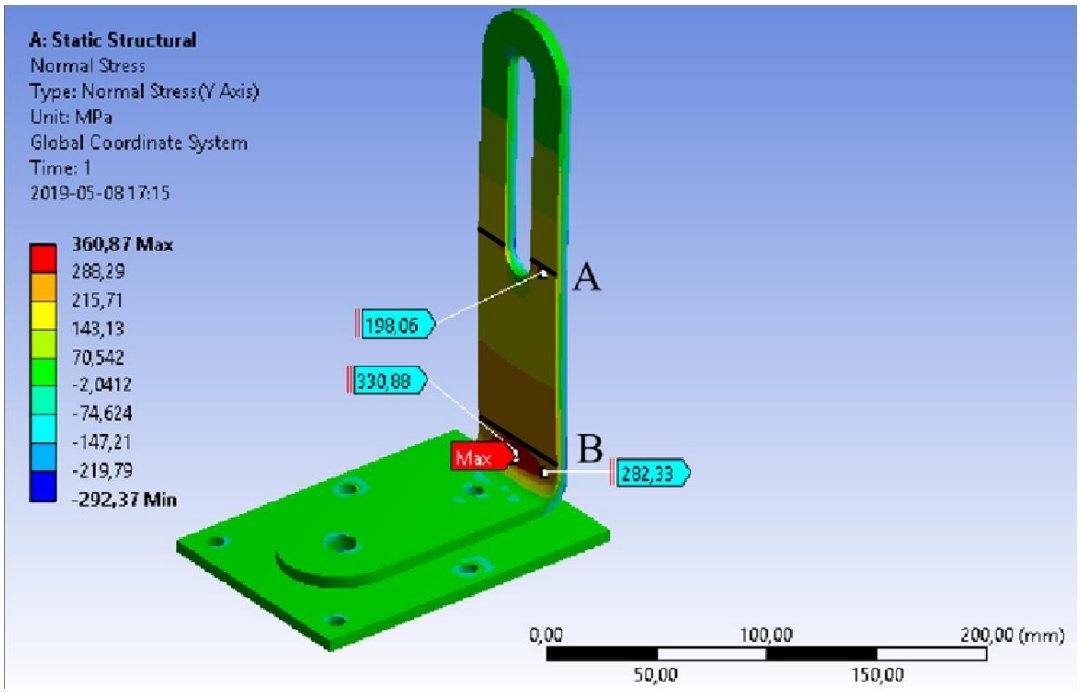

Figure 41 Normal stress in vertical direction.

When neglecting areas subject to notch effect, the numerical results from *Ansys* seem to be consistently circa 10 MPa greater than the analytical results. This is likely due to that the 500 N force in the simulation was applied on the entire fillet in the uppermost part of the slot, creating a slightly longer lever than the point load used in the analytical computations. Both analytical and numerical results indicate significantly greater stresses in the bend of the post than in the area close to the slot.

To further validate the results of the first iteration, the general element size was increased to 6 mm to enable the use of finer mesh in the bend where maximum stress was found. Convergence was found by decreasing the element size in the bend stepwise. Maximum stresses for different element sizes are summed up in Table 10. The refined area, as well as stress plots can be seen in Appendix P a).

Table 10 Maximum equivalent stresses for different sizes of mesh in the bend of the backrest post. Surrounding element size was fixed at 6 mm.

Element size in bend	**Max von-Mises stress**
2.0 mm	357.26 MPa
1.7 mm	356.79 MPa
1.5 mm	361.15 MPa
1.35 mm	358.90 MPa

Based on this, maximum von-Mises stress was assessed to converge toward circa 360 MPa.

7.2.2 Backrest Post Analysis Iteration 2

To decrease the maximum equivalent stress, it was decided to increase the bending radius from 10 mm to 20 mm, while material was removed at the ends of the posts to reduce mass. According to an initial simulation, using 5 mm element size, the redesign reduced the maximum stress to circa 314 MPa. This was tested through stepwise refinement of element size as in iteration 1. As before, surrounding element size was increased to 6 mm to allow refinement in the desired area. Maximum stresses for different element sizes can be seen in Table 11 while stress plots can be seen in Appendix P b).

Table 11 Maximum equivalent stresses for different element sizes in the bend of the backrest post. Surrounding element size was fixed at 6 mm.

Element size in bend	**Max von-Mises stress**
3 mm	319.47 MPa
2 mm	327.91 MPa
1.7 mm	326.17 MPa
1.6 mm	326.68 MPa

As seen in in Table 11, the maximum von-Mises stress increased and converged at circa 327 MPa as a result of the refined mesh.

8 Sheet Metal Material Selection

Since strength analysis was only implemented on the sheet metal components of the chair, material selection was limited to these components as well. It was decided to use the same material and thickness for all sheet metal components to simplify manufacturing. The greatest stress found in the final sheet metal parts during analysis was circa 327 MPa. Using a relatively small 30% safety factor produced a minimum allowed yield stress of circa 420 MPa [31].

No further changes in thickness were made at this point due to the complexity of such changes and the limited timeframe. Table 12 lists the functions, objectives, constraints and free variables of the sheet metal parts.

Table 12 Functions, objectives, constraints and free variables of the sheet metal parts.

Functions	Fastening for other modules
	Support weight and forces asserted by user
Objectives	Resistant to fatigue
	Not subject to brittle fracture
	Low weight
	Low cost
Constraints	Geometries, including thickness
	Minimum yield strength 420 Mpa
	Manufacturing process: cutting, bending and welding
Free variables	Choice of material

8.1 Material Selection CES Level 2 Database

An initial screening for materials was done using the level 2 database in CES Edupak. At first, yield strength was compared to fatigue strength at 10^7 cycles (Figure 42). The number of cycles is a fixed preset in CES and cannot be changed. The minimum fatigue strength was set to 420 MPa to match the minimum yield strength, making sure that the performance of the material still is adequate after some time of using the working chair.

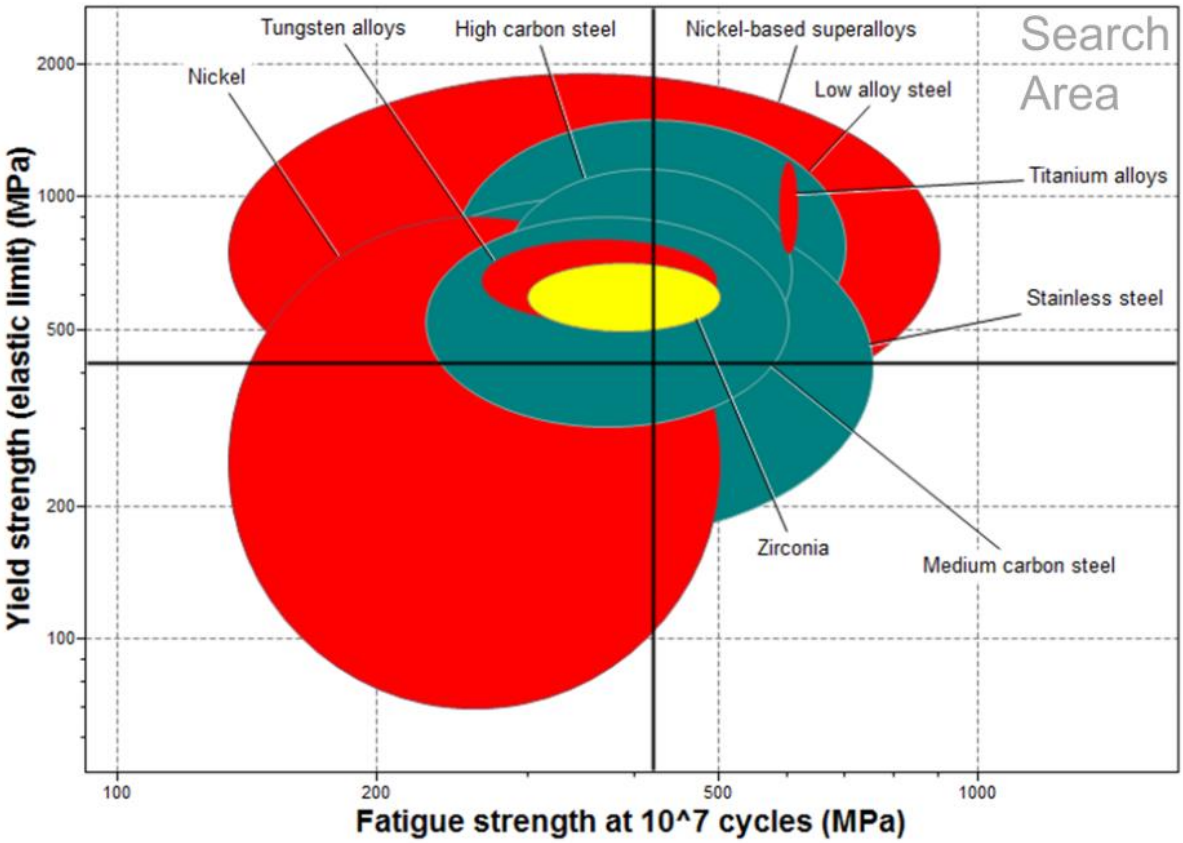

Figure 42 Graph for yield strength versus fatigue strength, generated in CES.

Secondly, the ratio between tensile strength and yield strength was compared to price multiplied with density. The ratio between tensile and yield strength was intended to compare plastic deformation prior to failure in different materials. Materials with a high ratio should deform plastically rather than being subject to brittle failure, and therefore be safer for the user. Since the volume of the sheet metal components already was fixed, price (defined in CES as USD/kg) was multiplied with density (kg/m^3) to produce the unit USD/m^3. In this comparison, the cost of medium and high carbon steel along with low alloy steel, stood out as significantly smaller than for all other material groups.

When comparing formability (for bending) and weldability, medium carbon steel performed best, followed by high carbon steel and low alloy steel. Based on this, these three material groups were chosen for further investigation using the level 3 database of CES. All level 2 graphs can be seen in Appendix R a).

8.2 Material Selection CES Level 3 Database

Only including the three material groups from 8.1, the ratio between tensile and yield strength was compared to price multiplied with density. In this comparison, “Carbon steel, AISI 1095, normalized” stood out as non-brittle to a low price.

Comparing yield strength to fatigue strength at 10^7 cycles showed “Low alloy steel, AISI 9255, oil quenched & tempered at 205 °C” as the seemingly strongest material. However, looking closer at the scale of the fatigue strength axis reveals that the material might be severely weakened from use. Also, the previous comparison shows that the tensile and yield strength of the material seem to coincide (ratio 1), indicating great risk of brittle failure.

Comparing suitability for metal press forming (as this is similar to bending) with weldability presented a single material as the most appropriate from the perspective of manufacturing: “Low alloy steel, AISI 9310, normalized”. According to previous graphs, the mechanical properties of the material are similar to “Carbon steel, AISI 1095, normalized”, while being more expensive.

Even though the yield strength of “Carbon steel, AISI 1095, normalized” is relatively small, it will likely not be subject to brittle failure. Also, it is relatively well suited for the intended manufacturing processes. Based on this AISI 1095 was chosen as material for all sheet metal parts. All level 3 graphs can be seen in Appendix R b).

9 Final Product and Conclusions

Chapter 9.1 presents the final working chair, followed by conclusions in chapter 9.2 and ideas regarding further work in chapter 9.3.

9.1 Final Working Chair

Color of all plastic parts was changed to match the orange color of the Fysionord AB logo, which can be seen in Figure 43.

Figure 43 The final working chair with the Fysionord AB logo.

As a result of the further development of the hub and backrest post, minor changes were made in the rear part of the seat, which can be seen in Figure 44.

Figure 44 The working chair seen from above.

Appendix S presents an exploded view of all components developed during the project along with a table listing manufacturing process and material for each part.

Using Inventor “iProperties”, density for the pre-manufactured components was adjusted for the mass to correspond to measured values in Appendix B. To find an approximate center of gravity, material of all metal parts was defined as carbon steel. The plastic parts were defined as ABS plastic since it is commonly used for vacuum forming [32]. This resulted in an approximate total weight of circa 13 kg, 6 kg lighter than the goal of 19 kg but heavier than the ideal 10 kg. The resulting position of the center of gravity can be seen in Appendix T. However, these results will vary with individual adjustments of the chair. *iProperties* of the working chair model can also be seen in Appendix T, along with Inventor material data for carbon steel and ABS plastic.

In addition to rendered images, a 3D-printed prototype in scale 1:3 was created. Images of the prototype can be seen in Appendix U.

Technical drawings of all parts developed during the project can be seen in Appendix V.

9.2 Conclusions

No known competing solution has a footrest that enables the foot position described in chapter 1.1.4, making the working chair both functionally and visually unique. Whether or not the chair is visually appealing is a matter of subjective opinion. However, by not resembling a traditional medical device, it has fulfilled the aesthetic vision of the project.

Linking back to wishes in the requirement specification, interface was created for adding a waist belt and fastening for the feet of the user. However, the chair lacks the options to fasten armrests and a grip for guardians to handle the chair. Due to the modular design, the undercarriage can be removed in favor of a solution with electric height adjustment.

Most components of the chair are newly developed and not standardized, which might lead to high manufacturing costs. However, since no manufacturers were contacted during the project and material was not selected for all components, these costs were still unknown at the end of the project. Production quantity, which was not considered during the project, is likely to affect costs and may also affect the chosen manufacturing processes listed in Appendix S.

In addition, problems may arise in the newly developed and untested components once being subject to actual use rather than virtual analysis.

Real life data, for instance pressure between the back of a user and the backrest, could have created more accurate finite element simulations. In addition, dedicating more time to numerical analysis would have enabled more extensive experimenting with mesh refinement to validate results.

9.3 Further Work

At the end of the project, following activities remained to finalize the working chair:

- The maximum stress found in the hinge during analysis (chapter 7.1.4) should be further investigated.
- Material must be selected for vacuum formed plastic parts and remaining metal parts. Material selection should be based on strength analysis and manufacturing process.
- Fastening elements such as bolts, nuts, threaded holes and possibly weld nuts must be defined.
- Padding for the backrest and seat must be designed.

A full scaled prototype should be built in order to:

- Test if the working chair is comfortable and whether the attempts to follow theories regarding ergonomics have been successful.
- Test if the working chair is convenient for its intended everyday use.
- Measure real life data for more accurate strength analysis.

It must also be ensured that the working chair fulfills all laws and regulations regarding medical devices mentioned in chapter 1.1.6.

Once the working chair is finished, accessories, such as waist belt and straps for fixating the feet of the user, are intended to be developed in order to expand the target group. However, this can likely be done after the initial product has been introduced to the market.

References

[1] fysionord.se. 2019. *Krabat Jockey>Dokumentation*. [ONLINE] Available at: https://www.fysionord.se/produkter/krabat-jockey/dokumentation-34005222. [Accessed 22 January 2019].

[2] vardgivare.skane.se. 2016. *Förekomst av smärta, fatigue och undernäring hos vuxna med cerebral pares*. [ONLINE] Available at: https://vardgivare.skane.se/siteassets/1.-vardriktlinjer/habilitering/fou-rapporter/2016/fourapport-2016nr07.pdf. [Accessed 22 January 2019].

[3] cdc.gov. 2012. *Anthropometric Reference Data for Children and Adults: United States, 2007–2010*. [ONLINE] Available at: https://www.cdc.gov/nchs/data/series/sr_11/sr11_252.pdf. [Accessed 22 January 2019].

[4] nettdoktor.no. 2018. *Jenters høyde og vekt i forhold til alder*. [ONLINE] Available at: https://www.nettdoktor.no/helseraad/fakta/jentervekstttabell.php. [Accessed 22 January 2019].

[5] teachmeanatomy.info. 2018. *THE HIP JOINT*. [ONLINE] Available at: https://teachmeanatomy.info/lower-limb/joints/hip-joint/. [Accessed 22 January 2019].

[6] body-motion.co.uk. 2019. *Improve Your Sitting Posture*. [ONLINE] Available at: https://body-motion.co.uk/injuries/postural-pain/improve-your-sitting-posture/. [Accessed 22 January 2019].

[7] aimphysio.com.au. 2019. *The Importance of Ergonomics in the Office*. [ONLINE] Available at: http://aimphysio.com.au/importance-ergonomics-office/. [Accessed 22 January 2019].

[8] verywellhealth.com. 2019. Anatomy of the Iliac Crest. [ONLINE] Available at: https://www.verywellhealth.com/iliac-crest-definition-3120351. [Accessed 24

May 2019].

[9] www.amazon.com. 2019. *Bambach Saddle Seat*. [ONLINE] Available at: https://www.amazon.com/Bambach-Saddle-Seat/dp/B00079H9FS. [Accessed 22 January 2019].

[10] Wemmenborn, C. (2019) Interviewed by Ludvig Larsson, 9 January.

[11] Elam, K., 2001. *Geometry of Design-Studies in Proportions and Composition*. 1st ed. New York: Princeton Architectural Press.

[12] riksdagen.se. 1993. *Lag (1993:584) om medicintekniska produkter*. [ONLINE] Available at: https://www.riksdagen.se/sv/dokument-lagar/dokument/svensk-forfattningssamling/lag-1993584-om-medicintekniska-produkter_sfs-1993-584. [Accessed 22 January 2019].

[13] lakemedelsverket.se. 2014. *Vägen till CE-märket*. [ONLINE] Available at: https://lakemedelsverket.se/malgrupp/Foretag/Medicinteknik/Vagen-till-CE-market/. [Accessed 22 January 2019].

[14] tuv.com. 2019. *Safety standards for wheelchairs and mobility scooters*. [ONLINE] Available at: https://www.tuv.com/content-media-files/master-content/services/products/1319-tuv-rheinland-wheelchair-and-mobility-scooter-testing/tuv-rheinland-wheelchair-leaflet-en.pdf. [Accessed 22 January 2019].

[15] EUROPEISKA GEMENSKAPERNAS OFFICIELLA TIDNING. 1993. *RÅDETS DIREKTIV 93/42/EEG*. [ONLINE] Available at: https://eur-lex.europa.eu/legal-content/SV/TXT/PDF/?uri=CELEX:31993L0042&from=EN. [Accessed 22 January 2019].

[16] lakemedelsverket.se. 2003. *Läkemedelsverkets föreskrifter om medicintekniska produkter*. [ONLINE] Available at: https://lakemedelsverket.se/upload/lvfs/LVFS_2003-11.pdf. [Accessed 22

January 2019].

[17] lakemedelsverket.se. 2014. *Registrering*. [ONLINE] Available at: https://lakemedelsverket.se/malgrupp/Foretag/Medicinteknik/Registrering/. [Accessed 22 January 2019].

[18] iso.org. 2014. *ISO 7176-1:2014*. [ONLINE] Available at: https://www.iso.org/standard/56817.html. [Accessed 22 January 2019].

[19] fysionord.se. 2019. Krabat Jockey Lite. [ONLINE] Available at: https://www.fysionord.se/produkter/krabat-jockey-lite-33207296. [Accessed 24 May 2019].

[20] leckey.com. 2012. PAL classroom Seat. [ONLINE] Available at: https://www.leckey.com/media/1551/pal_brochure_new_2012.pdf. [Accessed 24 May 2019].

[21] eurovema.com. 2019. Eurovema Creates mobility and ergonomics. [ONLINE] Available at: http://www.eurovema.com/en-gb/pdf/product_catalogue.pdf. [Accessed 24 May 2019].

[22] sunrisemedical.no. 2018. Real 9000 plus. [ONLINE] Available at: https://www.sunrisemedical.no/produkter/andreprodukter/real. [Accessed 24 May 2019].

[23] vela.eu. 2019. VELA Hip Hop 100. [ONLINE] Available at: https://www.vela.eu/media/com_reditem/files/customfield/75/23a87255fdc766113c99bcbe56a57a8fbae1a87a2c620846801947fb6986c4bb.pdf. [Accessed 24 May 2019].

[24] Richard G. Snyder. 2019. *ANTHROPOMETRY OF INFANTS,CHILDREN, AND YOUTHS TO AGE 18 FOR PRODUCT SAFETY DESIGN*. [ONLINE] Available at: http://mreed.umtri.umich.edu/mreed/downloads/anthro/child/Snyder_1977_Chil

d.pdf. [Accessed 23 January 2019].

[25] Pheasant, S., 2006. *Bodyspace*. 3rd ed. Boca Raton: Taylor & Francis.

[26] 3dcontentcentral.com. 2014. 3D Human Model Child 8-9 year P95 Sitting. [ONLINE] Available at: http://www.3dcontentcentral.com/download-model.aspx?catalogid=10260&id=496588. [Accessed 24 May 2019].

[27] grabcad.com. 2014. caster 50mm. [ONLINE] Available at: https://grabcad.com/library/caster-50mm-1. [Accessed 24 May 2019].

[28] grabcad.com. 2014. cross for office chair 4. [ONLINE] Available at: https://grabcad.com/library/cross-for-office-chair-4-1. [Accessed 24 May 2019].

[29] grabcad.com. 2014. Human Skeleton. [ONLINE] Available at: https://grabcad.com/library/human-skeleton-1. [Accessed 24 May 2019].

[30] studentcommunity.ansys.com. 2019. Numerical Problem Size limits Student License. [ONLINE] Available at: https://studentcommunity.ansys.com/thread/numerical-problem-size-limits-student-license/. [Accessed 24 May 2019].

[31] engineeringtoolbox.com. 2010. Factors of Safety. [ONLINE] Available at: https://www.engineeringtoolbox.com/factors-safety-fos-d_1624.html. [Accessed 24 May 2019].

[32] daroproducts.co.uk. 2015. What plastics do we use for plastic vacuum forming?. [ONLINE] Available at: http://www.daroproducts.co.uk/plastics-for-plastic-vacuum-forming/. [Accessed 24 May 2019].

Appendix A Current Solutions

Commentary regarding advantages (+) and disadvantages (-) with existing solutions were made by Charlotte Wemmenborn and Anders Larsson at Fysionord AB. These observations were made while selling and repairing aids, as well as through communication with users. The word “relative” refers to the other mentioned chairs:

- **Krabat Jockey Lite:**

  +Looks good.

  +Relatively good sitting position for children with mild physical disabilities.

  +Modular; multiple sizes all using the same wheels but different seats.

  +Good curvature of the backrest, providing lateral stability.

  -Back rest subject to fatigue.

  -Hip angle not ideal due to positioning of footrest.

  -Hard to enter and exit independently due to the front shape of the seat.

  -User must exit chair for sitting height to be adjusted.

  -Height of footrest adjusted separately from seat.

  -No central brake, separate brake mechanism for each of the 5 wheels.

  -No armrests (could have facilitated entering and exiting of the chair).

  -The tilt mechanism of the seat is too easily accessible, leading to accidental forward tilt of the chair, which in turn can lead to the user falling.

- **Leckey PAL Size 4:**

  +The user is seated in the same height as other children.

  -Relatively unsuitable for sitting at external table when eating or playing.

  -Inadequate personalization/adjustment.

  -Does not offer enough guiding of the user into a sustainable sitting position.

- **Euroflex ABC SitRite:**

  +Central brake, rear wheels are locked using a lever.

  +Removable armrests.

  +Removable footrest.

  +Large selection of accesories.

  +Electric/automatic sitting height adjustment.

  +The seat can be tilted forward to achieve desired hip flexion angle.

  +Joint in undercarriage enables ground contact with all 4 wheels on uneven surfaces.

  -Heavy; minimum 20 kg.

-Posterior pelvic tilt, leading to exaggerated kyphosis, curved shoulders and bent neck.
-Not good looking.

- **Mercado Real 9000 Plus:** (Similar to Euroflex)
  +The curvature of seat and backrest provides lateral support and good positioning.
  +Central brake.
  -As a side effect of the brake system the chair rotates when subject to uneven weight distribution from the user.
  -Heavy
  -Not visually appealing.
- **•Vela Hip Hop 100:** (similar to Mercado and Euroflex)
  +Relatively light weight.
  +Relatively good looking.

Following non-medical products were studied as inspiration:

- **Bambach:**
  +Good looking
  +Light weight
  +Hip angle ok…
  -…but counteracted by forward foot position.
  -Rear shape of the seat reduces the ability to find a natural position of the pelvis.
  -Backrest lacks curvature for lateral support.
- **Salli:** (Similar to Bambach)
  +Adjustable seat width.
  -Possibly too much pressure on thighs.
- **Stokke Balans:**
  +Good looking
  +Good leg position.
  +Simple construction.
  -No height adjustment.
  -No backrest.
  -No wheels for moving around.

Appendix B Krabat Jockey Lite Undercarriage

Undercarriage from Krabat Jockey Lite chair:

Weighing the height adjustment component:

Weighing wheels, the star shaped “legs” and gas spring together:

Mass for the height adjustment component as well as for wheels, legs and gas spring together, can be seen in the table below.

Component:	**Mass:**
Height adjustment component	2.1 kg
Wheels, legs and gas spring	3,15 kg

Appendix C Time Plan

The blue bars refer to the nine main steps of the project, which answer to one chapter each in the report.

The green bars refer to sub-steps needed to fulfill the main steps.

The black cells show deadlines.

Week / Task	2	3	4	5	6	7	8	9	10	11	12	13	14	15	16	17	18	19	20	21	22	23	24
1-4 Preliminary Study																							
Pilot Study																							
Fuctions & System Boundary																							
Requirement Specification																							
5 Concept Generation																							
Foot- /Legrest Concept																							
Seat Concept																							
Backrest Concept																							
6 Detailing																							
7-8 FEM & Material Selection																							
Ansys Course, Gothenburg																							
FEM																							
Material Selection & 3D Print																							
9 Conclusions																							
Delivery, May 5																							
Deadline, May 11																							

Appendix D Objectives Tree Diagram

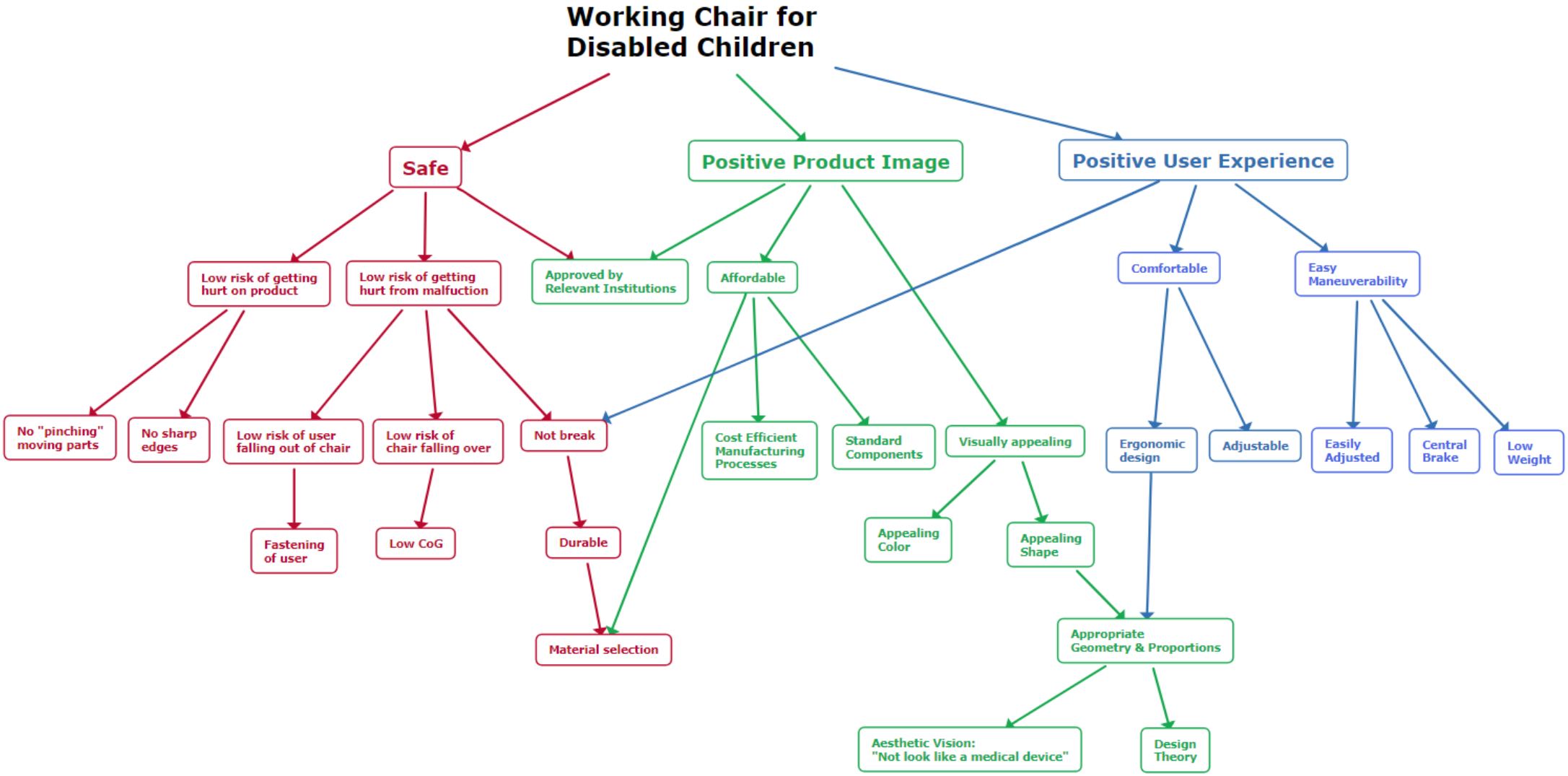

Appendix E Morphological Matrix for Foot-/Legrest

The same morphological matrix as in chapter 5.1.6 but without lines to facilitate reading.

Fastening	**Support Area**	**Knee Angle**	**Femur Length**	**Knee height**
Front of seat	Bar	Hinge at fastening		Translation along shin
Under seat	Flat foot pad	↔ translation	↔ translation	↕+↔ translation
Back of seat	Curved foot pad	Curved foot pad		
Undercarriage	Shin pad	↕ translation		

Appendix F Foot-/Legrest Concepts

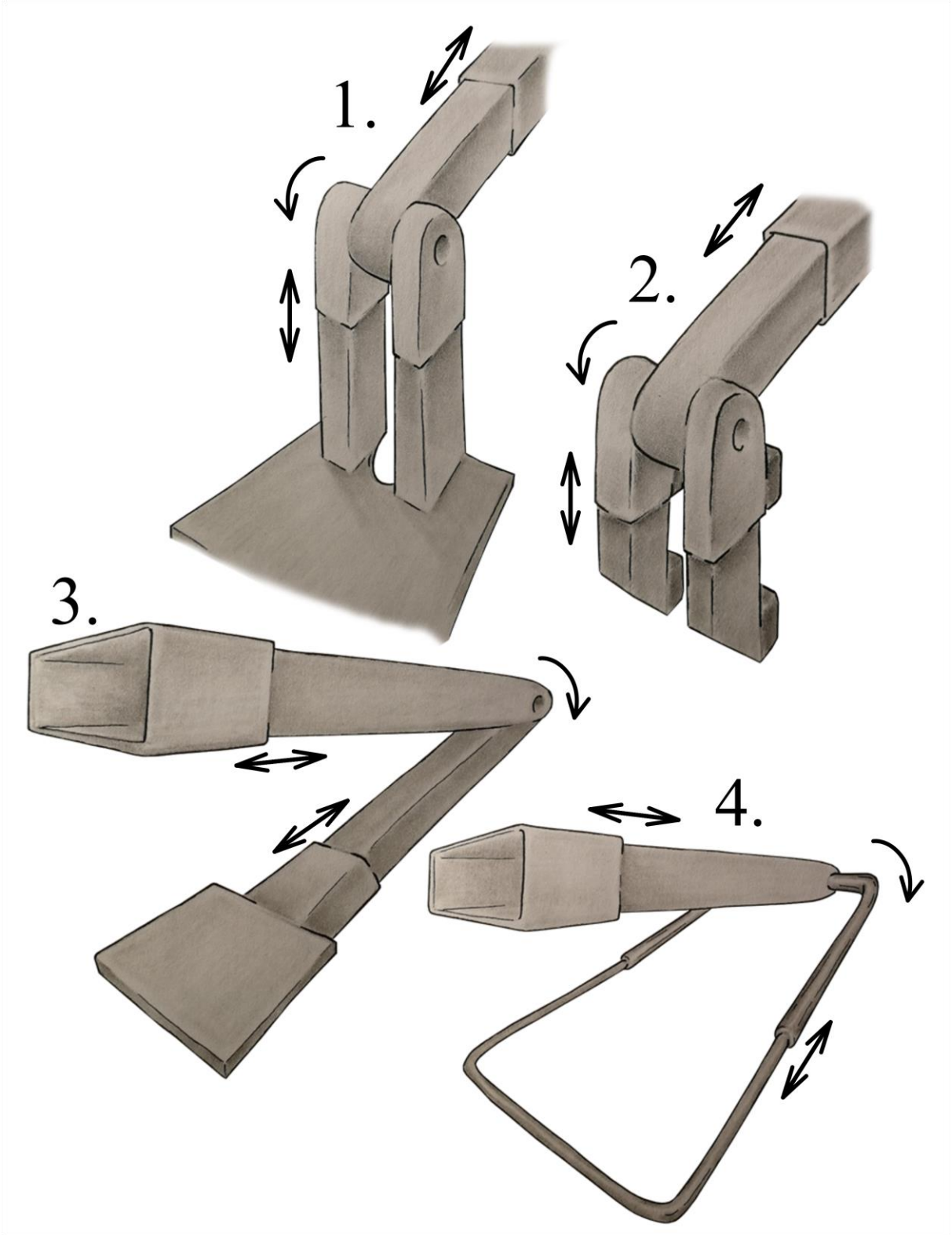

5.

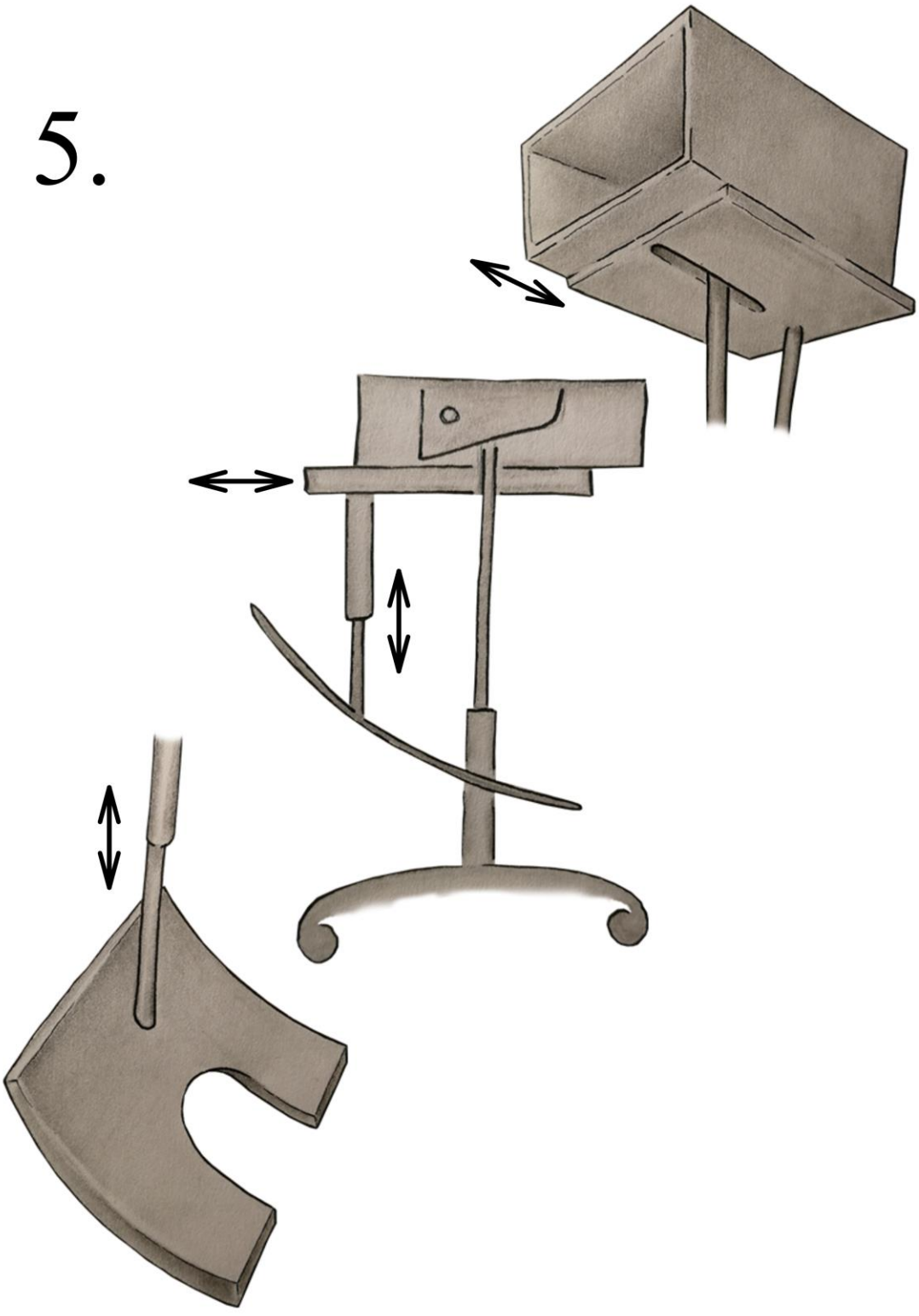

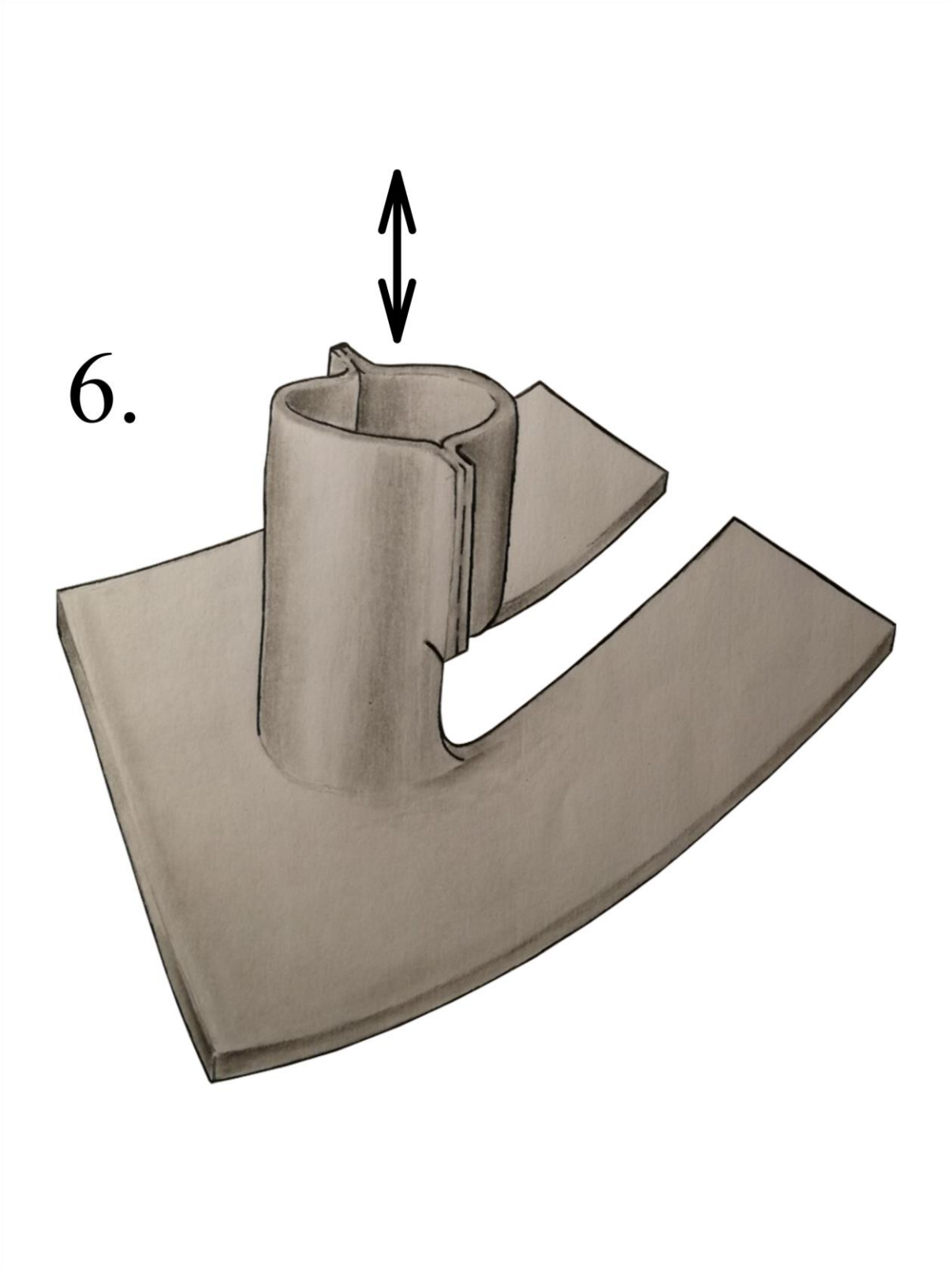
6.

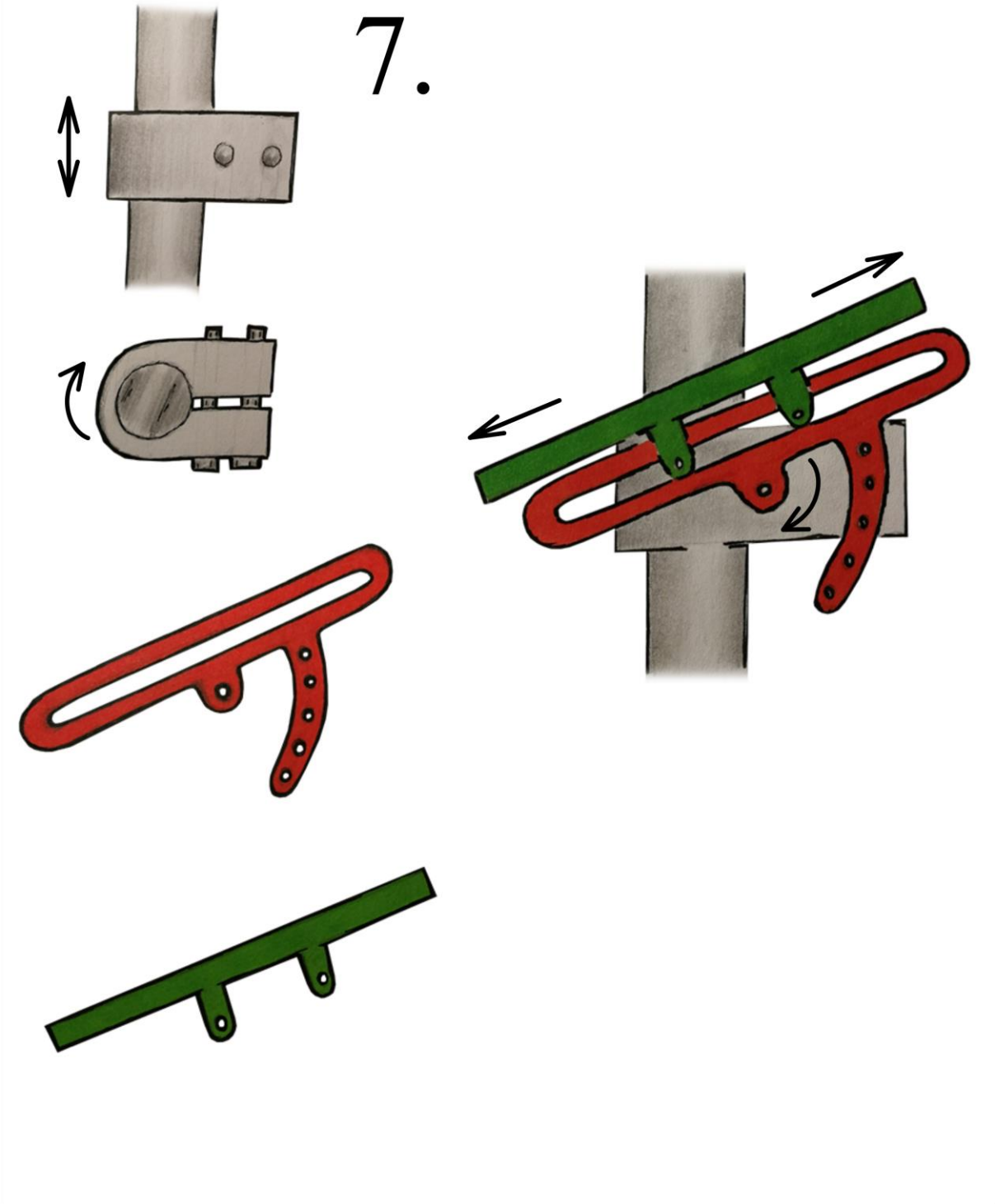
7.

Appendix G Concept 1 → Concept 3

Sketches and pictures of the physical prototype showing the development from concept 1 (left) to the modified concept 3 (right).

Appendix H Development of Final Seat Concept

Development of the final seat concept from basic geometric shapes shown in two-point perspective.

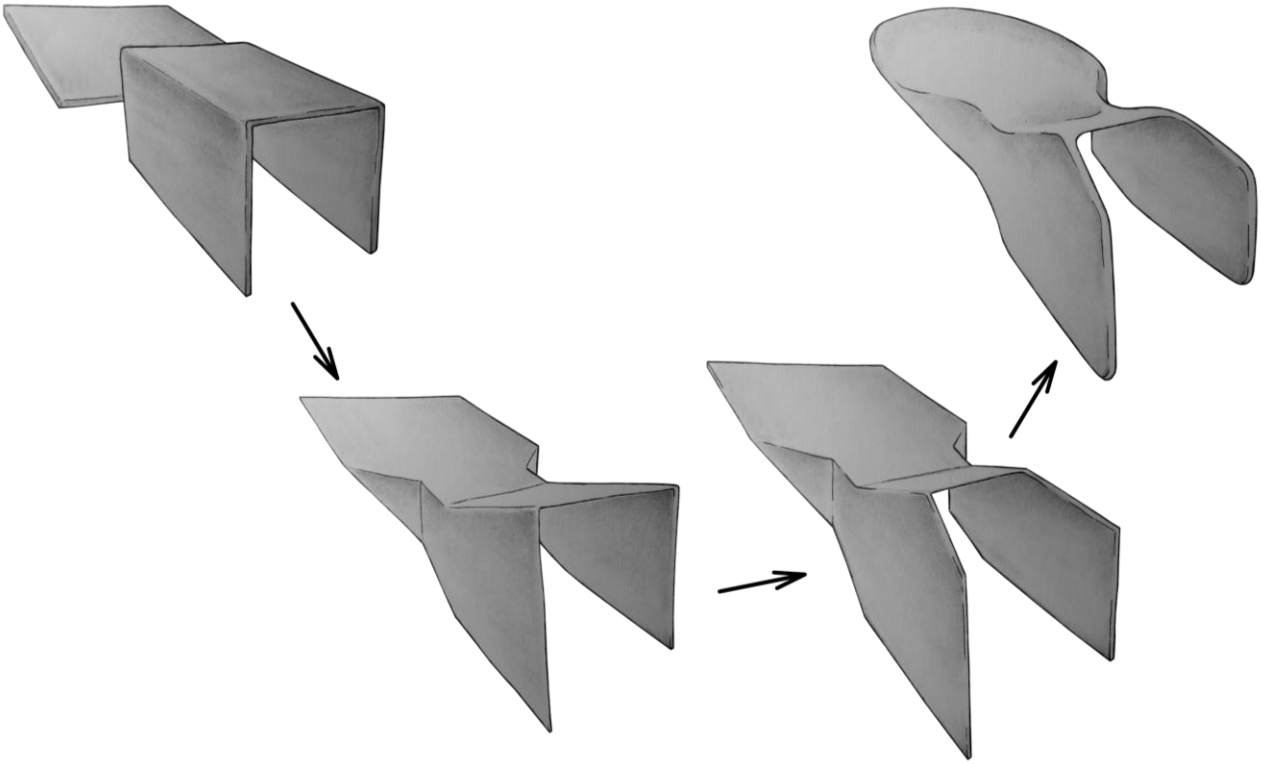

1. The seat was initially based on two geometric shapes; a plane and a box.
2. Material was removed to create space for the thighs of the user, linking together the plane and the box, creating more subtle angles and 15° hip abduction.
3. Excess material close to the knees of the user was removed.
4. Fillets were added for smoother round shapes.

The same process shown in 2D from the side (left) and from above (right).

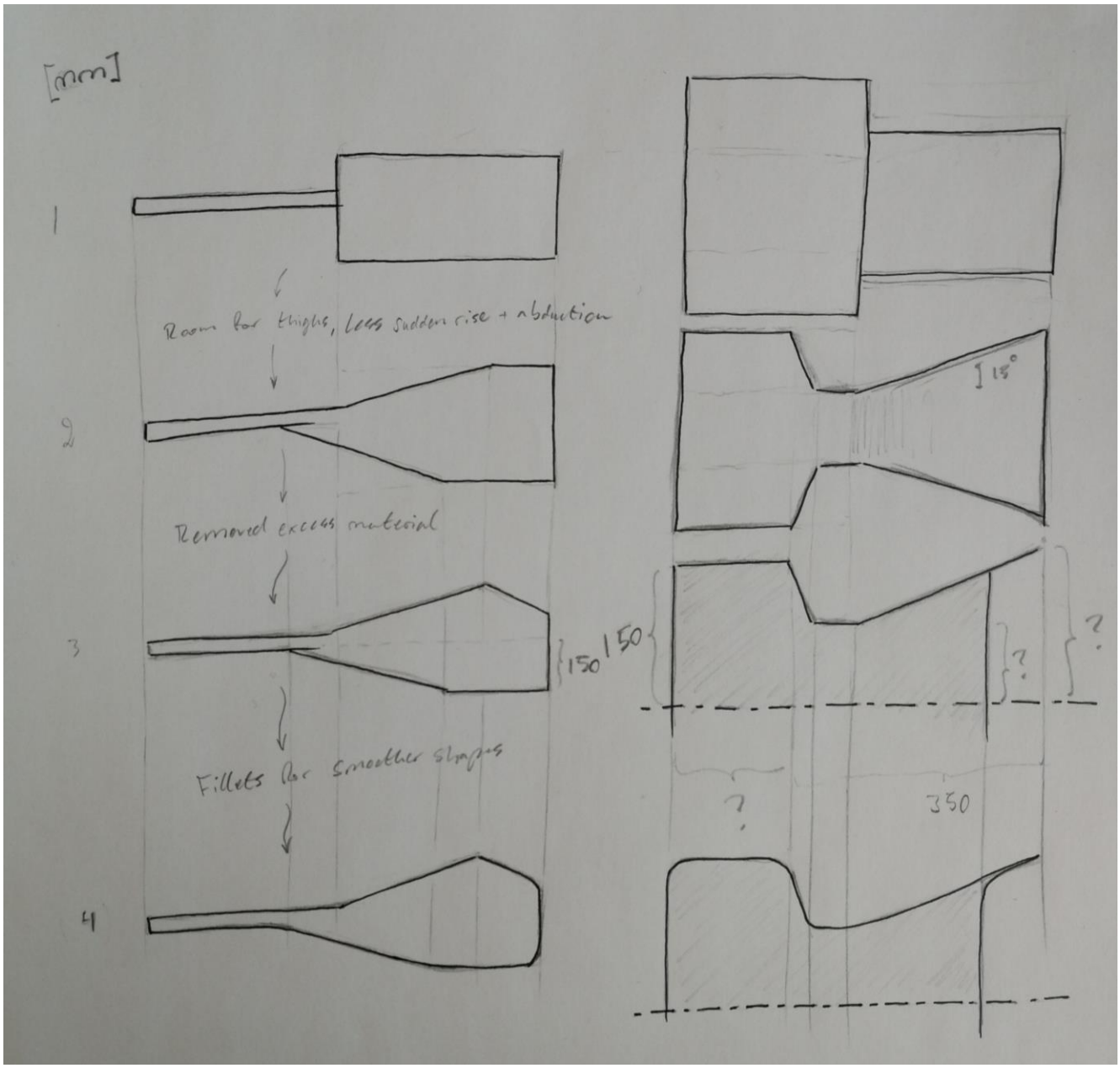
[mm]
1
Room for thighs, Less sudden rise + abduction
2
Removed excess material
3
150
150
Fillets for smoother slopes
4
15°
?
?
?
350

Appendix I Iterative Backrest Sketch Process

1. A slightly tapered rectangular shape reaching from the top of the iliac crests to the bottom of the scapulas.

2. The top and bottom of the initial shape were extended to support a longer part of the spine, without interfering with the pelvis or scapulas.

3. The uppermost kyphosis-like curve in step 2 was deemed to make the backrest less likely to fit differently sized users. Therefore, the protruding shape between the scapulas was removed, creating a more subtle hexagonal shape.

4. The initial taper was removed to allow place for the midsection of the user. Also, lateral support was added at the waist of the user.

5 The lateral support in step 4 was extended upwards, creating the final shape of the backrest.

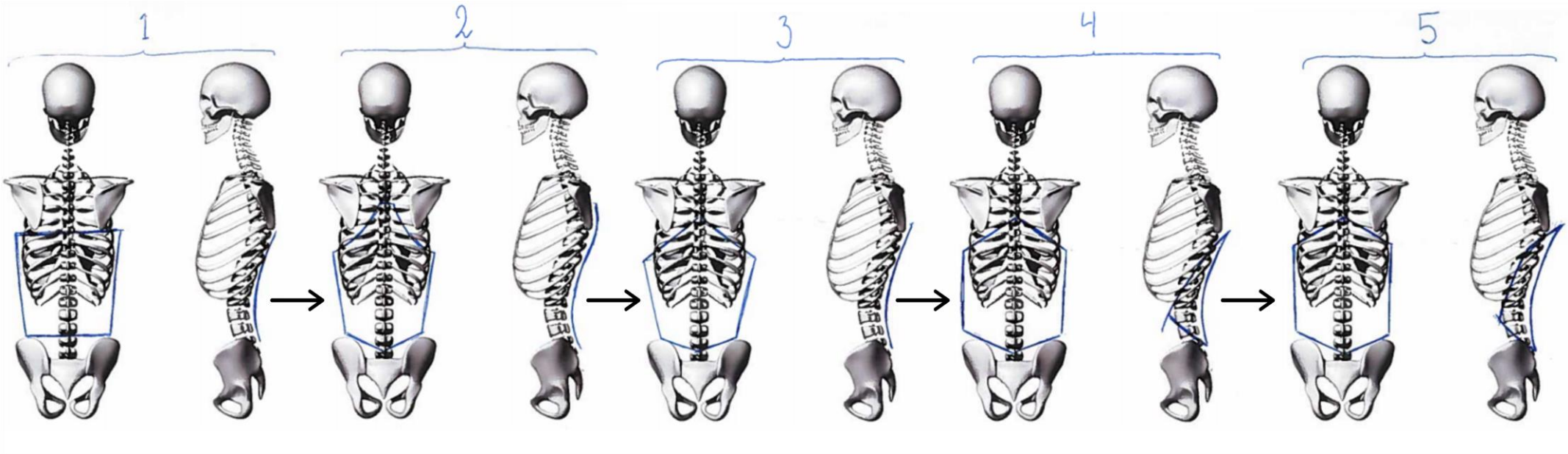

Appendix J Backrest Post Concepts

Seven combinations of post geometry 1-6 and height adjustment location A-C:

1B: A bent round pipe fastened to the backrest and height adjustment inspired by a medical crutch.
2A: An elliptic pipe with a slot for stepless height adjustment. The pipe is fastened to a cutout in the back of the backrest with a bolt.
4A: A bent strip of sheet metal with a slot for stepless height adjustment of the backrest, which is fixated by a bolt. This solution is intended to be fastened under the seat.
4B: Similar as 4A but divided into two parts, moving the height adjustment away from the backrest.
5A: A U-beam with trimmed off top end and similar height adjustment as A4.
5C: Bent sheet metal, fastened to backrest while the stepless height adjustment mechanism is found in the interface to the rest of the chair though two slots with corresponding bolts.
6A: Bent or welded sheet metal with the same functionality as 5A.

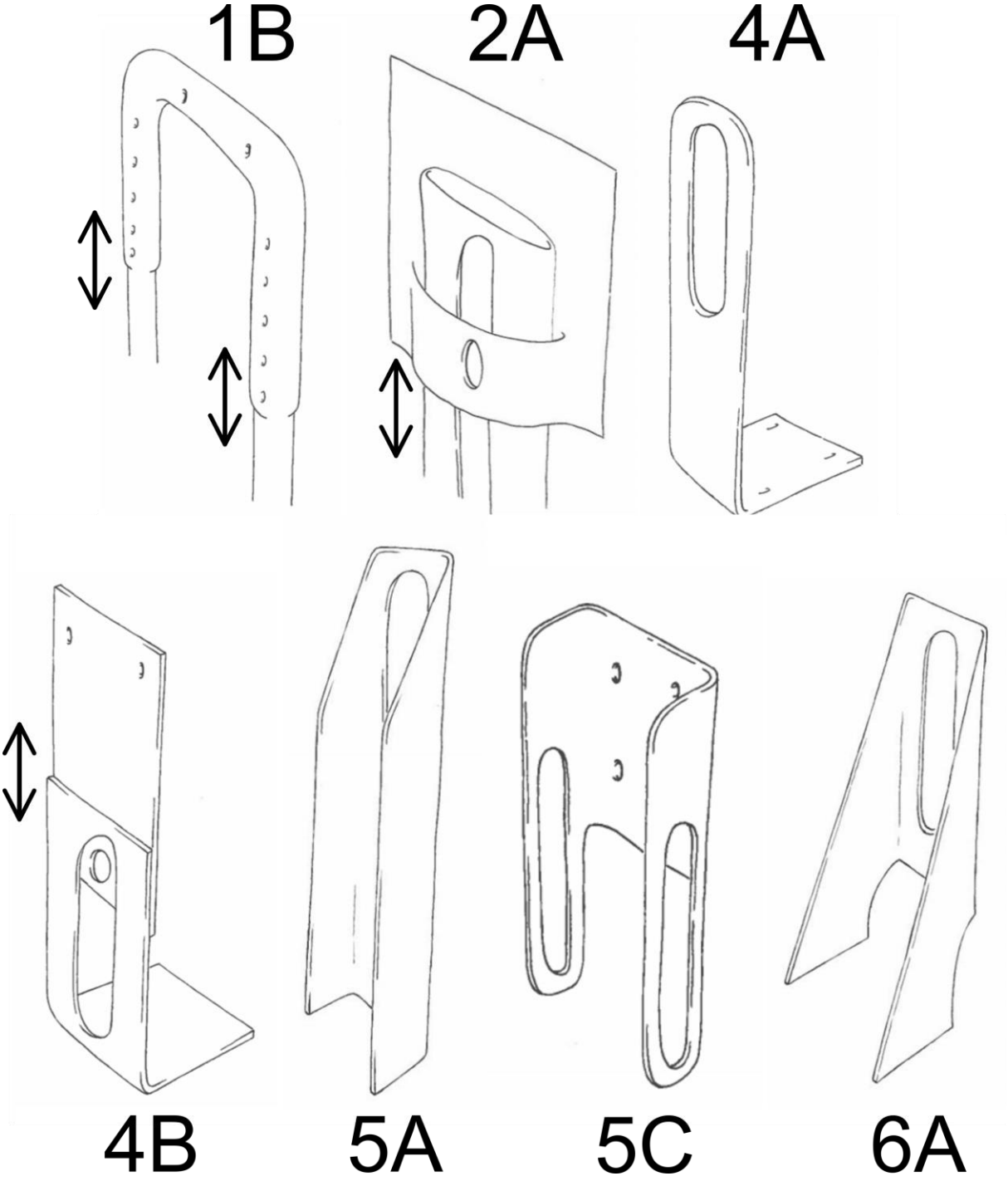
1B
2A
4A
4B
5A
5C
6A

Appendix K Friction Joint for Footpad Angle Fixation

3D model created in Inventor from measured dimensions.

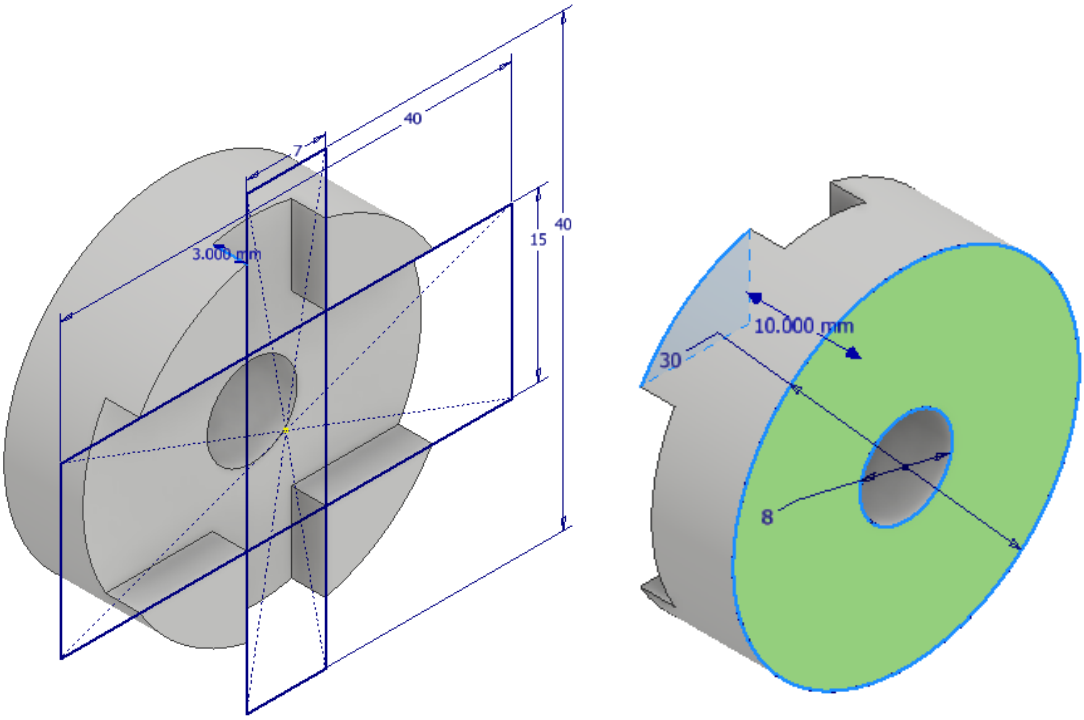

Appendix L Detailing of Plastic Parts and “Hub”

Description of how shapes were generated for plastic components intended for vacuum forming; footpad, seat and backrest. Followed by a description of the development of the sheet metal hub for fastening all modules of the chair.

a) Footpad Detailing

Footrest Iteration 1: An initial flat footpad was created based on the size and position of the feet of a model for anthropometrical validation scaled according to body dimensions listed in Table 6. However, when removing material to avoid interference with the undercarriage a weak link in the middle of the footpad appeared.

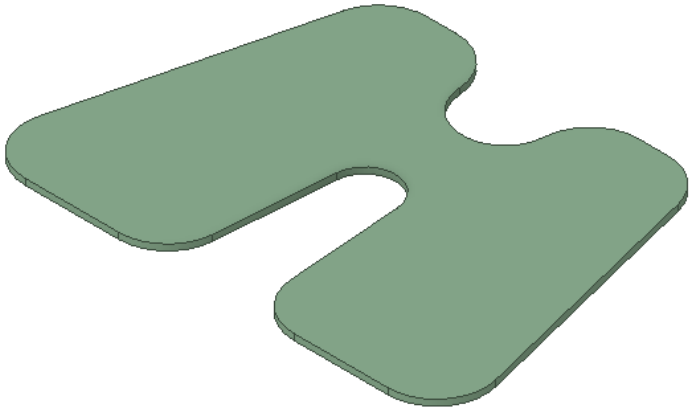

Footrest Iteration 2: The cutout in the front part of the footpad was replaced with a curved geometry.

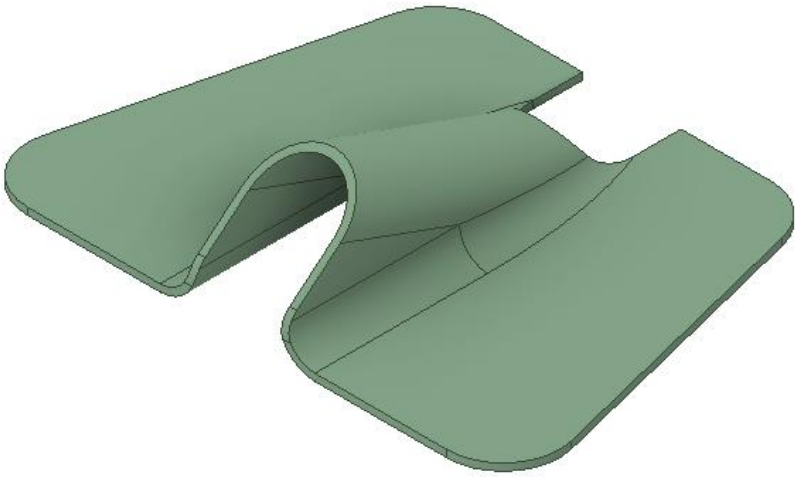

Footrest Iteration 3: Slots for fastening straps for fixating the feet of the user were added, as well as a slot for the strap adjusting the height of the footrest. A solution for fastening the footpad was added at its rear end.

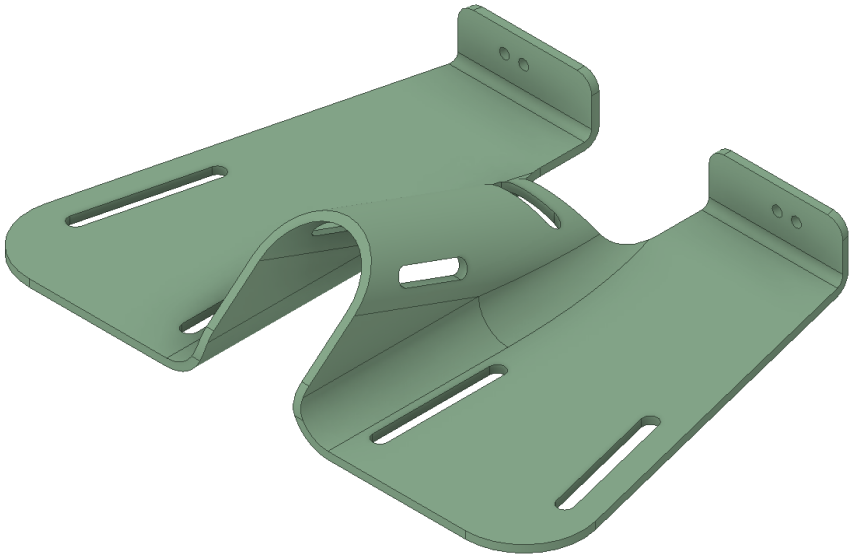

b) Seat Detailing

To include more potential users it was decided to increase the hip breadth to 300 mm when designing the rear part of the seat. It was deemed unlikely that this would cause problems for smaller users. An initial model of the seat was created in Inventor Professional 2018. It was then changed iteratively by testing it with a CAD model for anthropometrical validation

Seat Iteration 1: An initial seat was created from sketches and given desired dimensions. The total length of the seat, which was calculated through trigonometric expressions based on anthropometrical data and joint angles, was discover to be too large. It was also discovered that the most rear part of the seat was redundant and that the shapes close to the middle of the seat should be less angular to allow room for the thighs of the user.

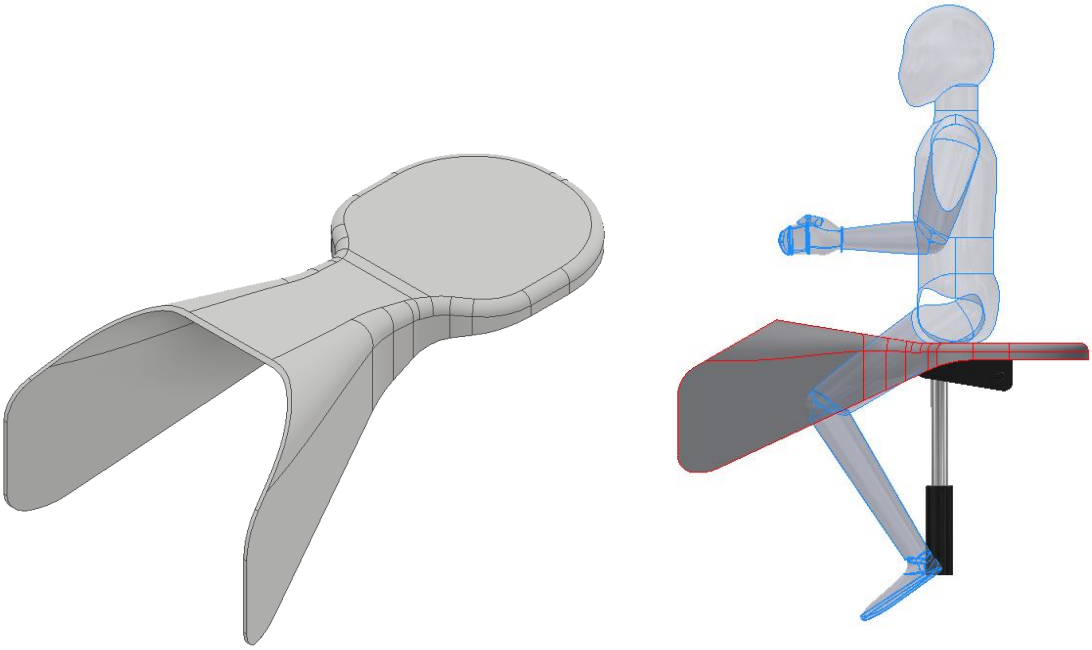

Seat Iteration 2: After adjusting the shape according to the discoveries in iteration 1, it was understood that the middle part of the seat should be narrower to fit smaller users.

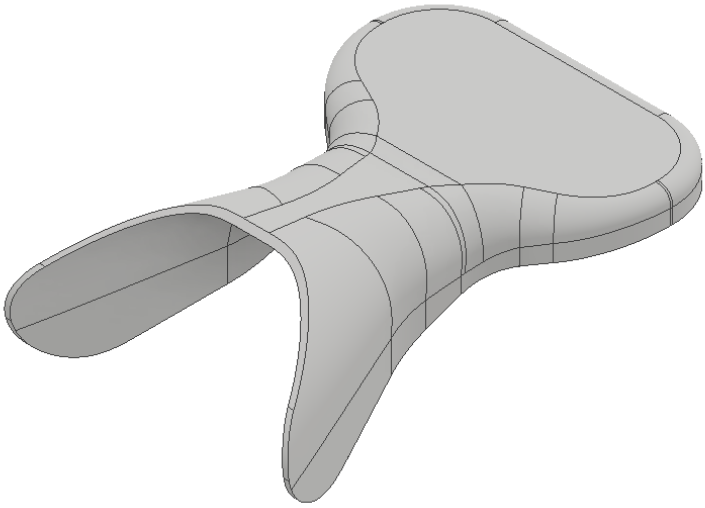

Seat Iteration 3: The narrow middle part of the seat complicates fastening to the undercarriage of the chair while keeping the users center of gravity securely within the support area offered by the chair. Also, reinforcement is needed for the seat to able of supporting the weight of the user. These two issues were addressed by adding a steel frame to the seat consisting of two hollow bars and sheet metal. The transitioning of the frame into a hub for all surrounding modules is described in d), later in this appendix.

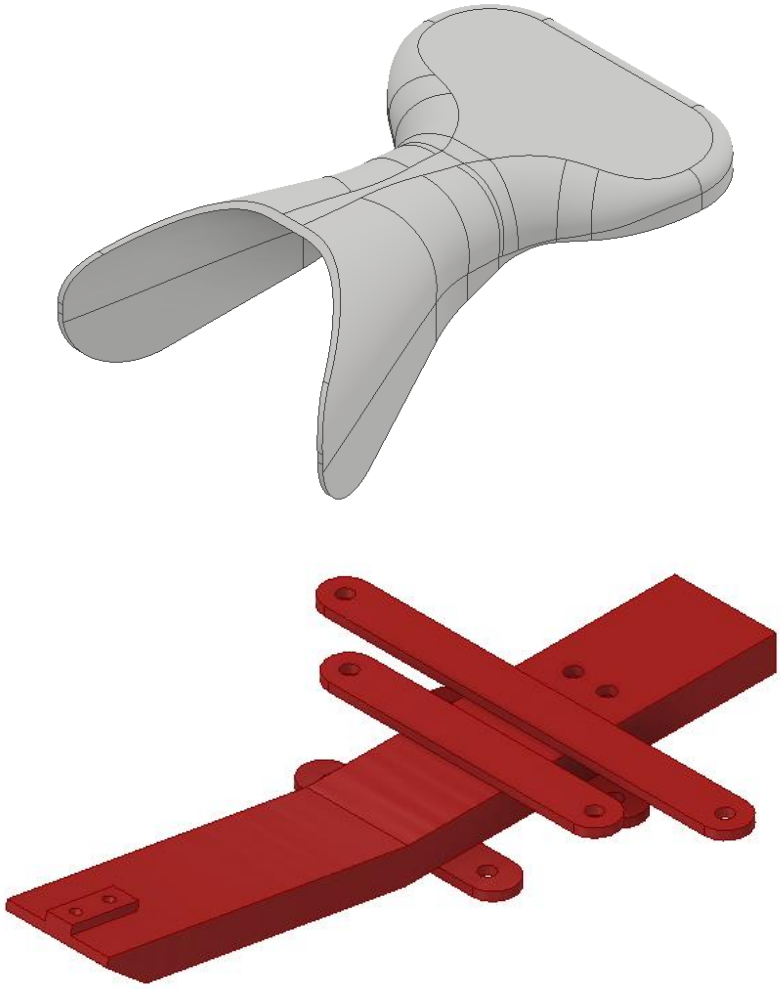

Seat Iteration 3: Holes were added in the seat for fastening on the reinforcement component. Holes were also added to make fastening of the backrest into the steel frame accessible, while a cutout was added to give space for the backrest post. Additional changes were made to the rear part of the seat to remove excess sitting area.

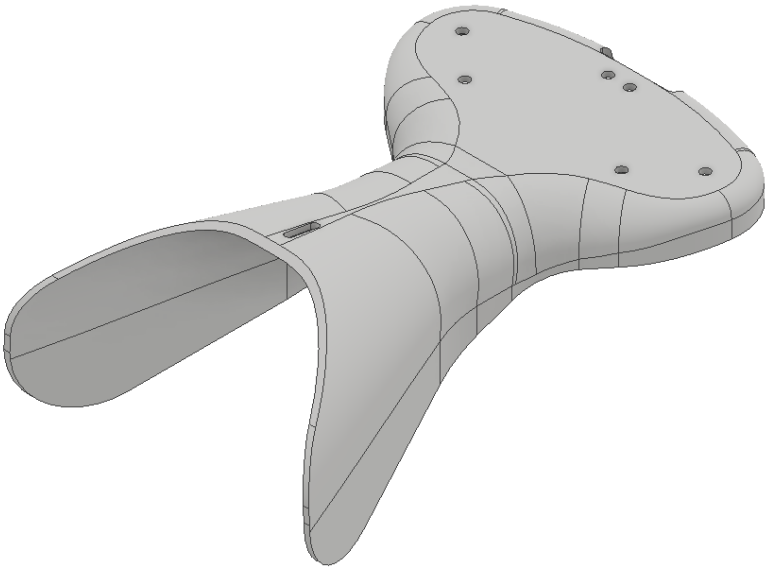

Seat Iteration 4: Cutouts were made in the rear part of the seat to enable fastening of a waist belt underneath it, using the bolts that fixates the seat itself onto the steel reinforcement frame.

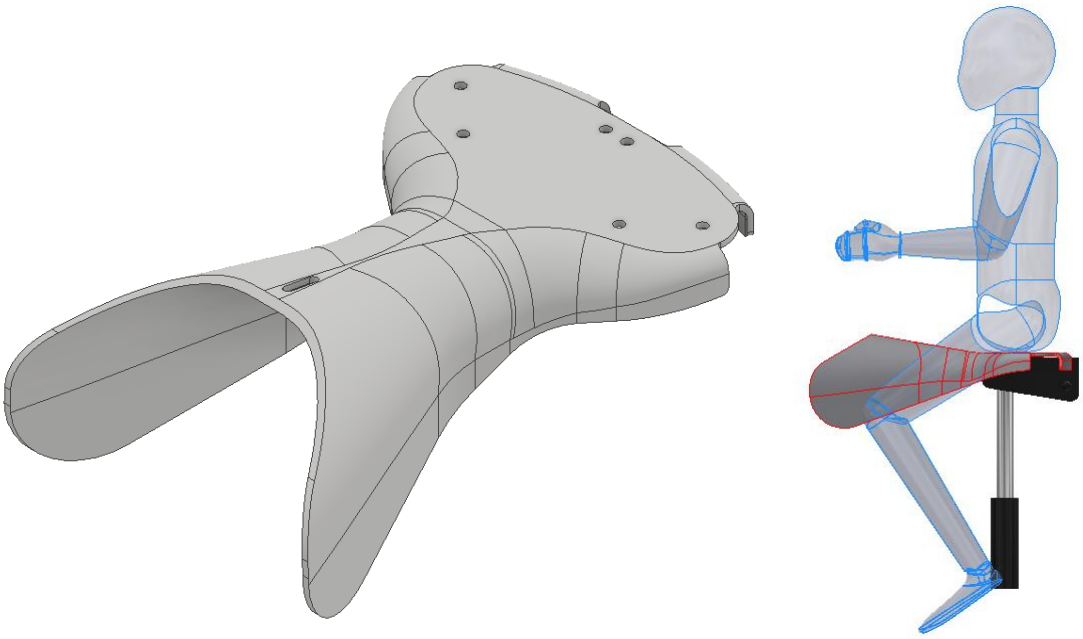

c) Backrest Detailing

The same CAD model of a skeleton that was used for sketching during the concept generation phase was used to generate an approximate spinal curvature for the backrest.

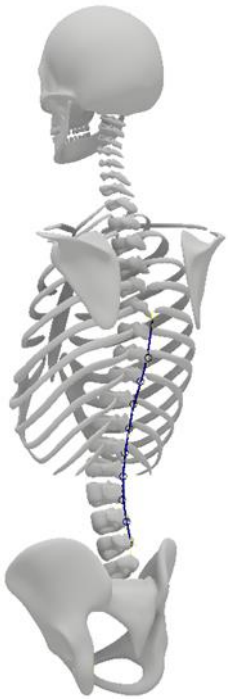

The curvature, originally sketched as an interpolating spline going through the most protruding part of each vertebra, was simplified to a b-spline within a control polygon with less control points to create a smoother curve. The curve was then extruded laterally into a surface to enable appropriate scaling with respect to the CAD-model for anthropometrical validation.

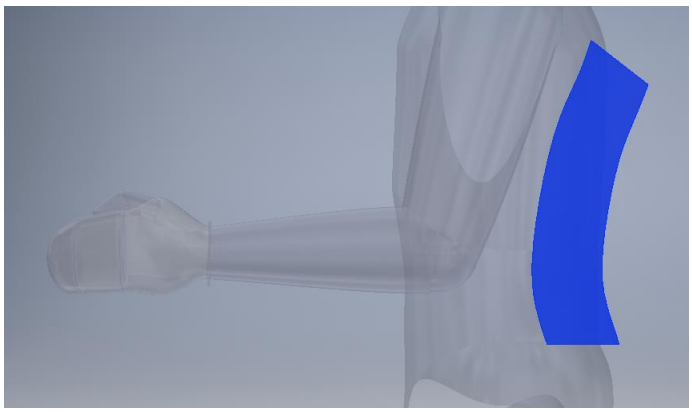

After scaling the spinal curvature of the backrest, the surface was deleted, only leaving the curve itself. Viewing the model from above, another curve was sketched and “sweeped” along the spinal curvature, creating a new, double curved surface. This was done arbitrarily to achieve lateral support. Viewing the model from the front, a hexagonal shape was cut out and thickened by 5 mm into a solid part.

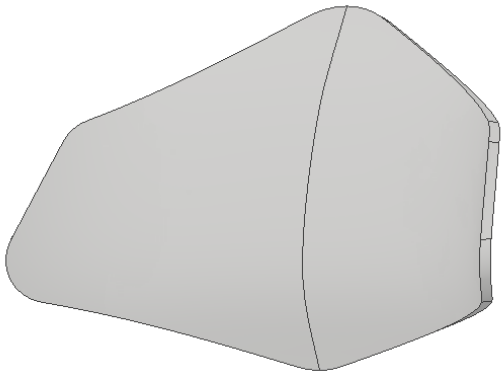

To enable an interface towards the backrest post, a cavity was created in the lower part of the backrest, intended for fastening of an external metal part that is in turn to be fastened to the post.

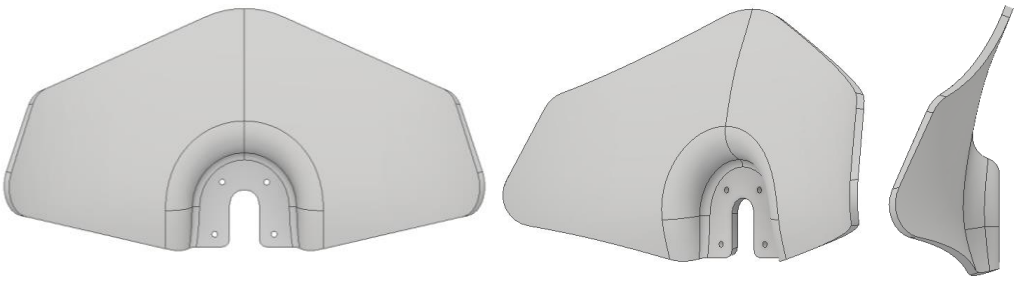

d) Development of the “Hub”

What was later to become the hub started solely as reinforcement for the seat and transitioned into fastening for other modules during the modeling process. The initial seat reinforcement consisted of two hollow bars with rectangular cross sections and five pieces of sheet metal welded together. It connected the flat surfaces on the underside of the seat to the height mechanism of the undercarriage while creating a distance between the seat and the height adjustment mechanism to avoid interference.

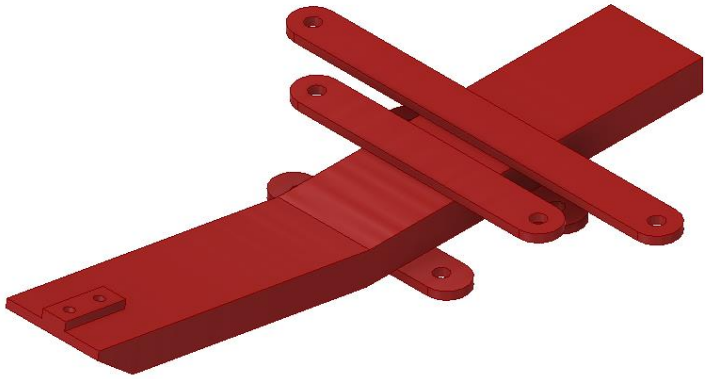

Two holes were added for fastening of the backrest post.

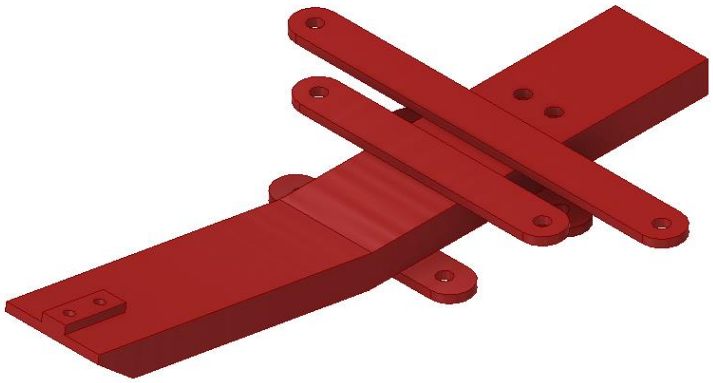

Another bar, placed vertically behind the height adjustment mechanism of the undercarriage, was added for fastening the hinges connecting the footrest.

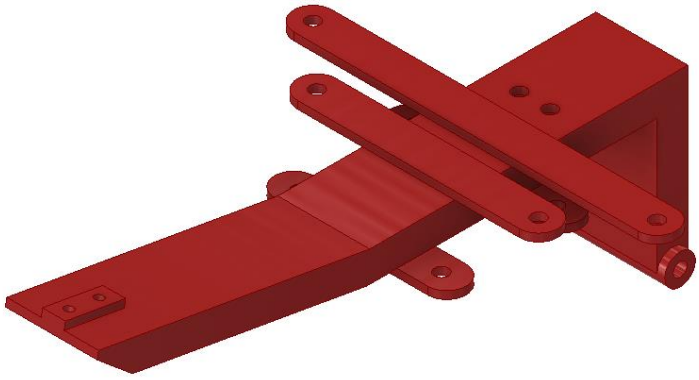

The two rear pieces of sheet metal were merged into a single bent piece.

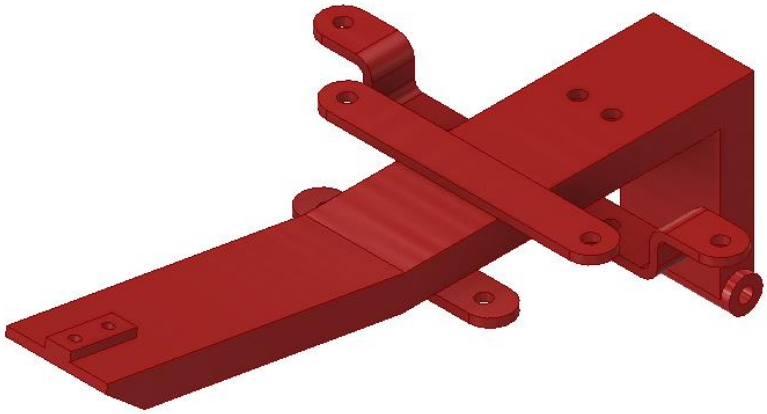

The component was redesigned to be made in bent sheet metal, eliminating all welds. The small protruding piece of sheet metal in the front was replaced with an external bushing. Fastening for the footrest height adjustment strap was added in the front.

Appendix M Height Adjustment Component

Main dimensions from measurements of the *Krabat Jockey Lite* height adjustment component and gas spring. Seen from the side, in isometric perspective and from above. The front of the component is facing left in all three views.

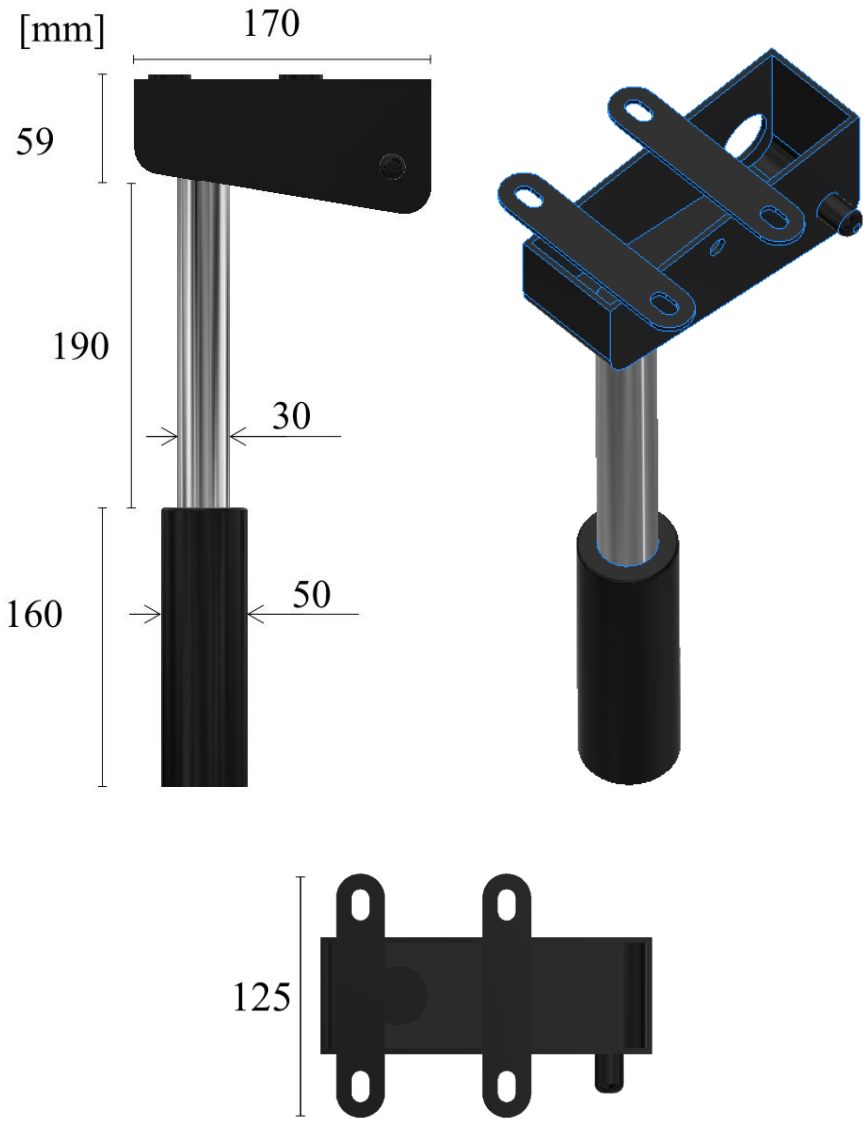

Appendix N Ansys Material Data

Screenshot of material data for Ansys pre-defined structural steel:

Properties of Outline Row 3: Structural Steel

	A	B	C	D	E
1	Property	Value	Unit		
2	Material Field Variables	Table			
3	Density	7850	kg m^-3		
4	Isotropic Secant Coefficient of Thermal Expansion				
6	Isotropic Elasticity				
7	Derive from	Young...			
8	Young's Modulus	2E+11	Pa		
9	Poisson's Ratio	0.3			
10	Bulk Modulus	1.6667E+11	Pa		
11	Shear Modulus	7.6923E+10	Pa		
12	Strain-Life Parameters				
20	S-N Curve	Tabular			
24	Tensile Yield Strength	2.5E+08	Pa		
25	Compressive Yield Strength	2.5E+08	Pa		
26	Tensile Ultimate Strength	4.6E+08	Pa		
27	Compressive Ultimate Strength	0	Pa		

Appendix O Numerical Analysis of the “Hub”

Additional images describing the 4 iterations of developing the hub, using the finite element method.

a) Hub Iteration 1

The difference in mesh from introducing virtual topologies:

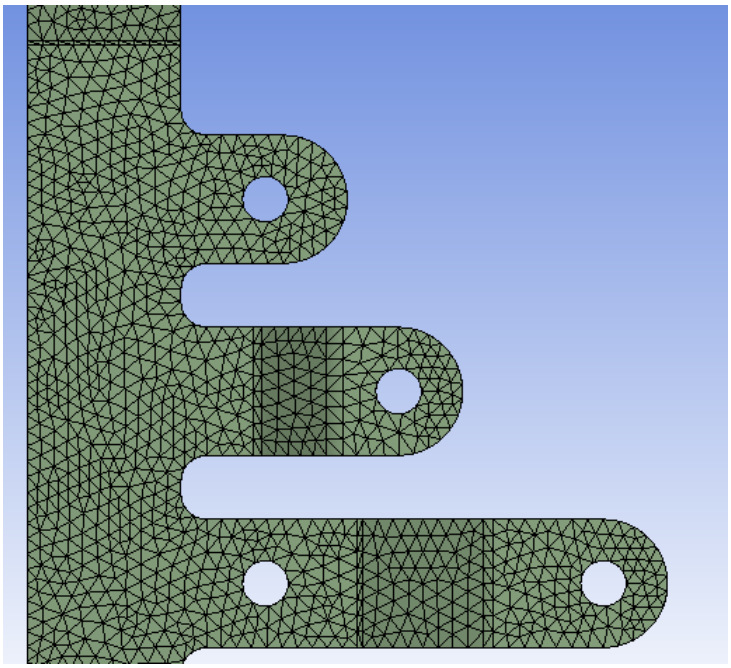

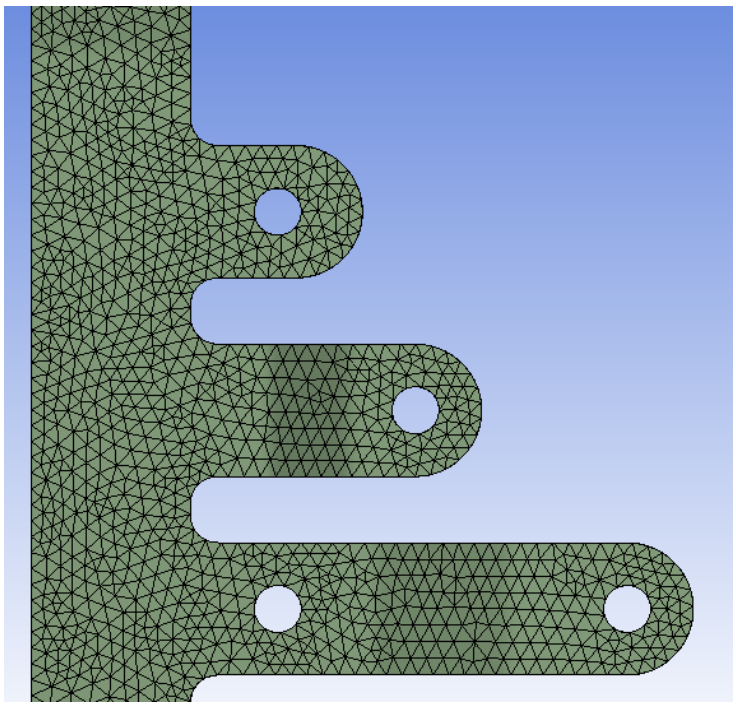

Additional images of the meshed model of the hub in iteration 1:

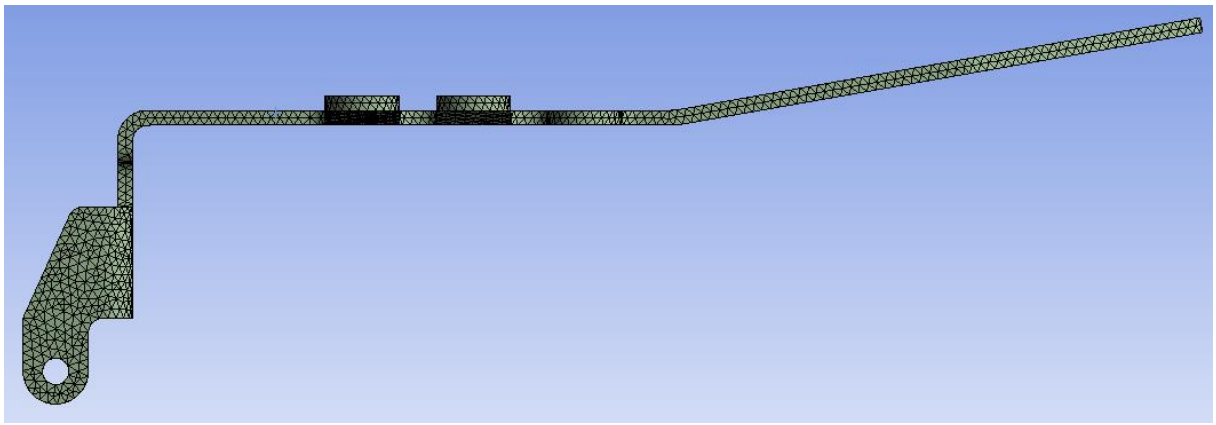

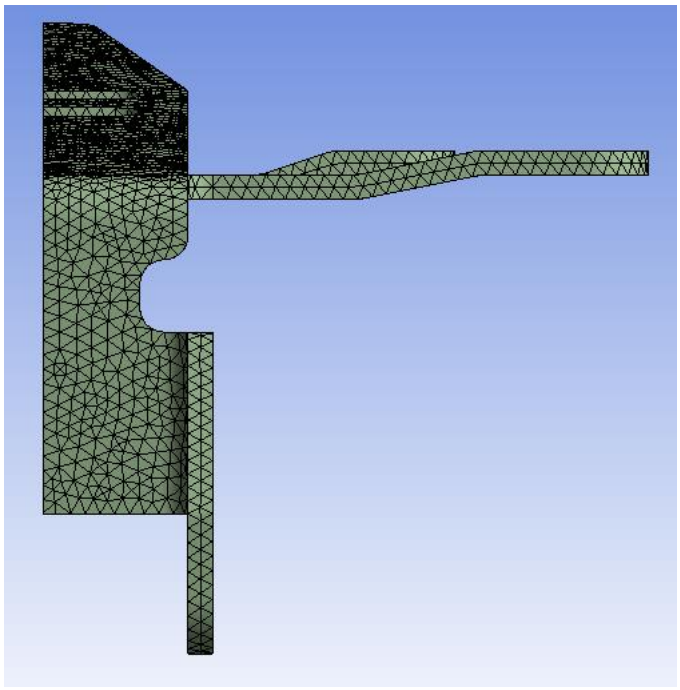

Equivalent stress distribution in the assembly used for validation of the use of a remote force to mimic moment from backrest. The backrest was hidden in the stress plot for visual purposes:
Element size: 3 mm, 136 993 nodes

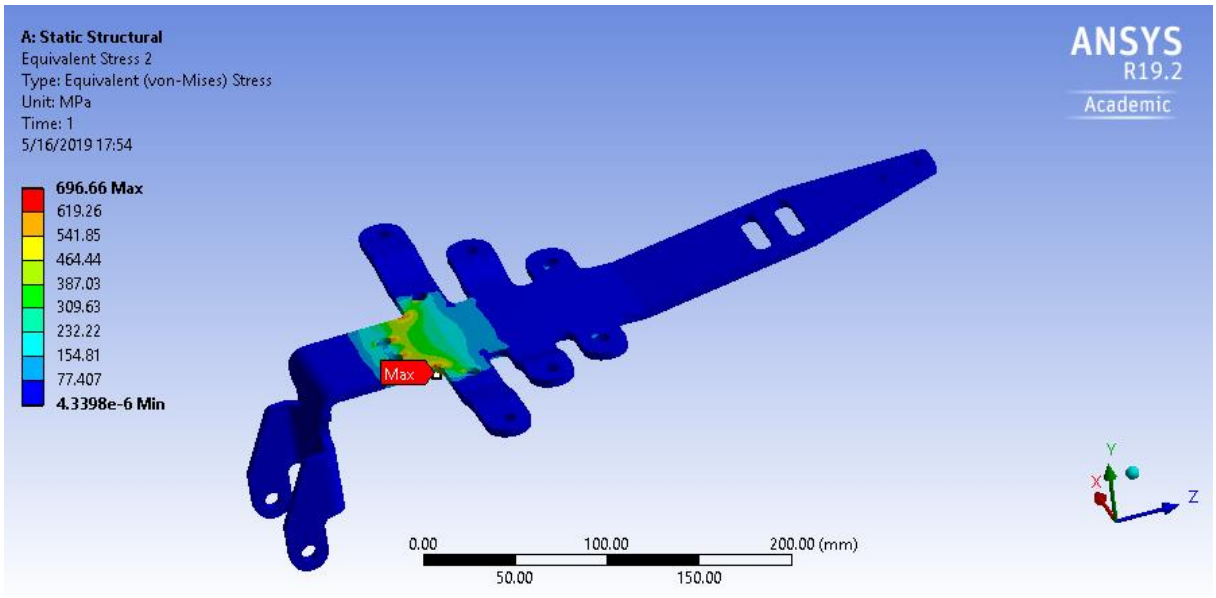

Stress plots of fillet contained in the refined area:

Refined element size 2 mm:

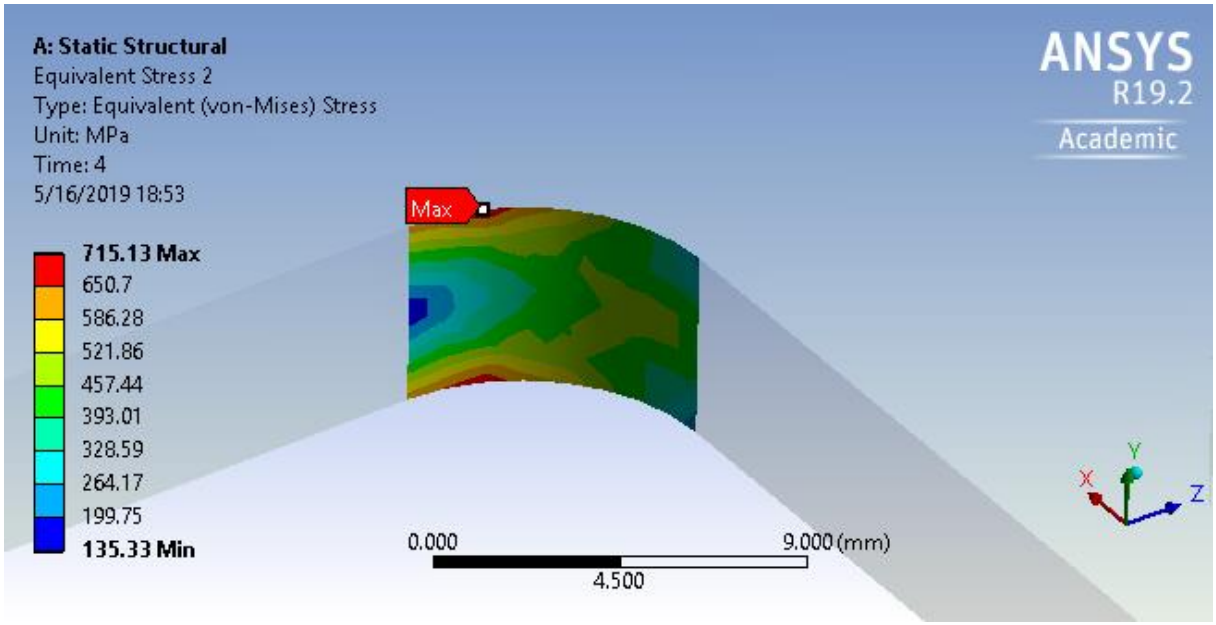

Refined element size 1 mm:

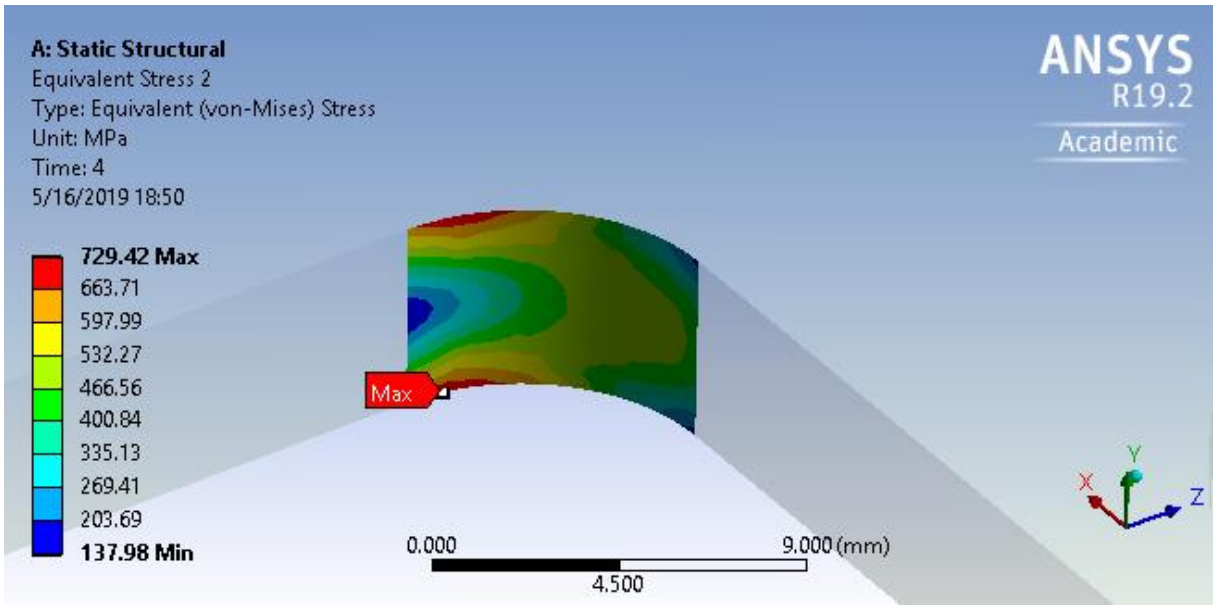

Refined element size 0.7 mm:

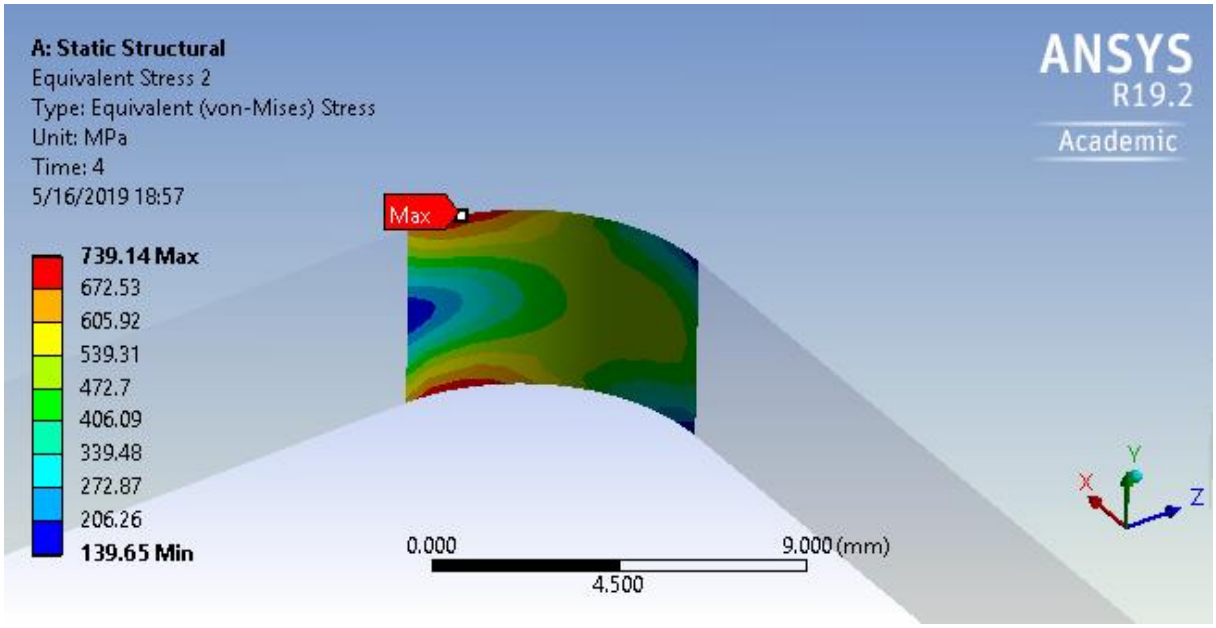

Refined element size 0.4 mm:

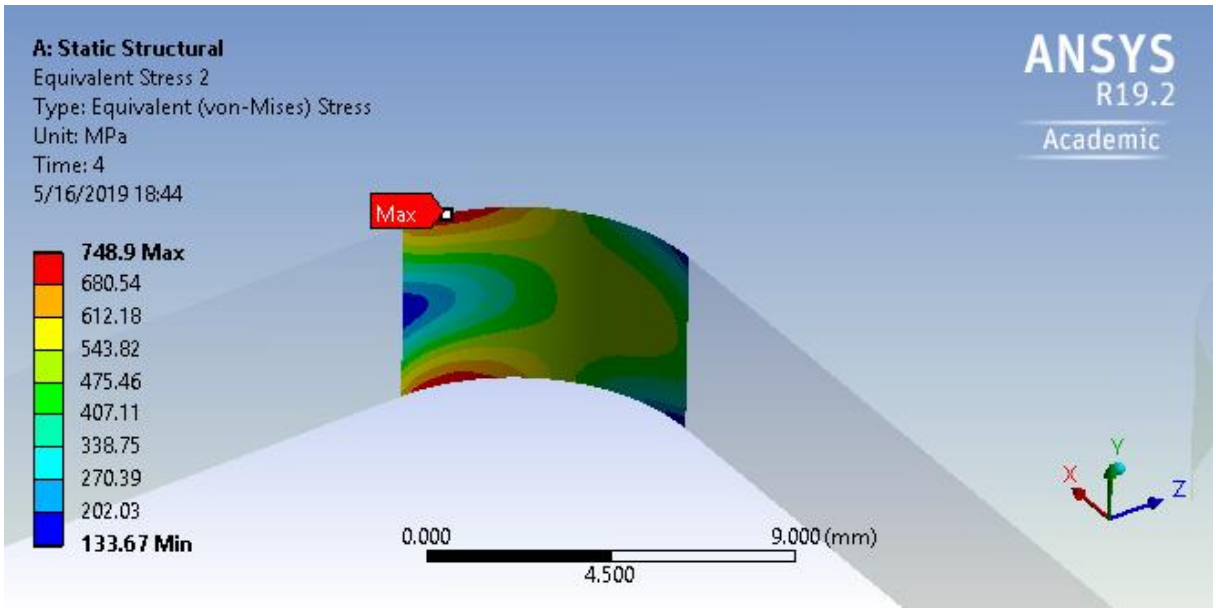

Refined element size 0.37 mm:

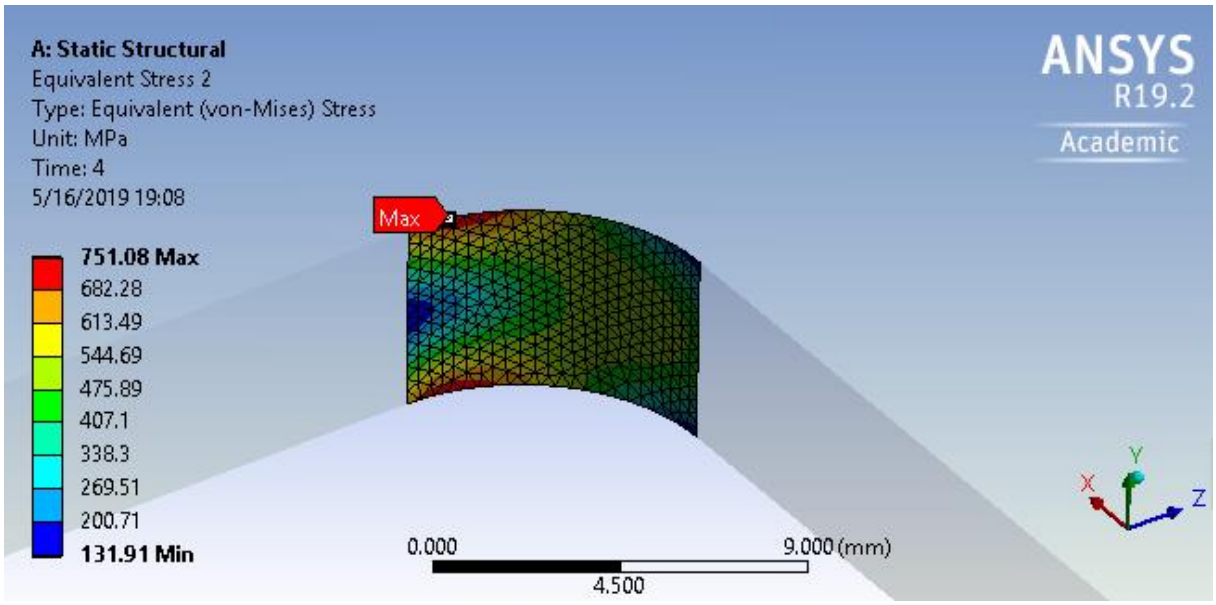

b) Hub Iteration 2

Stress distribution from lateral remote force on the rear hinges of the hub, as well as comparison of stress magnitude for different loads.

Element size: 3 mm, 102 964 nodes

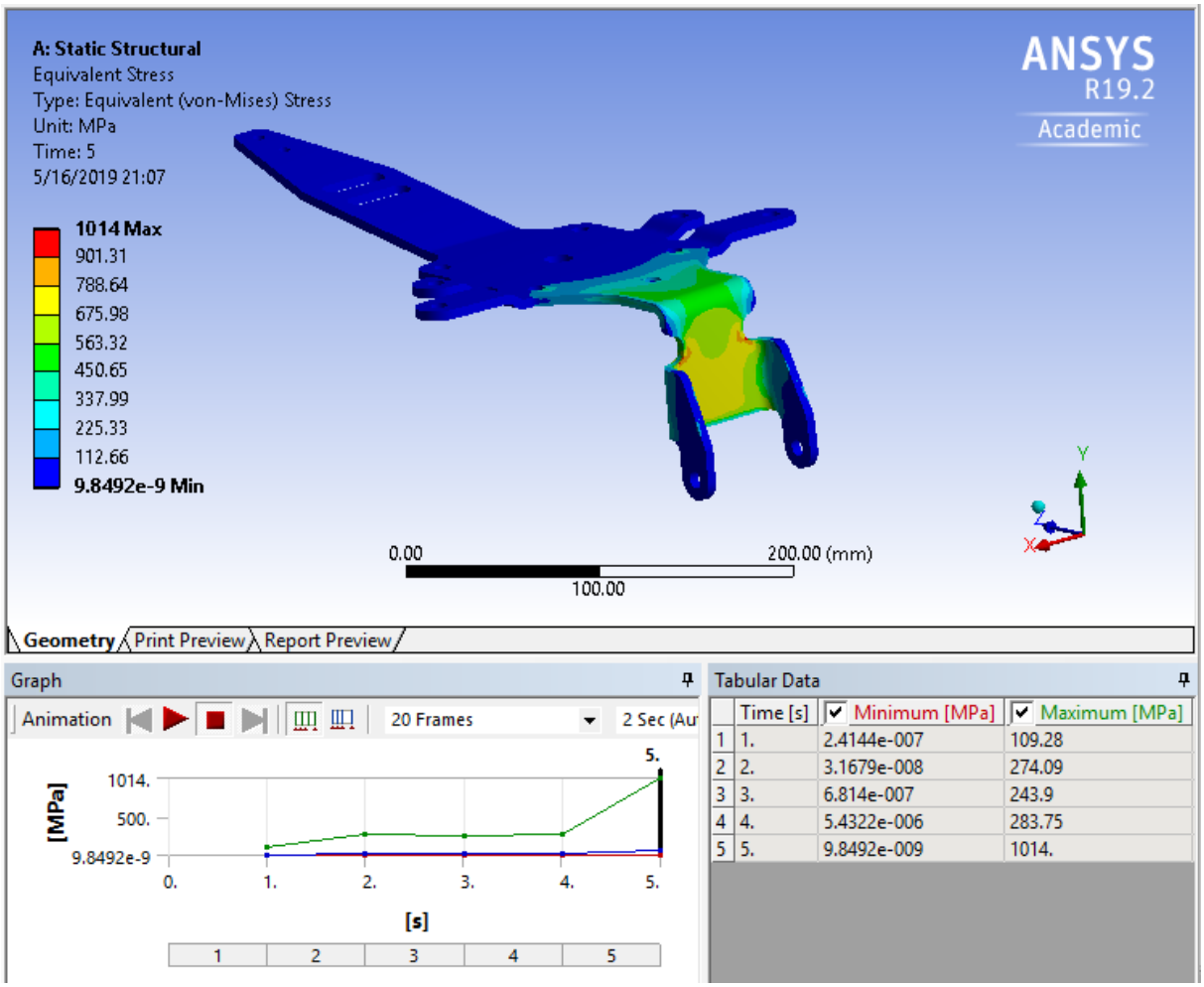

Force B active in step 1, force C active in step 2, bearing load D active in step 3, remote force E active in step 4 and remote force F active in step 5.

c) Hub Iteration 3

The two areas subject to refined mesh; one of the rear fastening holes to the undercarriage, followed by the lower of the two holes for fastening the hinges connecting the footrest.

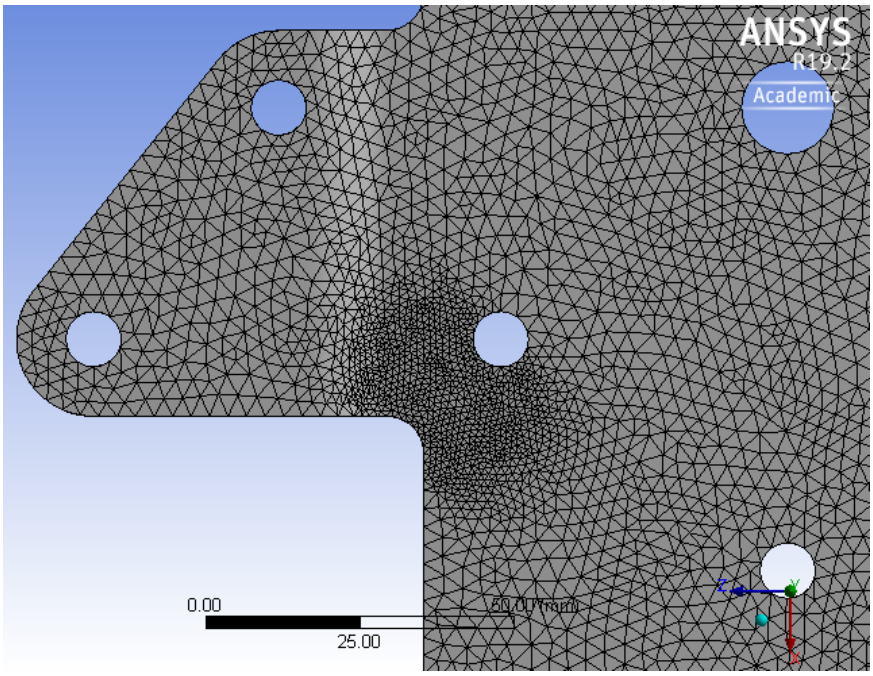

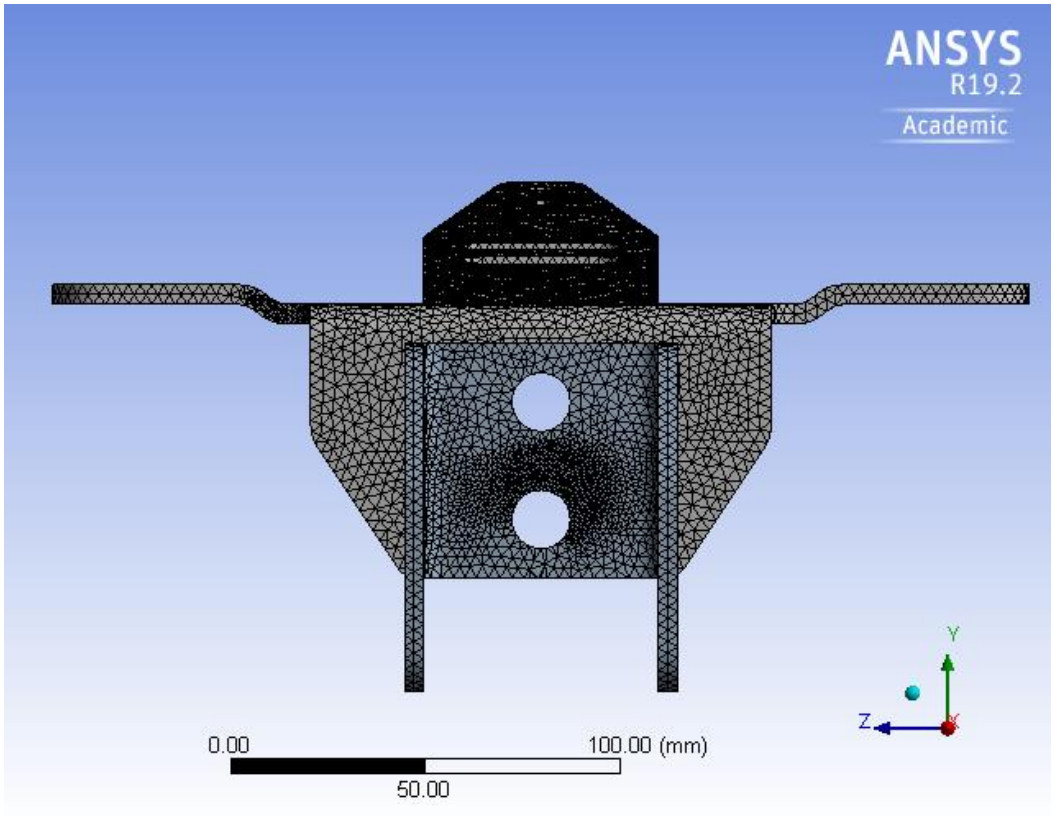

Stress distribution from lateral remote force after refining mesh.

3 mm surrounding mesh, 2 mm refined mesh, 145 768 nodes:

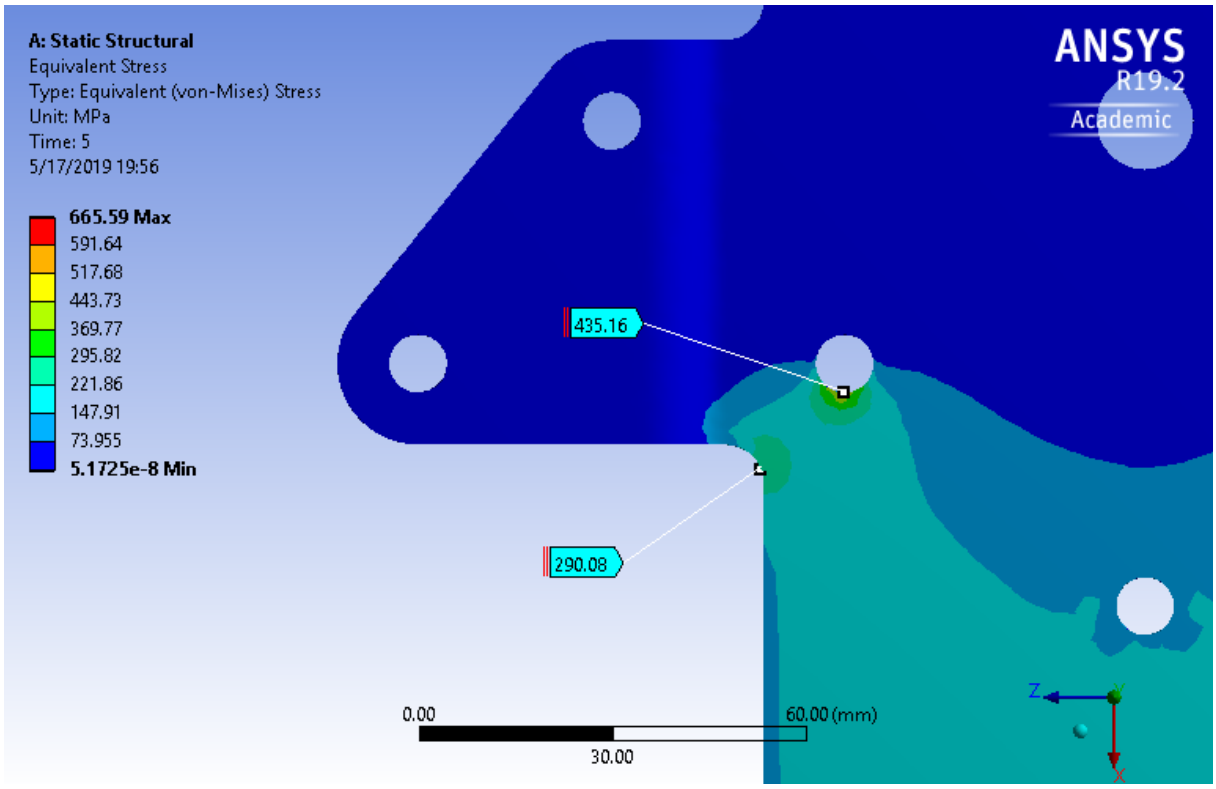

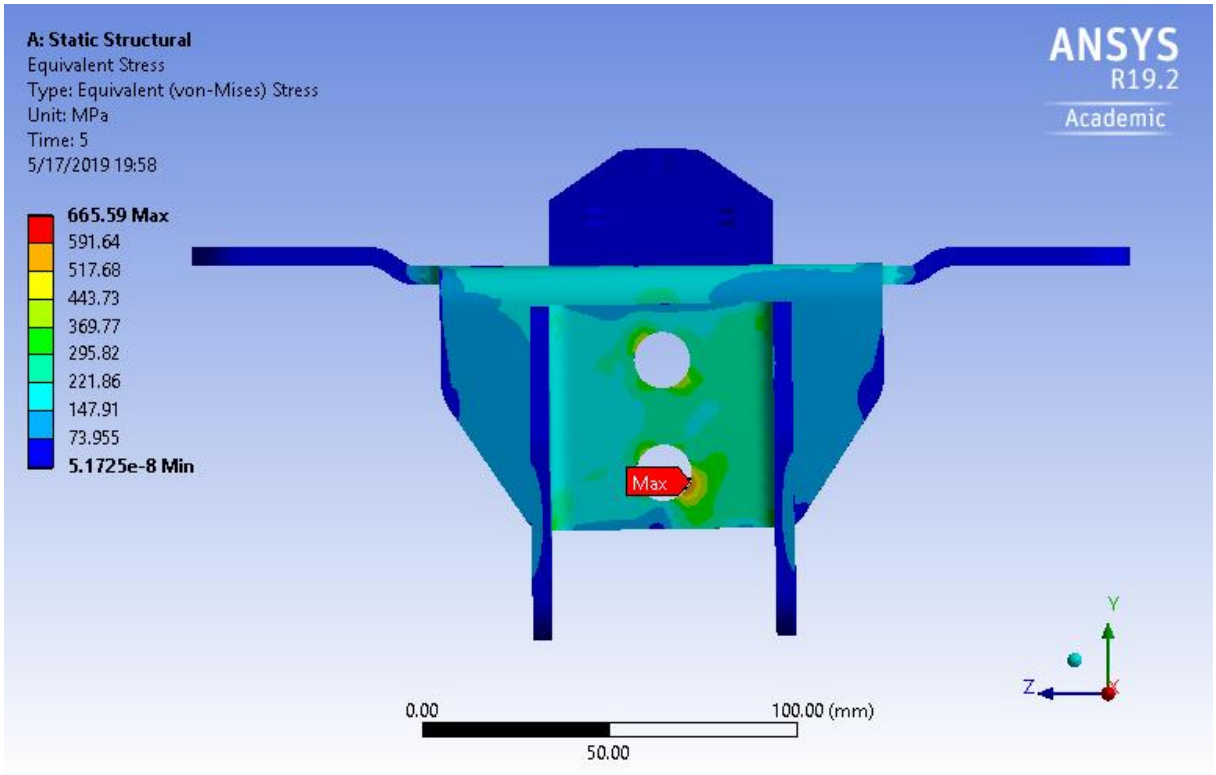

3 mm surrounding mesh, 1 mm refined mesh, 210 622 nodes:

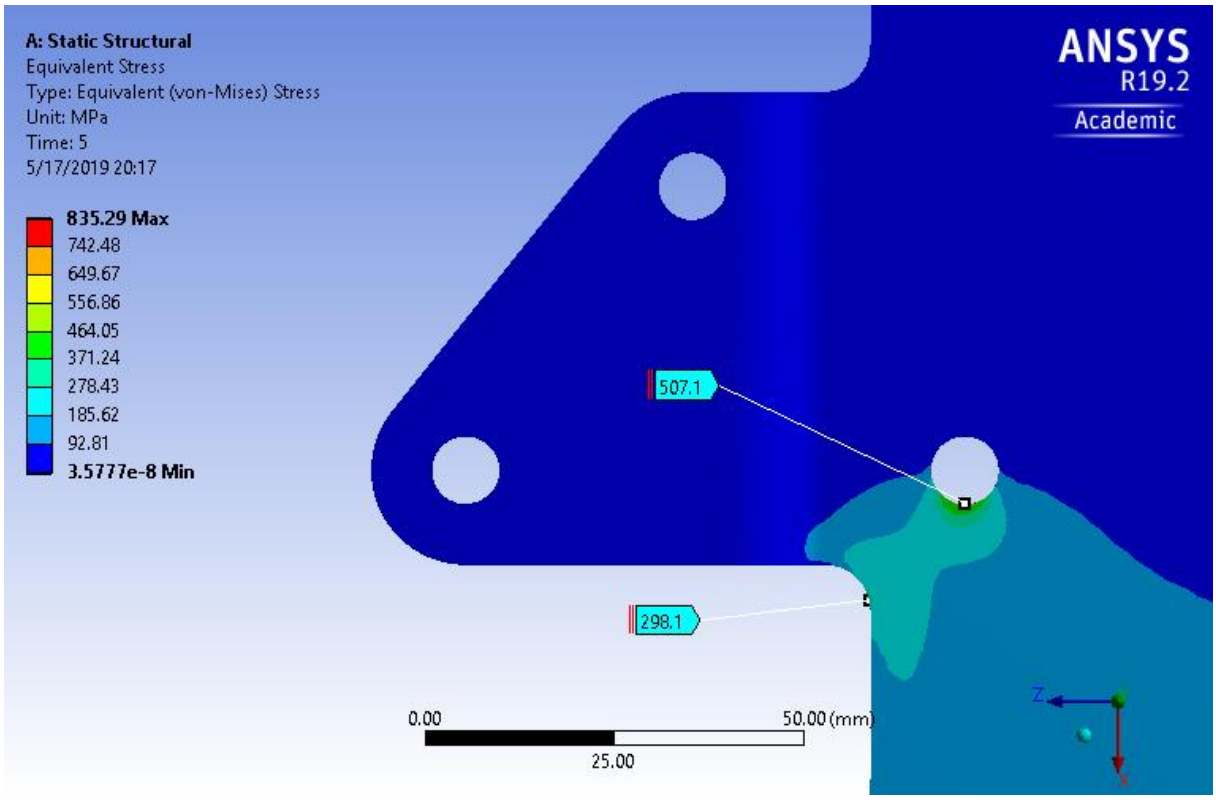

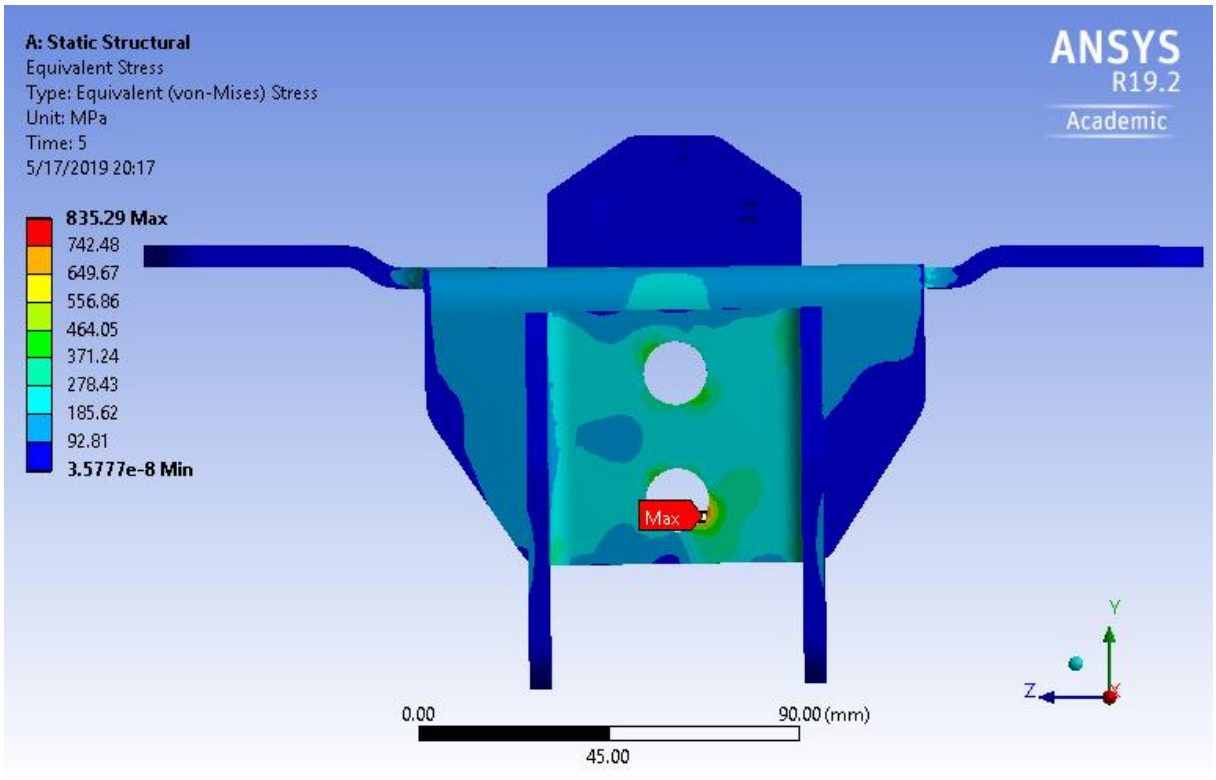

d) Hub Iteration 4

Multiple loads, lateral remote force active on hinge:

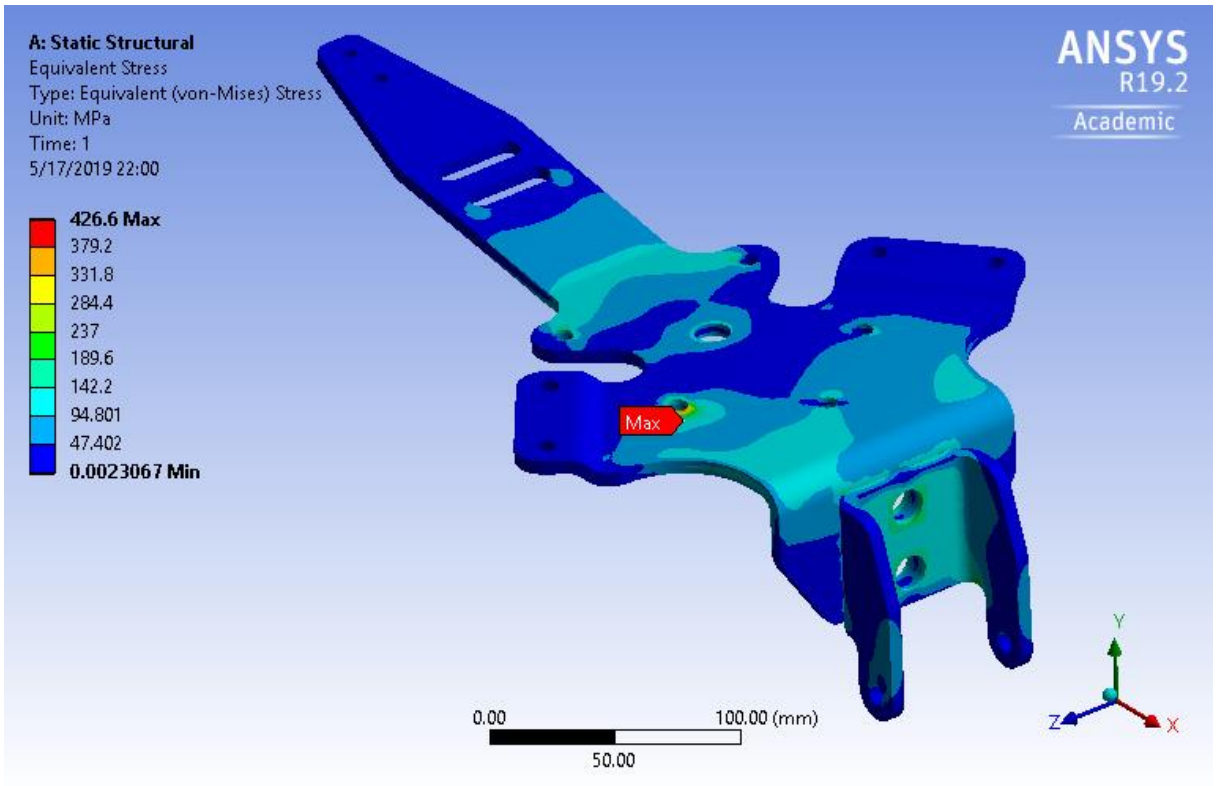

Multiple loads, vertical bearing load active on hinge:

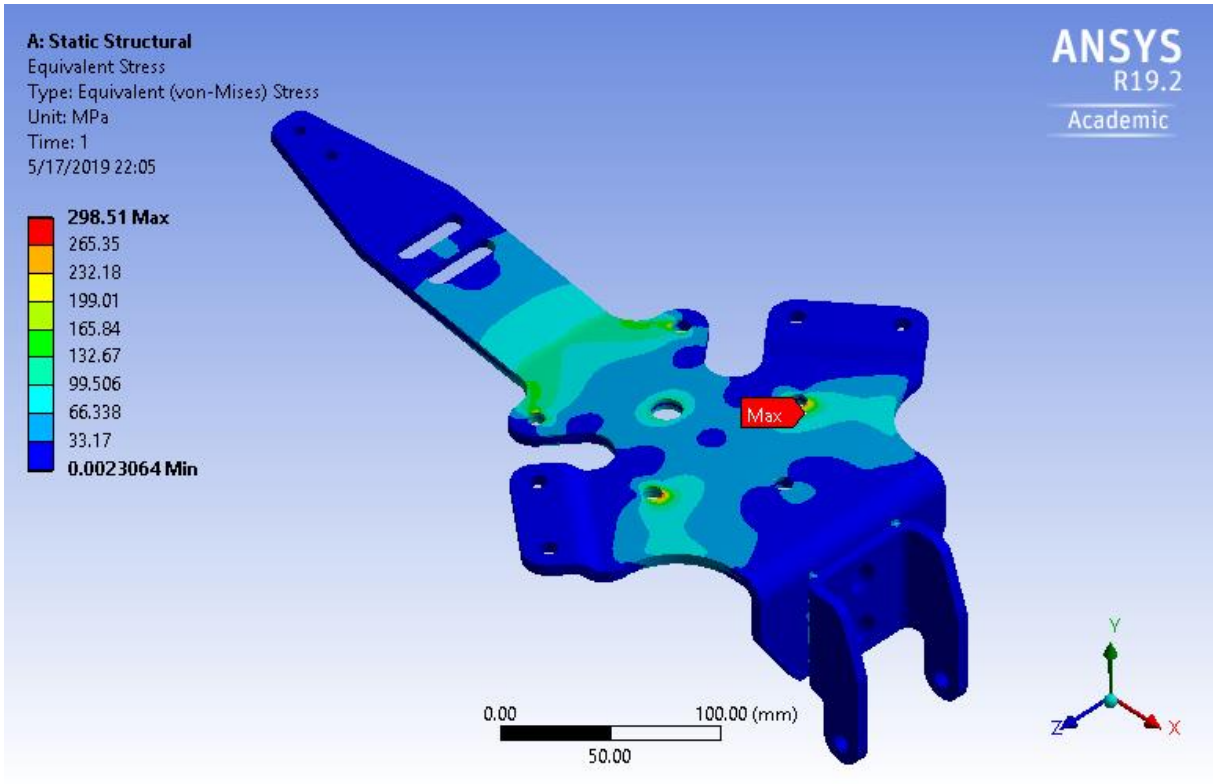

Area of refined mesh:

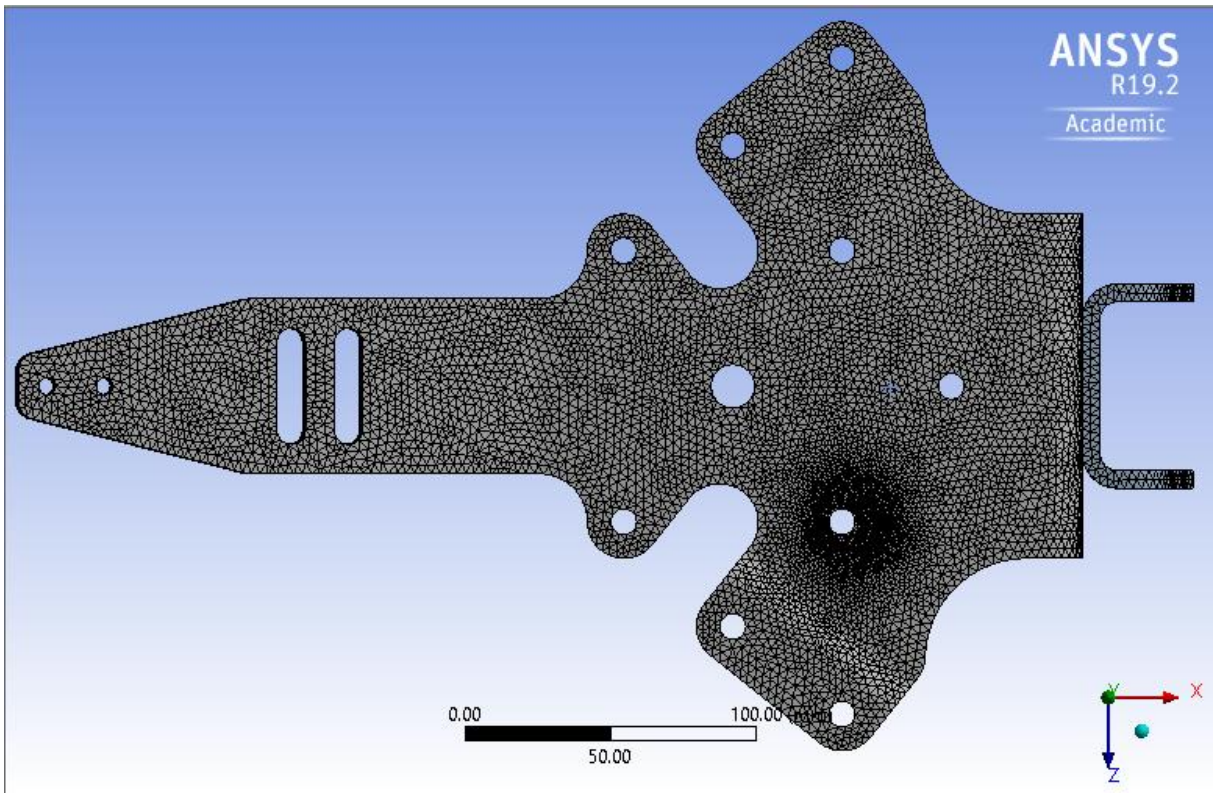

Stress plots for stepwise refined mesh:

Refined element size 2 mm:

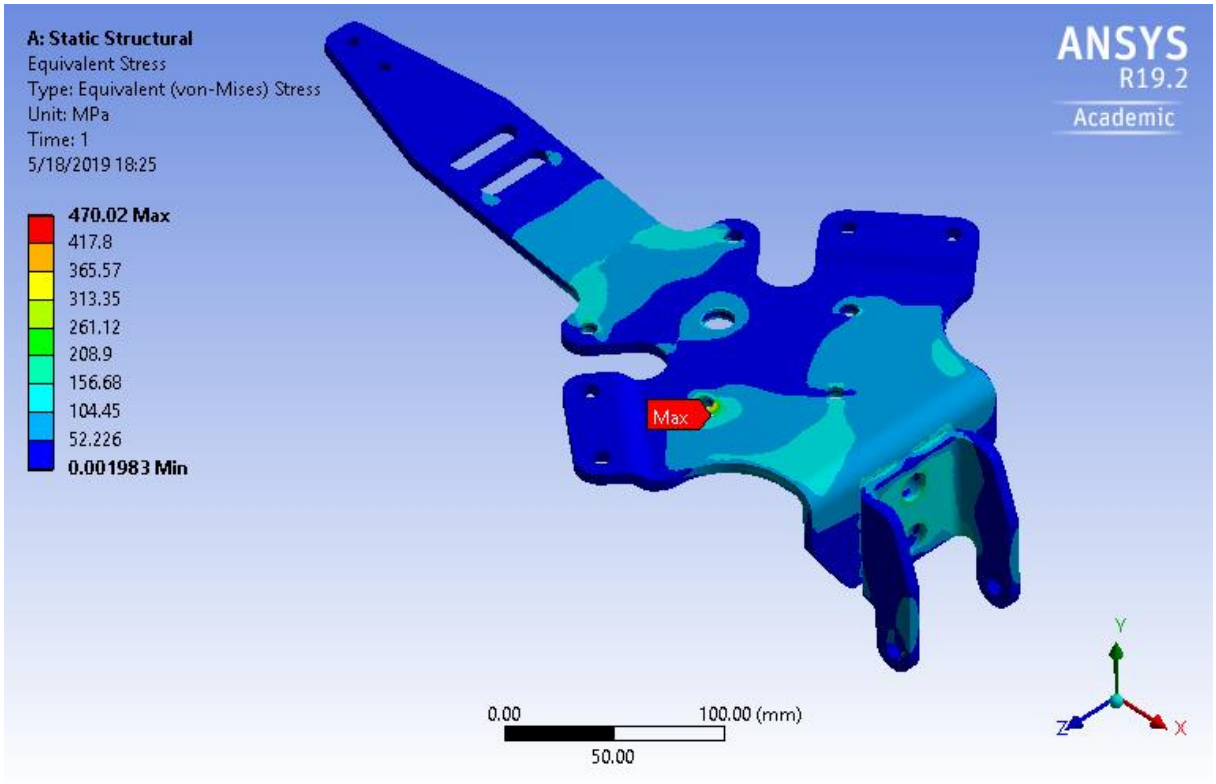

Refined element size 1mm:

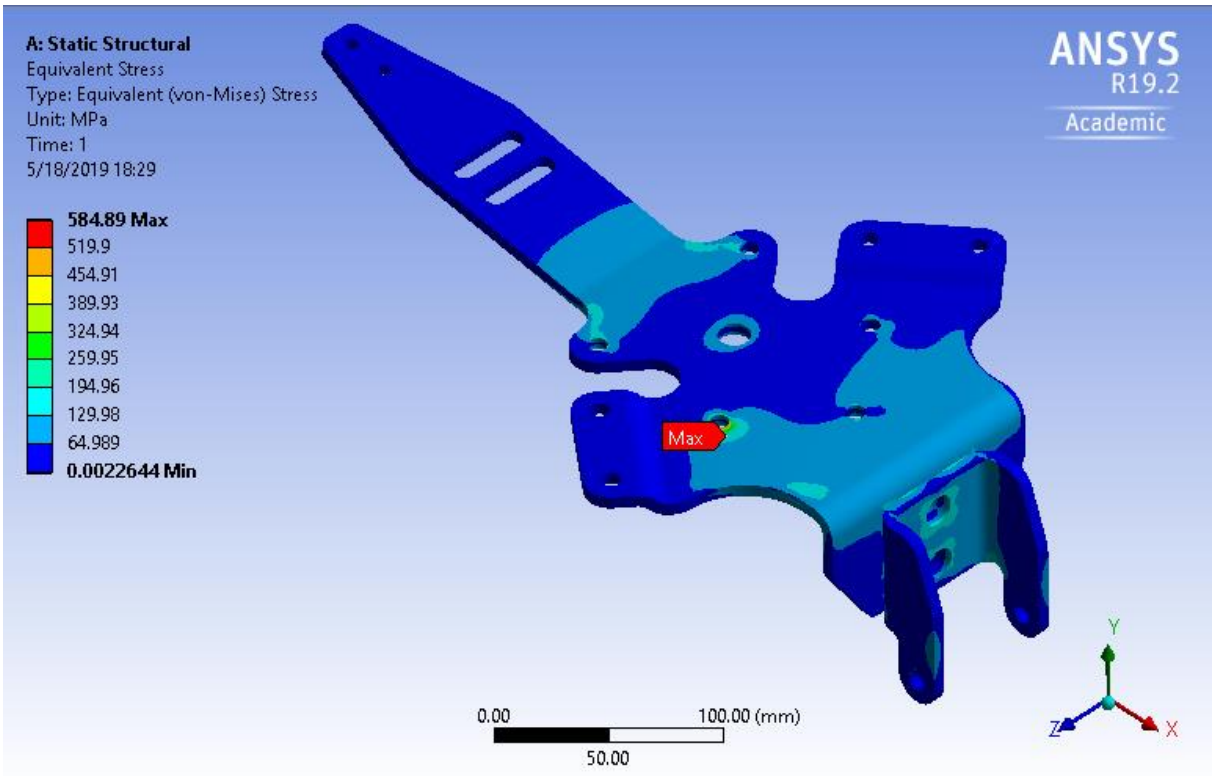

Refined element size 0.9 mm:

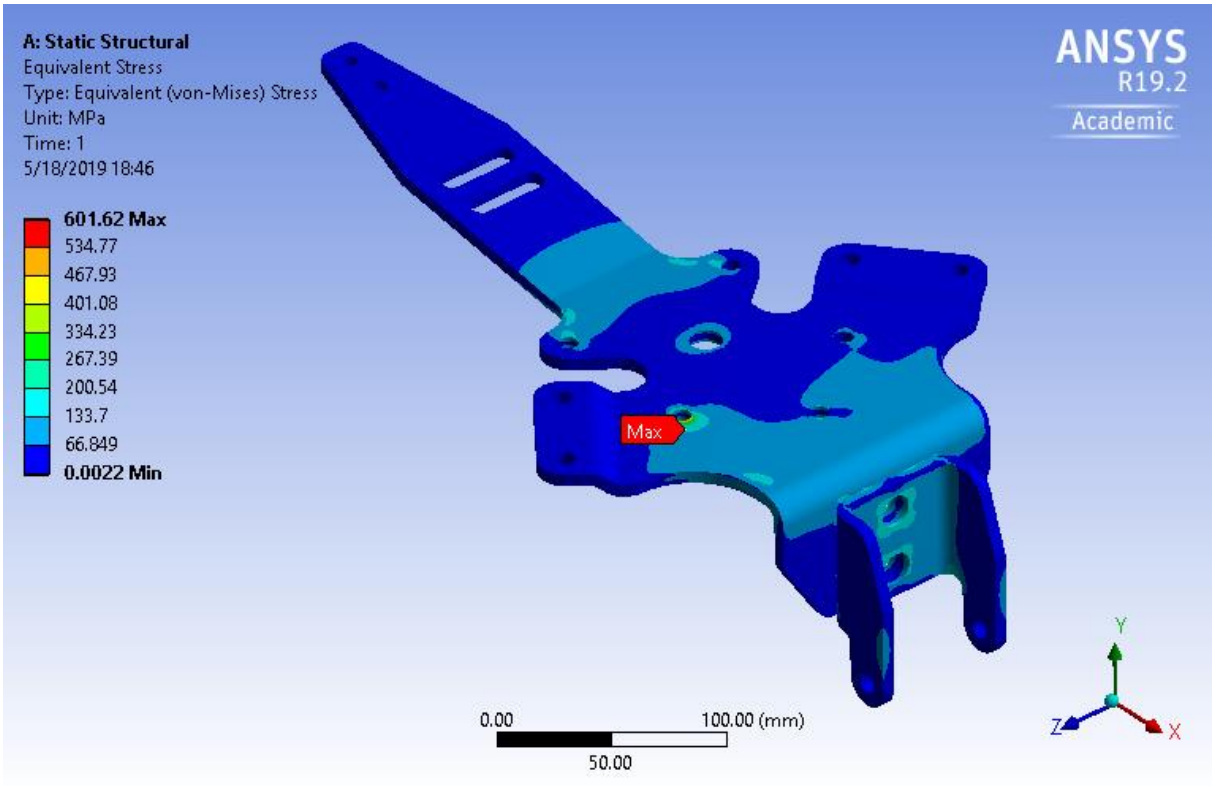

Adding undercarriage, using *Spaceclaim*:

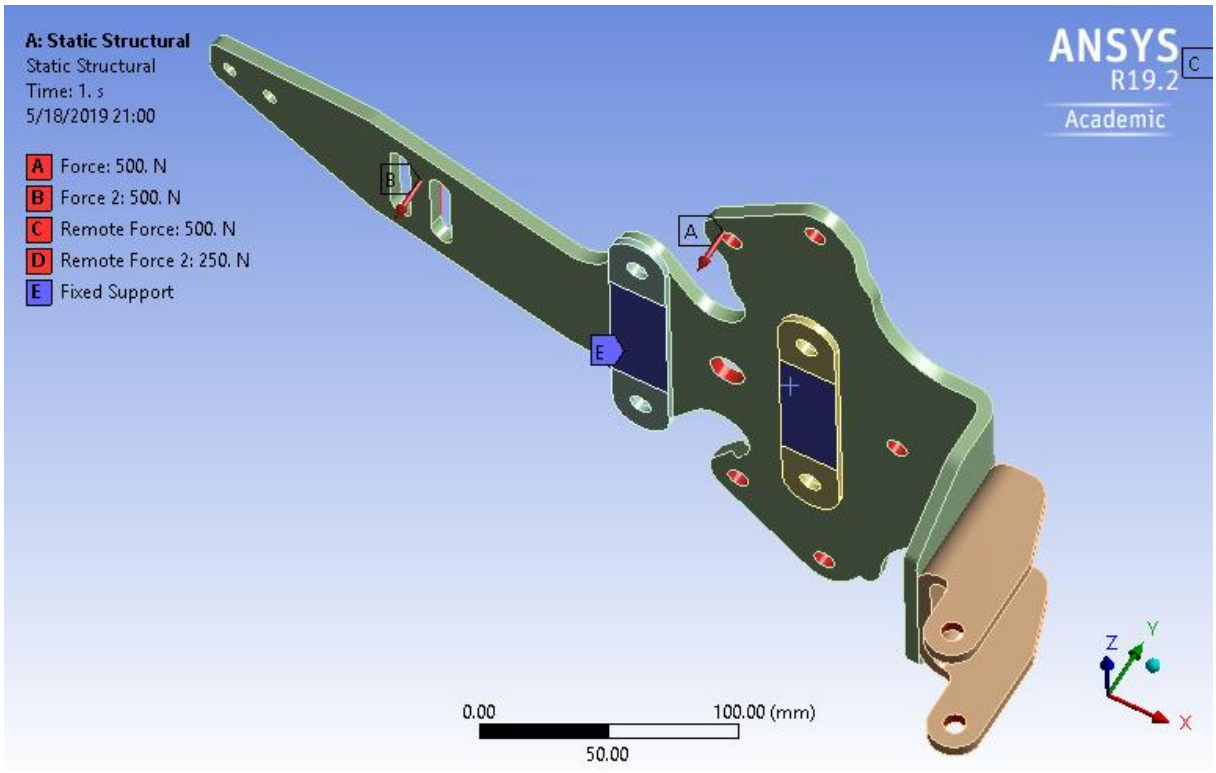

Note that the notation of the loads and supports in the image does not correspond to previous images.

Appendix P Numerical Analysis of Backrest Post

a) Backrest Post Iteration 1

Displacement and stress distribution

Element size 5 mm, 25 903 nodes

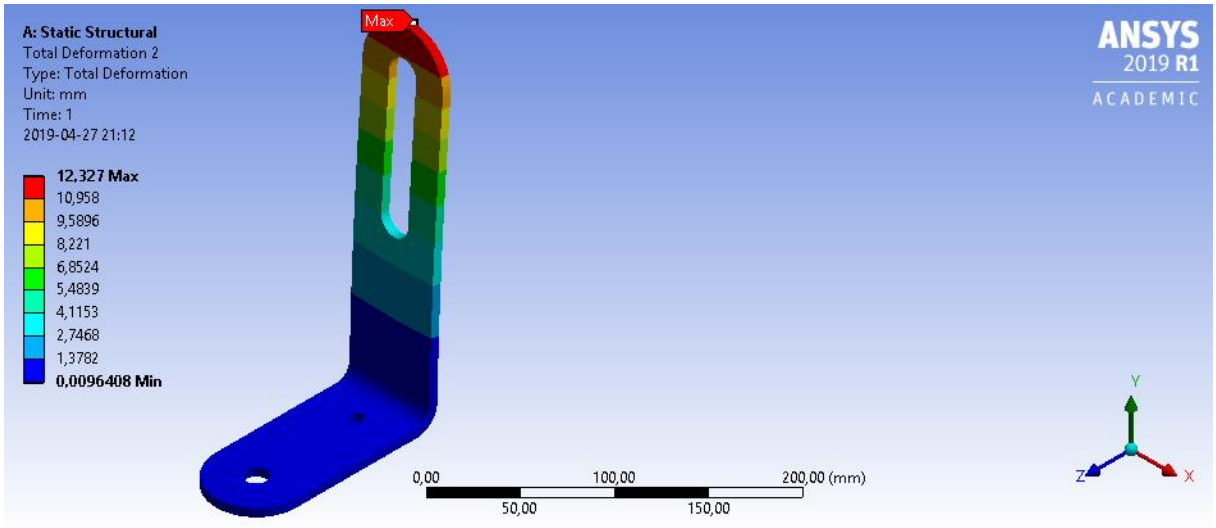

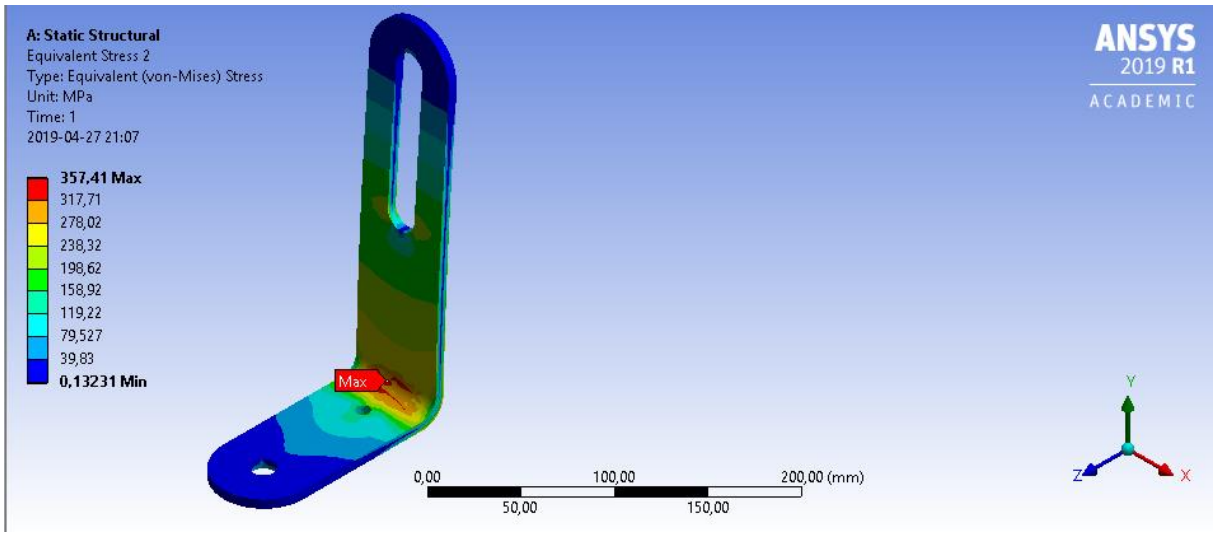

Surrounding element size was increased to 6mm to allow refinement in the bend of the post.

Meshed model, visualizing the refined area in the bend of the post:

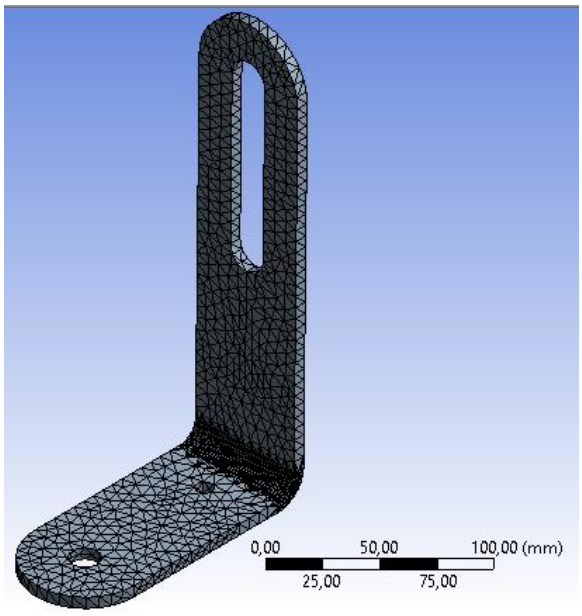

Element size in refined bend: 3mm:

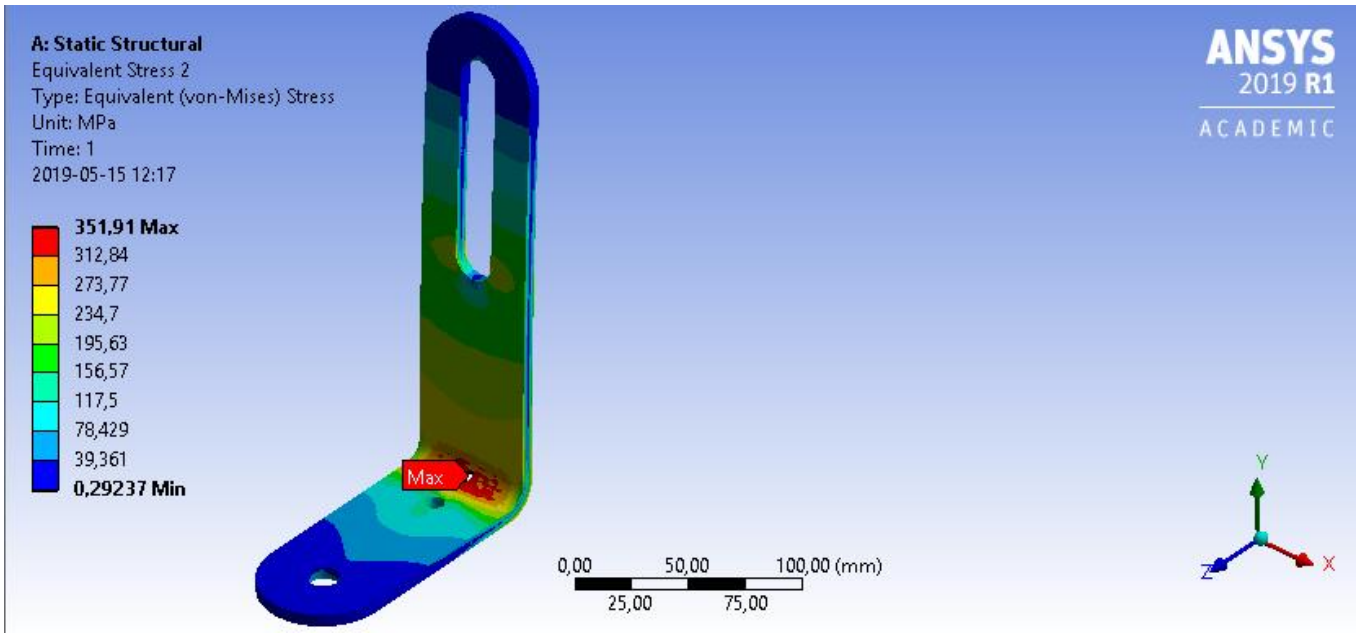

Element size in refined bend: 2mm:

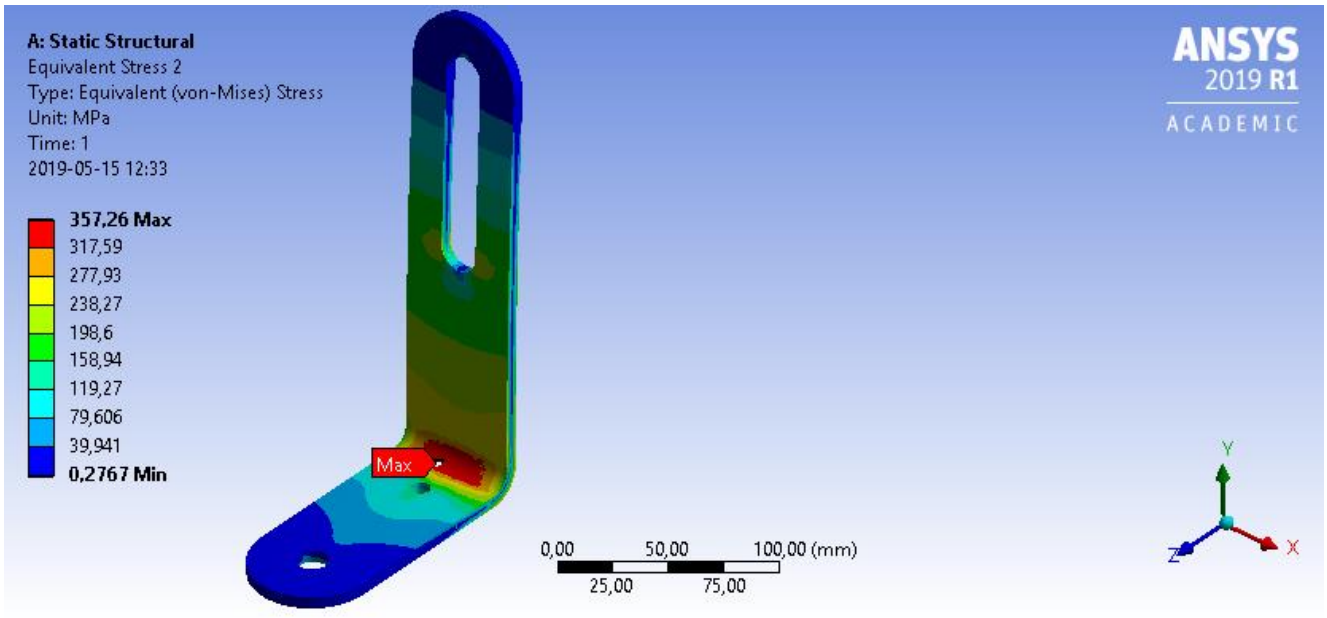

Element size in refined bend: 1.7mm:

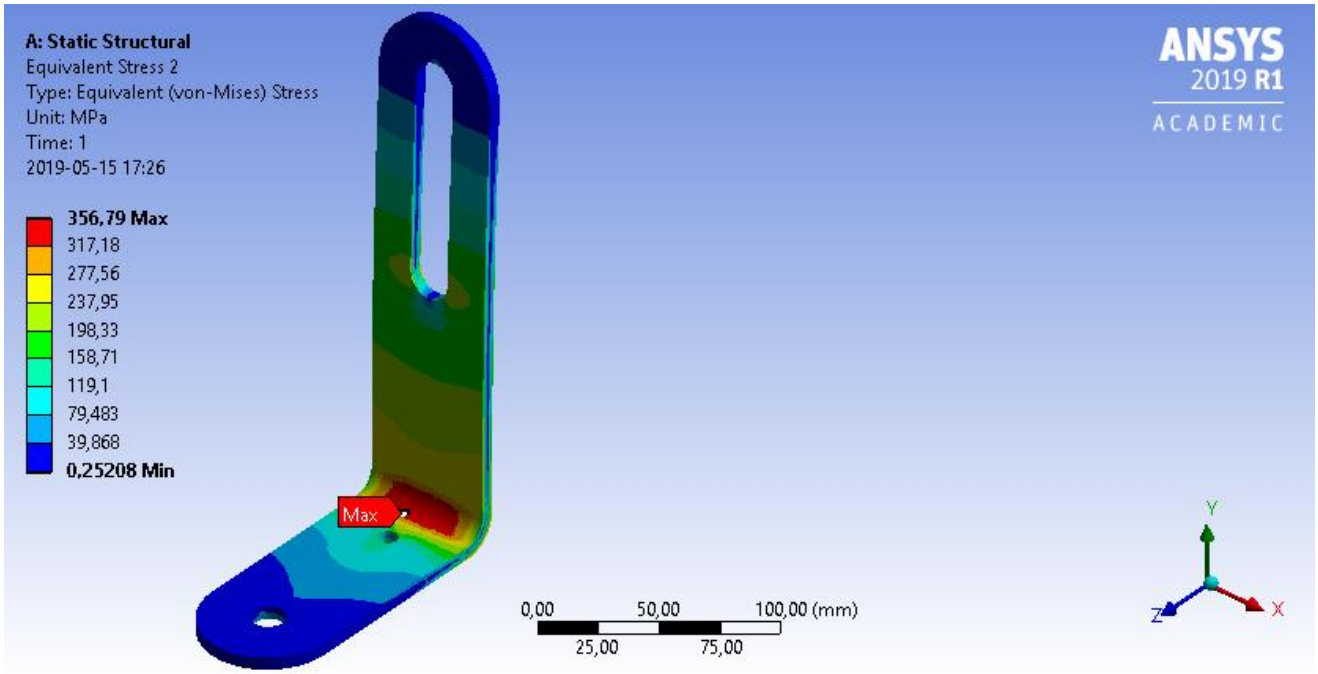

Element size in refined bend: 1.5mm:

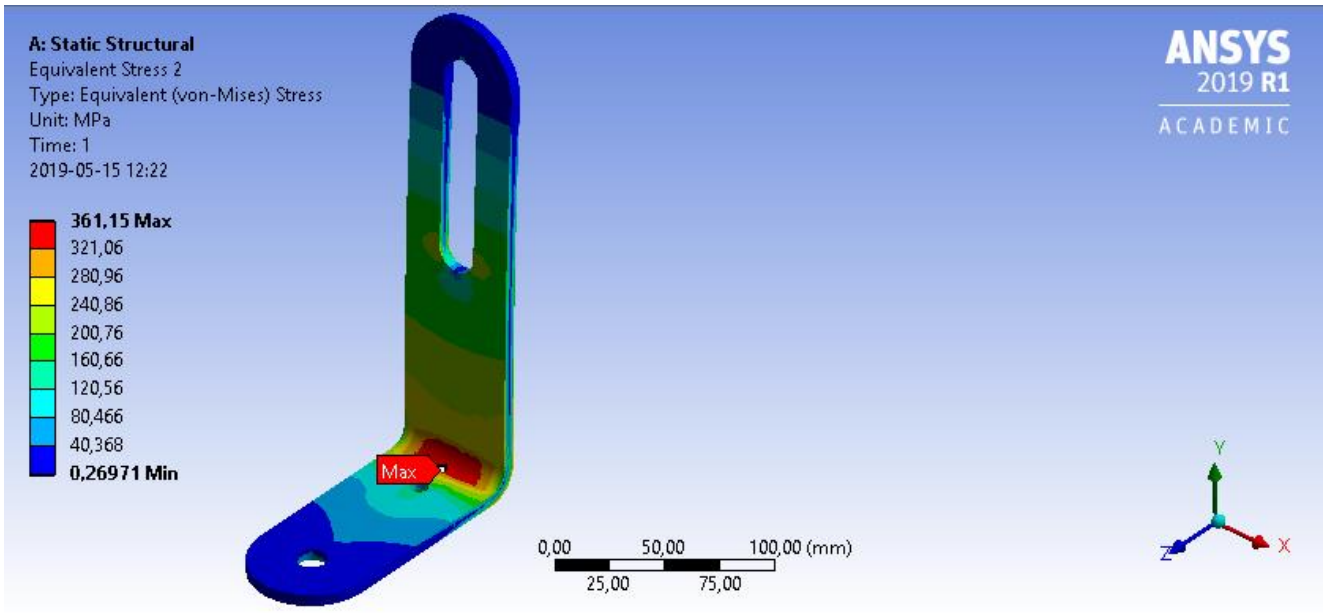

Element size in refined bend: 1.35mm:

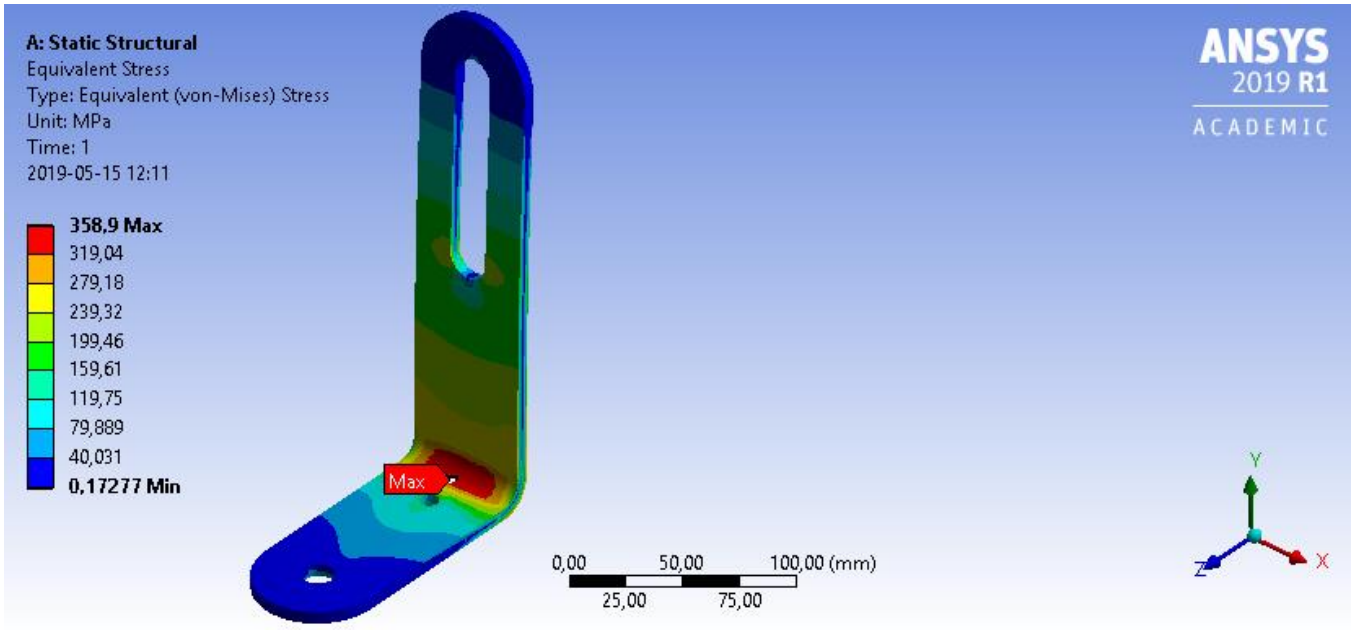

b) Backrest Post Iteration 2

Stress distribution

Element size 5 mm, 23 420 nodes.

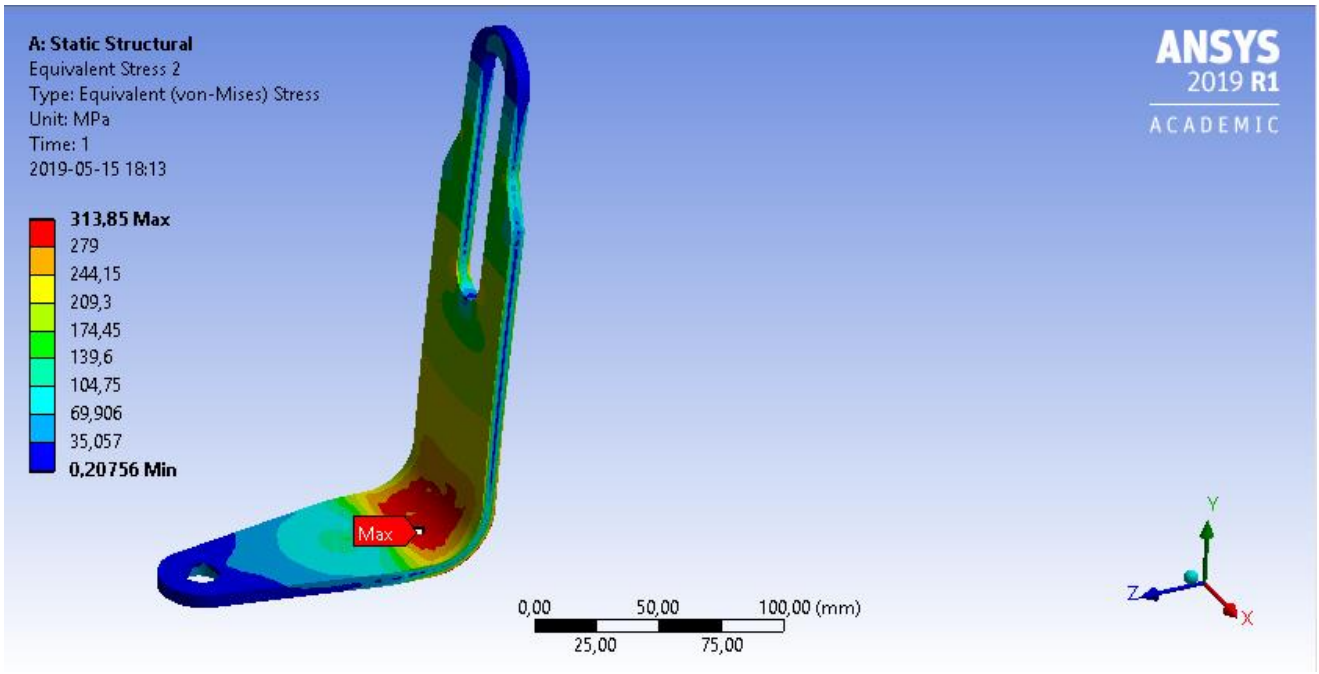

Surrounding element size was increased to 6mm to allow refinement in the bend of the post

Element size in refined bend: 3mm:

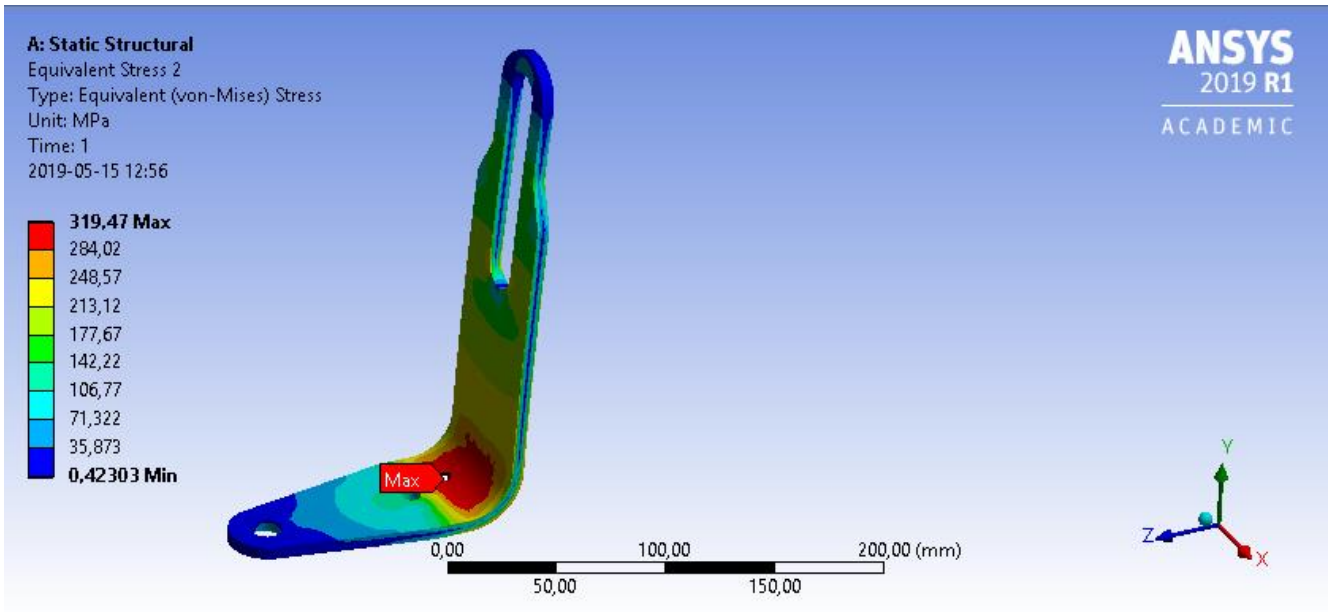

Element size in refined bend: 2mm:

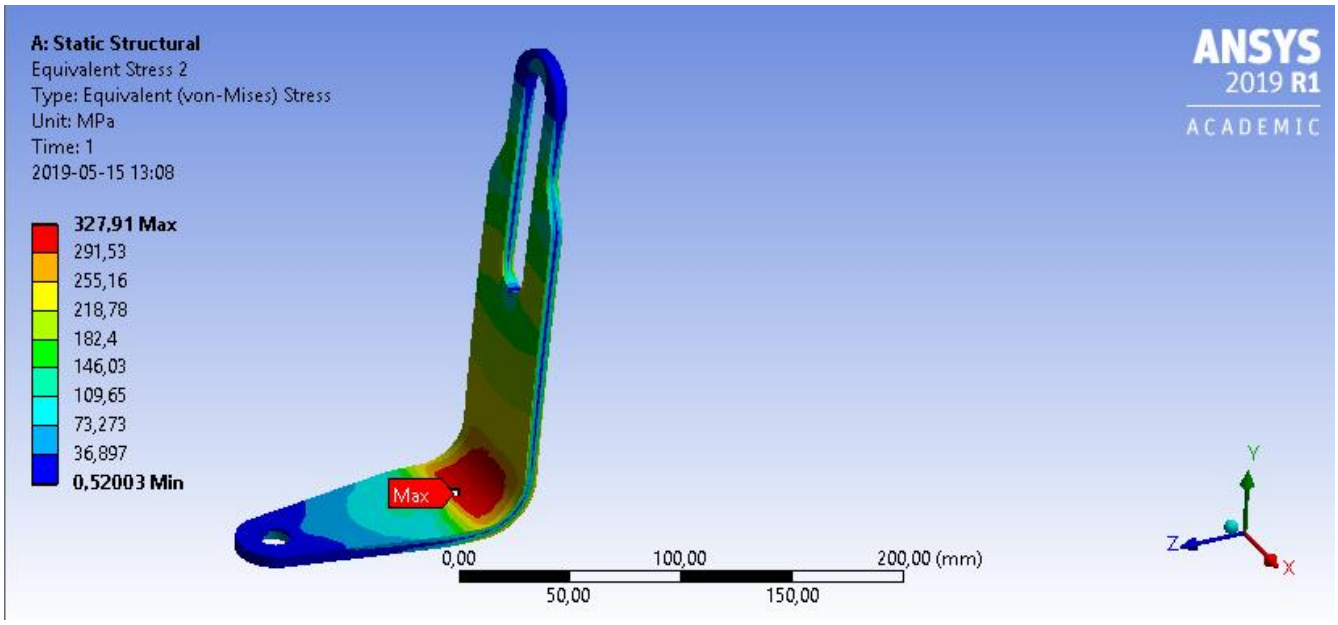

Element size in refined bend: 1.7mm:

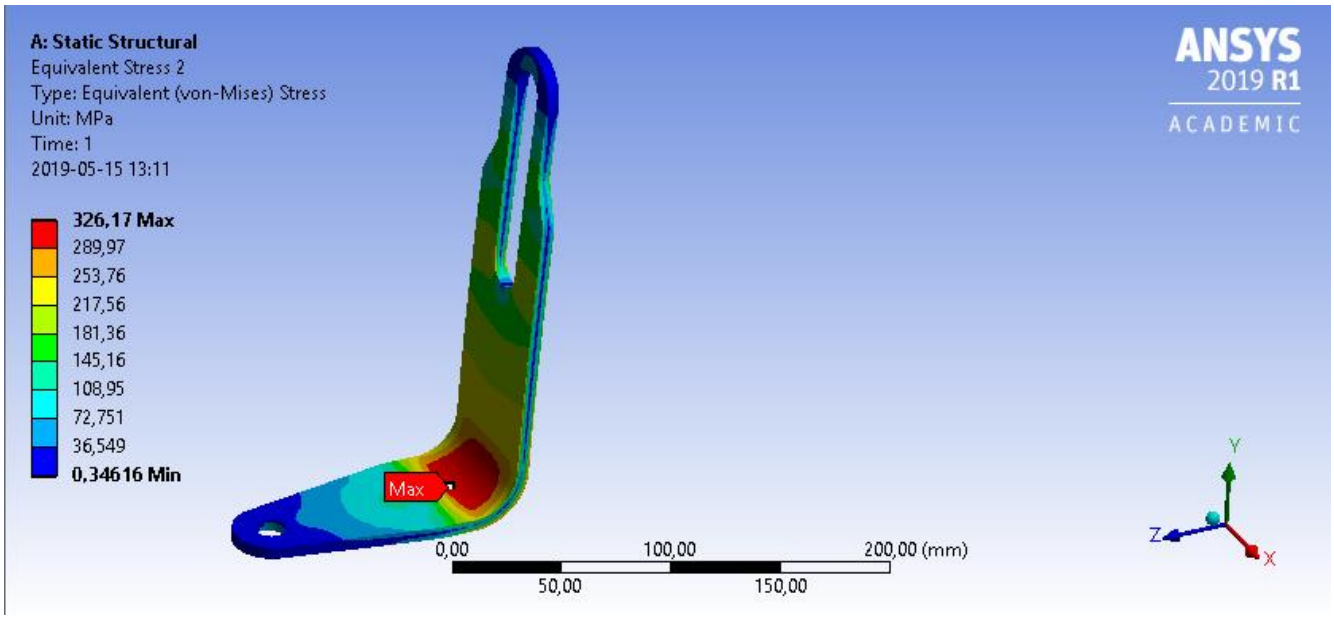

Element size in refined bend: 1.6mm:

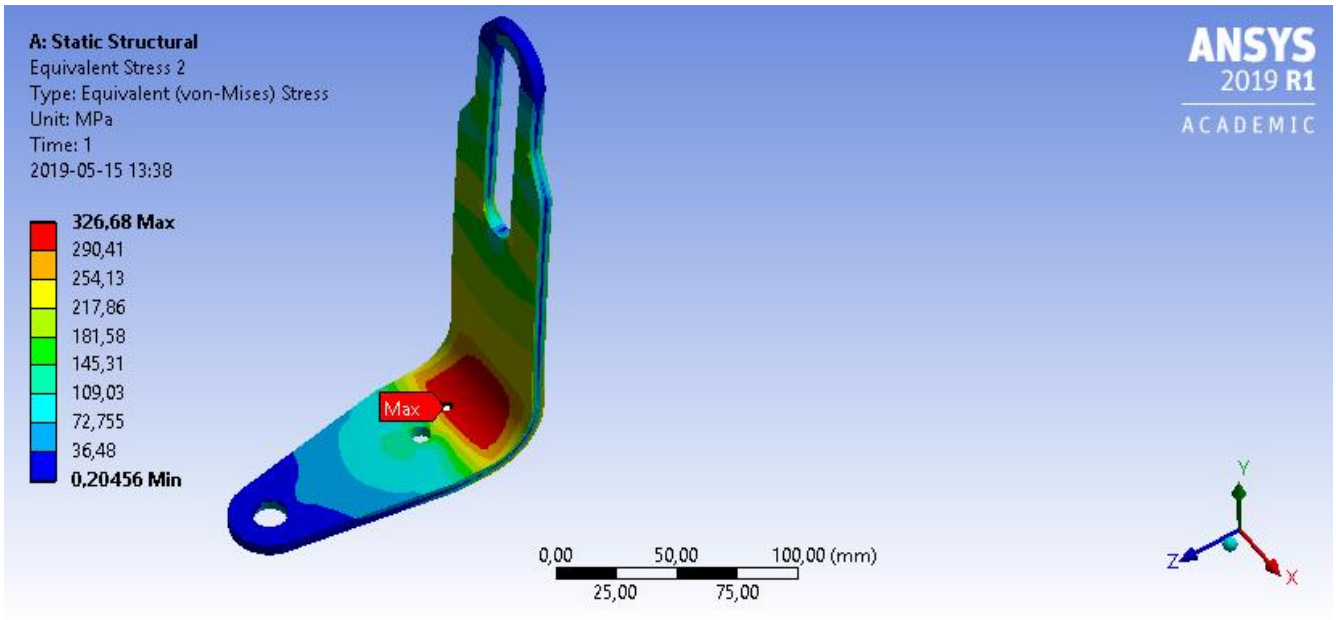
A: Static Structural
Equivalent Stress 2
Type: Equivalent (von-Mises) Stress
Unit: MPa
Time: 1
2019-05-15 13:38
326,68 Max
290,41
254,13
217,86
181,58
145,31
109,03
72,755
36,48
0,20456 Min
Max
0,00
50,00
100,00 (mm)
25,00
75,00
ANSYS
2019 R1
ACADEMIC
Y
Z
X

Appendix Q Analytical Stress Calculations

Bending stress was calculated analytically along two lines, A and B, in the vertical part of the backrest post. The 500 N force was simplified to a point load and located on the lowest part of the upper fillet of the slot. Point A was located close to corresponding position on the lower part of the slot. Point B was located on the upper part of the bend.

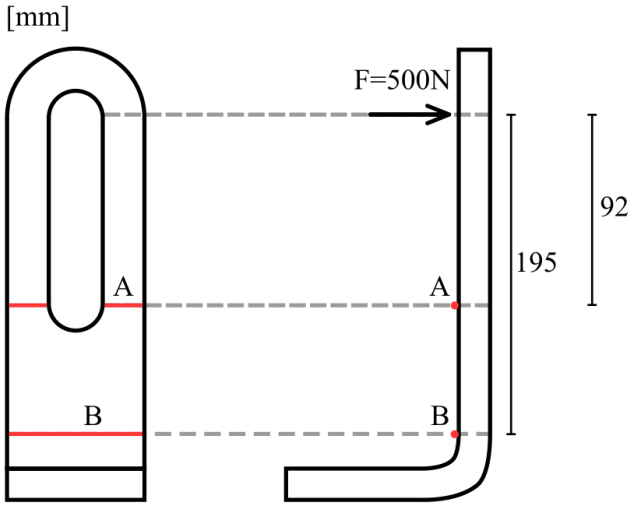

Bending stress, σ_b, can be expressed as

$$\sigma_b = \frac{My}{I_x}$$

where M is bending moment and y is distance from the neutral plane. I_x, second moment of area around the x-axis, can be expressed as

$$I_x = \frac{bh^3}{12}$$

for rectangular cross sections with a coordinate system as follows

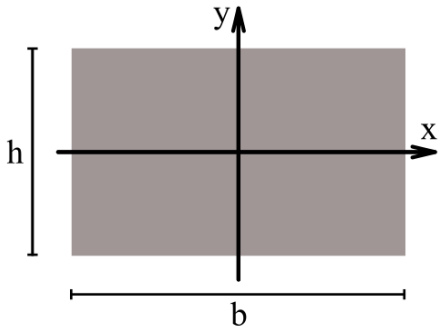

Calculating moment around A:

$$M_A = 500\ N \cdot 0.092\ m = 46\ Nm$$

Cross section around A

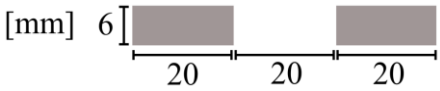

gives second moment of area

$$I_{xA} = \frac{2 \cdot 0.02\ m \cdot (0.006m)^3}{12} \approx 7.2 \cdot 10^{-10} m^4$$

Calculating bending stress on the surface gives $y = 6mm/2 = 3mm$. This gives bending stress

$$\sigma_{bA} = \frac{M_A y}{I_{xA}} = \frac{46\ Nm \cdot 0.003\ m}{7.2 \cdot 10^{-10}\ m^4} \approx 191.67\ MPa$$

Moment around B is calculated similarly:

$$M_A = 500\ N \cdot 0.195\ m = 97.5\ Nm$$

Cross section around B

gives second moment of area

$$I_{xB} = \frac{0.06\ m \cdot (0.006m)^3}{12} \approx 1.08 \cdot 10^{-9} m^4$$

Using $y = 3\ mm$ as previously gives

$$\sigma_{bB} = \frac{M_B y}{I_{xB}} = \frac{97.5\ Nm \cdot 0.003\ m}{1.08 \cdot 10^{-9}\ m^4} \approx 270.83\ MPa$$

Appendix R Sheet Metal Material Selections

Graphs using *CES Edupak* level 2 database are presented in a), while graphs using the level 3 database can be seen in b).

a) CES Level 2 Material Graphs

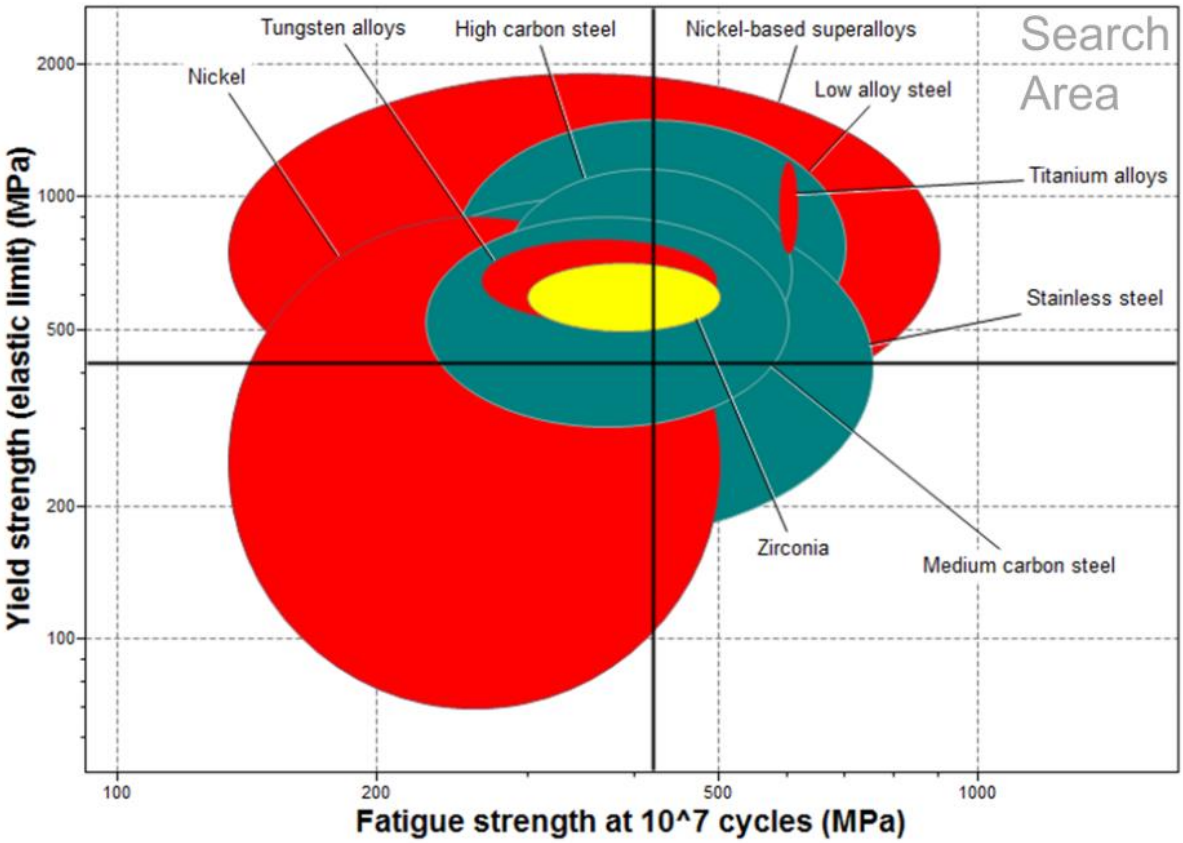

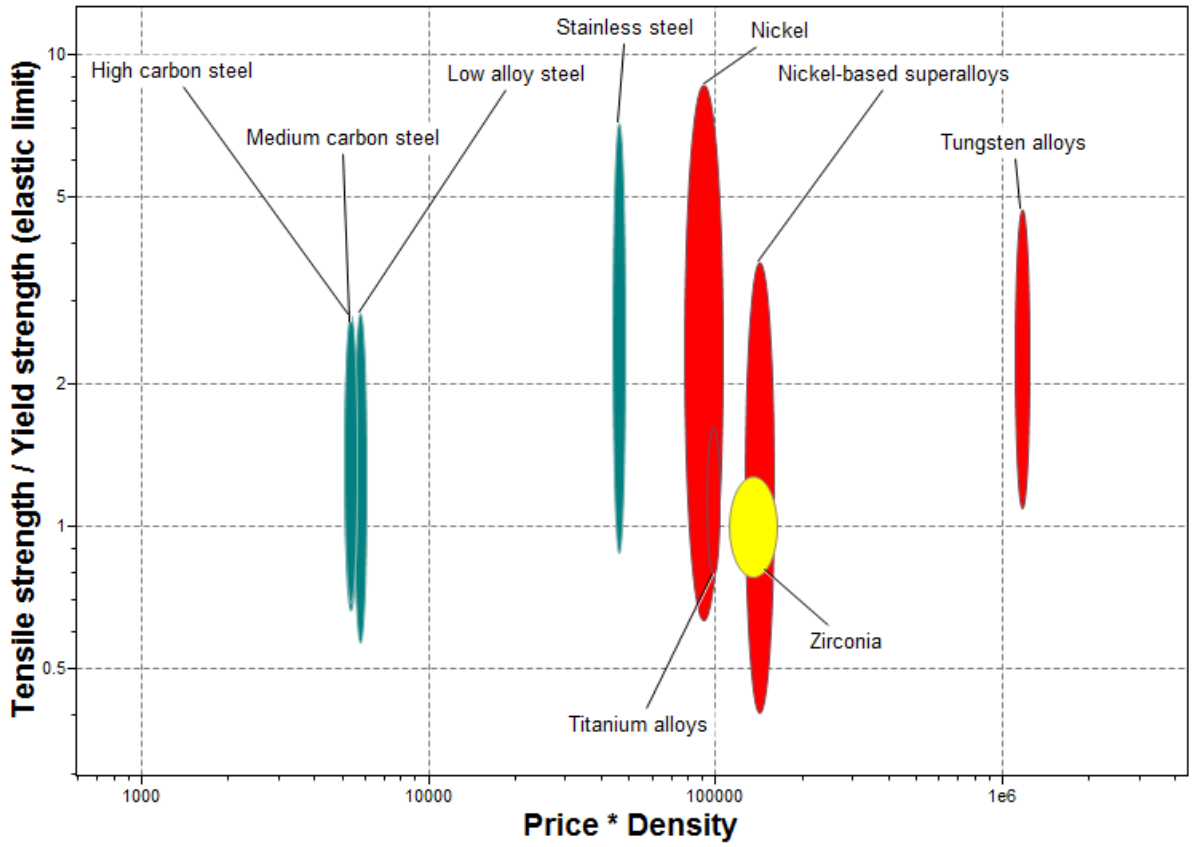
Tensile strength / Yield strength (elastic limit)
Price * Density
High carbon steel
Medium carbon steel
Low alloy steel
Stainless steel
Nickel
Nickel-based superalloys
Tungsten alloys
Zirconia
Titanium alloys
10
5
2
1
0.5
1000
10000
100000
1e6

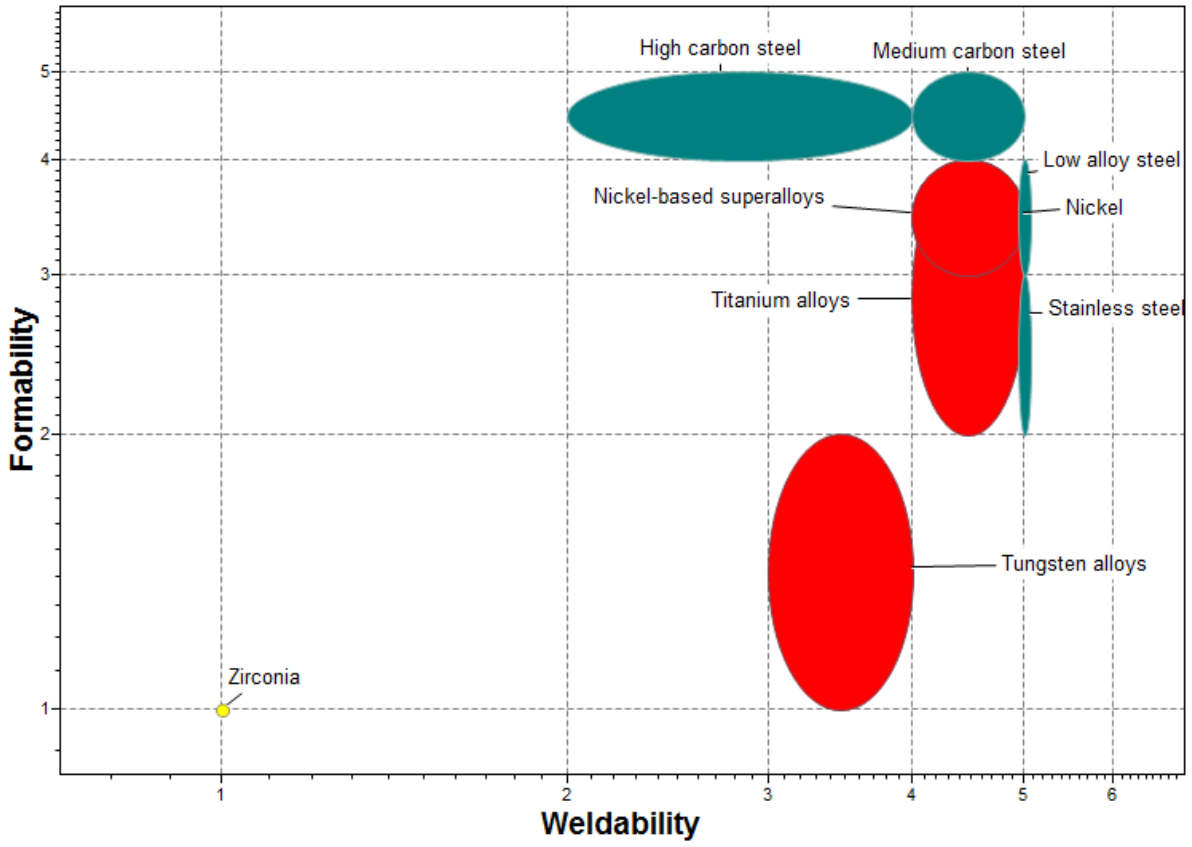
Formability
Weldability
High carbon steel
Medium carbon steel
Low alloy steel
Nickel-based superalloys
Nickel
Titanium alloys
Stainless steel
Tungsten alloys
Zirconia
5
4
3
2
1
1
2
3
4
5
6

b) CES Level 3 Material Graphs

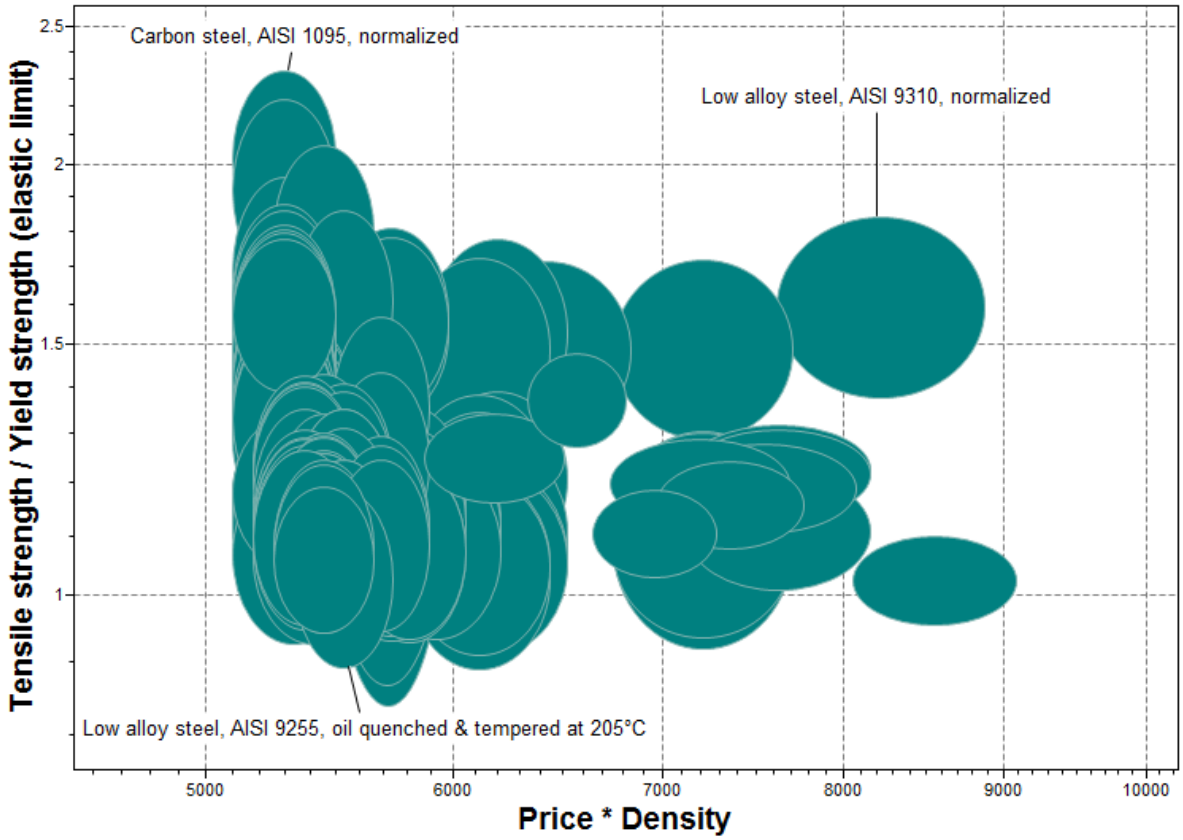

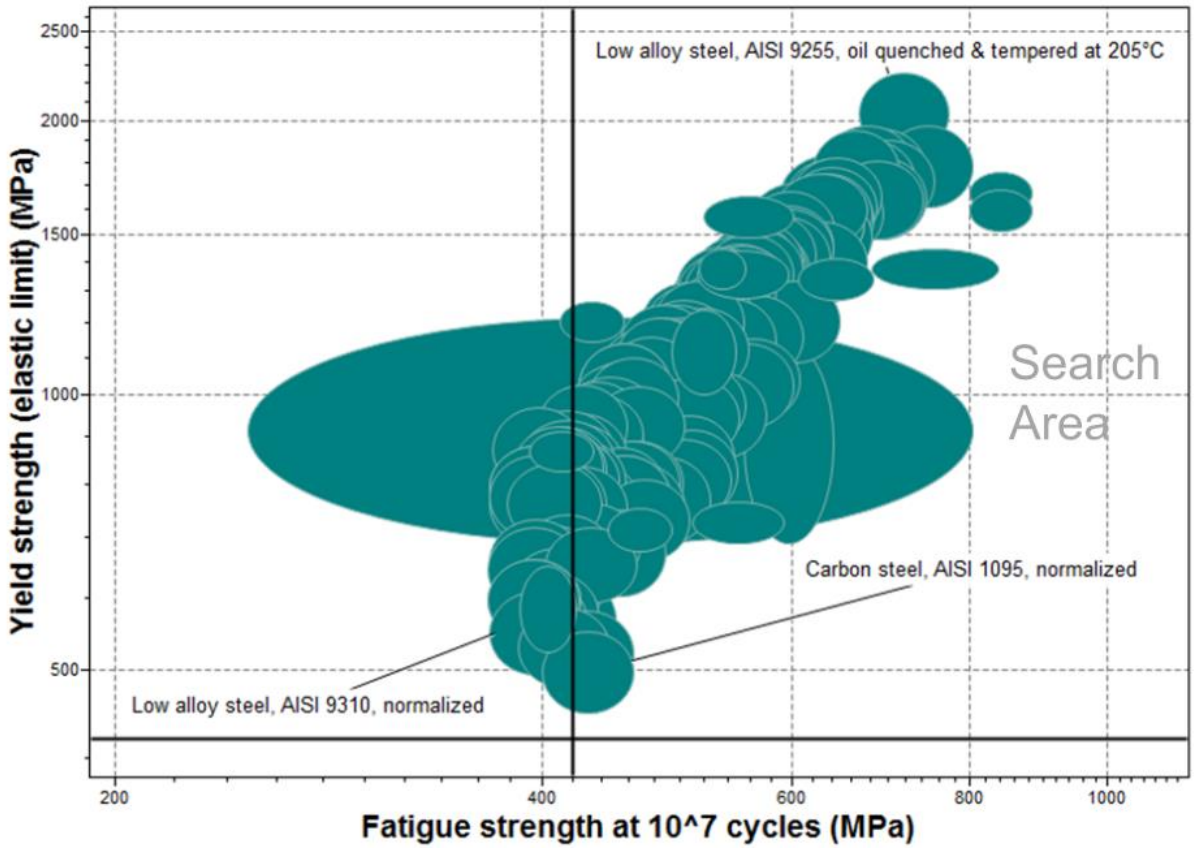

Metal press forming	Unsuitable	Poor	Good	Excellent
Excellent	0	27	95 Low alloy steel, AISI 9255, oil quenched & tempered at 205°C	1 Low alloy steel, AISI 9310, normalized
Acceptable	0	9	33 Carbon steel, AISI 1095, normalized	0
Limited use	0	0	0	0
Unsuitable	0	0	3	0

Weldability

Appendix S List of Manufacturing Processes

Exploded view of all components of the working chair developed during the project.

Followed by a table stating manufacturing process and material for each component.

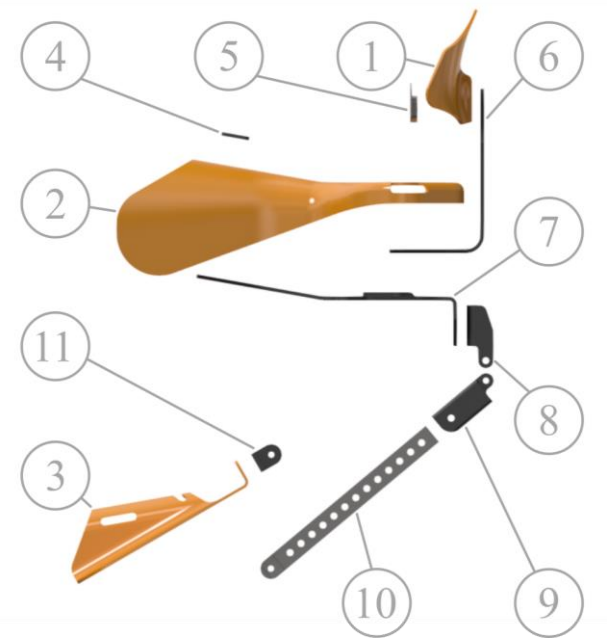

#	Component	Manufacturing	Material
1	Backrest	Vacuum forming	Thermoplastic
2	Seat	Vacuum forming	Thermoplastic
3	Footpad	Vacuum forming	Thermoplastic
4	Bushing	Cutting	Plastic
5	Backrest fastener	Casting	Metal
6	Backrest post	Bent sheet metal	Carbon steel, AISI 1095, normalized
7	Hub	Bent sheet metal	Carbon steel, AISI 1095, normalized
8	Upper hinge	Bent sheet metal	Carbon steel, AISI 1095, normalized
9	Lower hinge	Extrusion	Metal
10	Lever	Extrusion	Metal
11	Footpad fastener	Extrusion	Metal

Appendix T Working Chair Mass and Center of Gravity

Working chair center of gravity:

Working chair iProperties, including mass and center of gravity position:

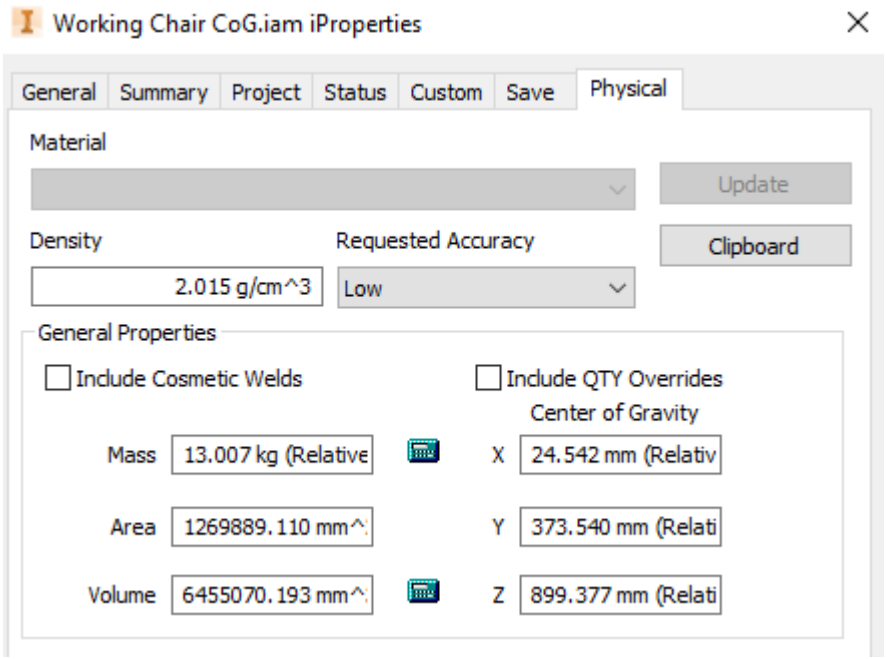

Material data for Inventor pre-defined carbon steel:

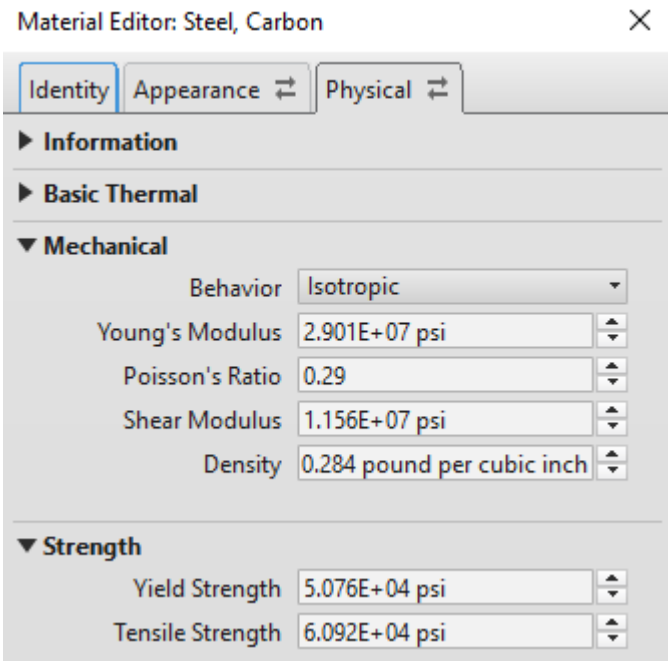

Material data for Inventor pre-defined ABS plastic:

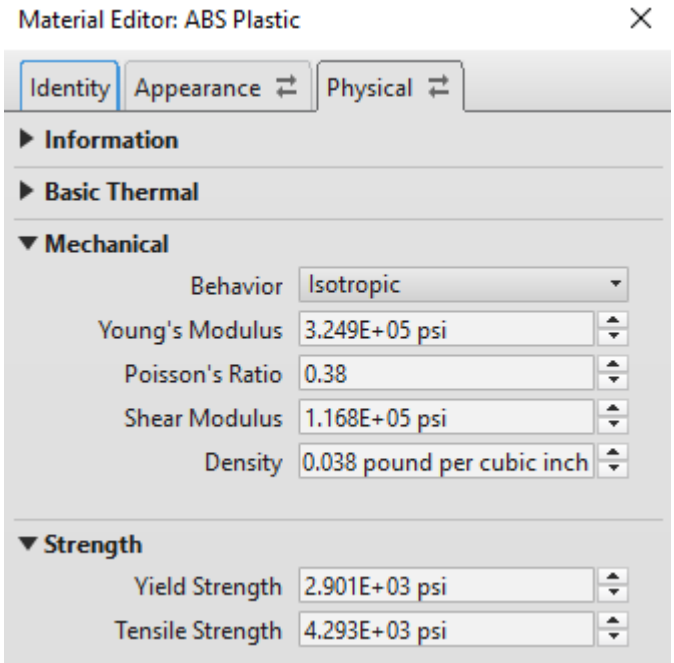

Note that all Inventor material data is displayed in imperial units.

Appendix U 3D Printed Prototype

Printed in scale 1:3 using a *Makerbot Z18* machine and PLA plastic.

The CAD model of the working chair was divided into 5 smaller assemblies in Inventor prior to being exported as .stl-files:

- Backrest and backrest post
- Seat, hub and height adjustment component
- Levers and hinge
- Footrest and footrest fasteners
- Gas spring, “legs” and wheels

Geometries of the undercarriage were simplified prior to printing.

Filler primer spray was used to improve surface finish prior to painting the model with water based acrylic paint. The strap, made of painted aquarelle paper, was added during the assembly of the prototype.

Appendix V Technical Drawings

Technical drawings of the components developed during the project. Followed by drawings of the entire working chair, including both newly developed and pre-manufactured components.

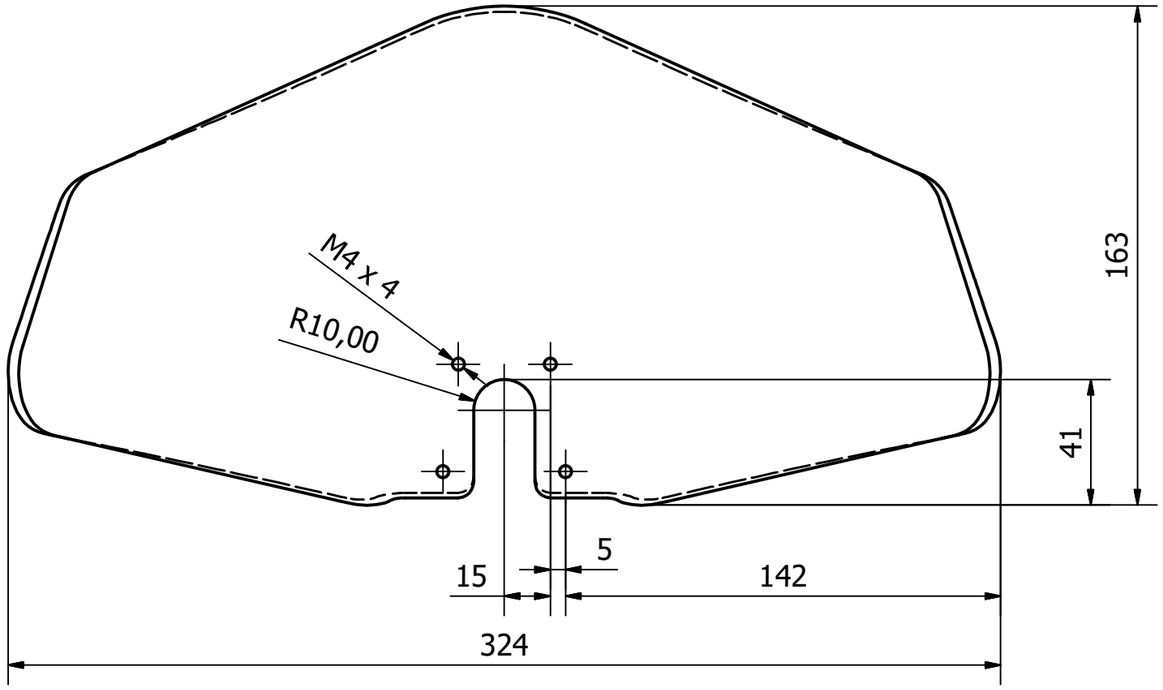

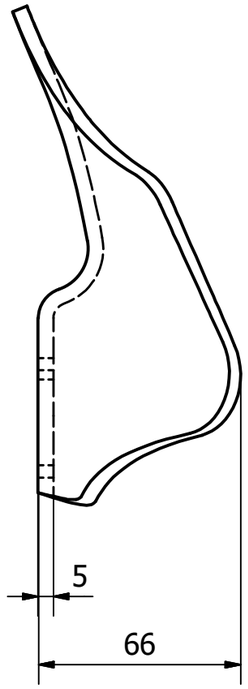

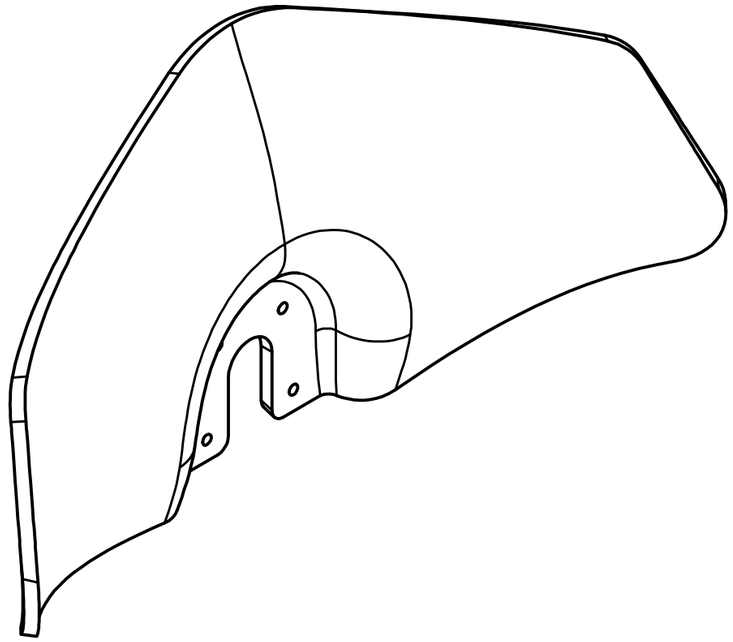

Designed by	Checked by	Approved by	Date		Date	
Ludvig					2019-04-30	

Backrest		Edition	Sheet 1 / 1

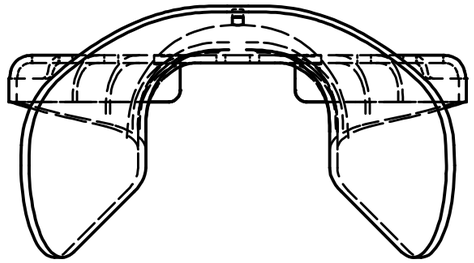

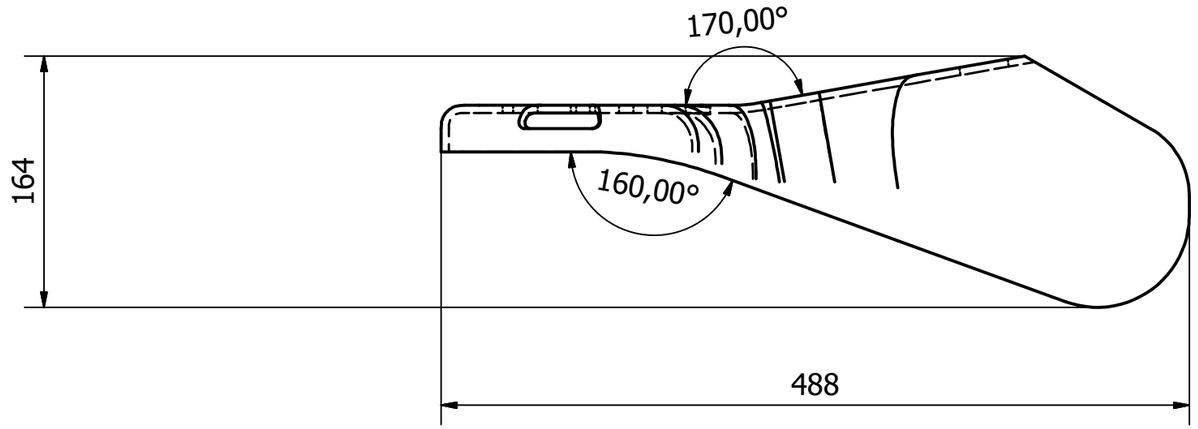

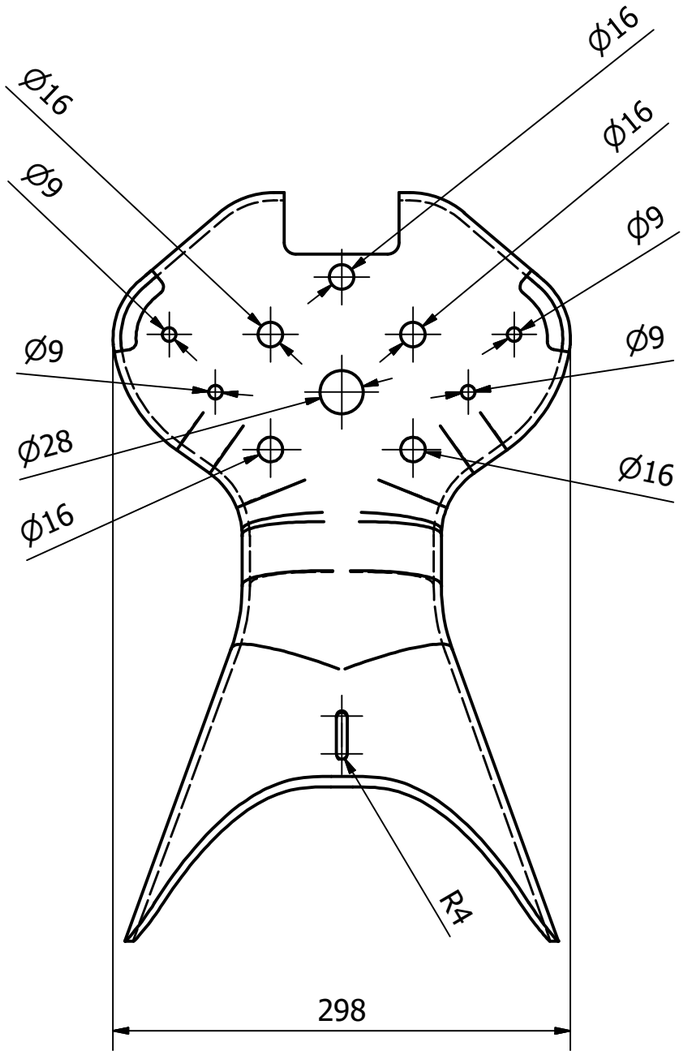

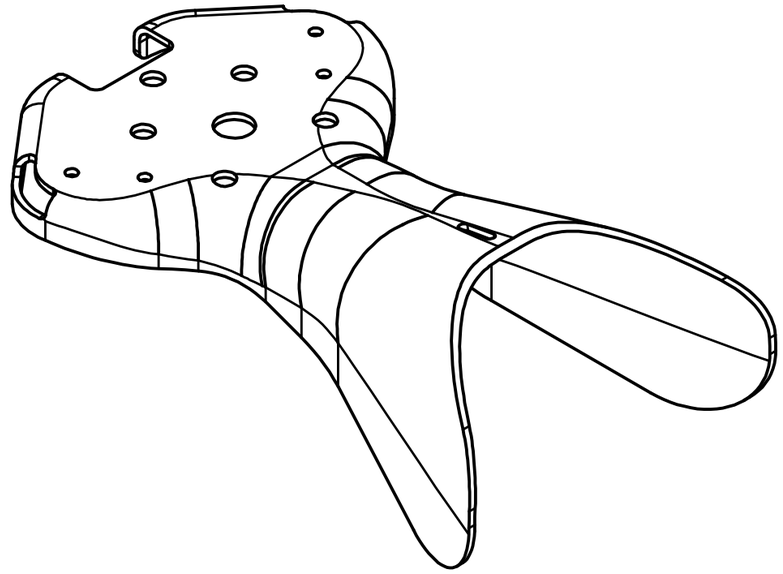

Designed by	Checked by	Approved by	Date		Date	
Ludvig					2019-05-01	

Seat		Edition	Sheet 1 / 1

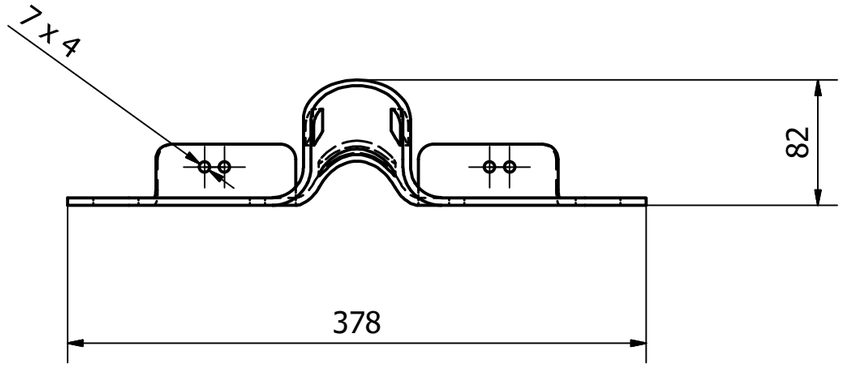

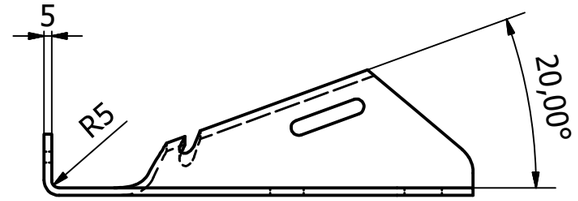

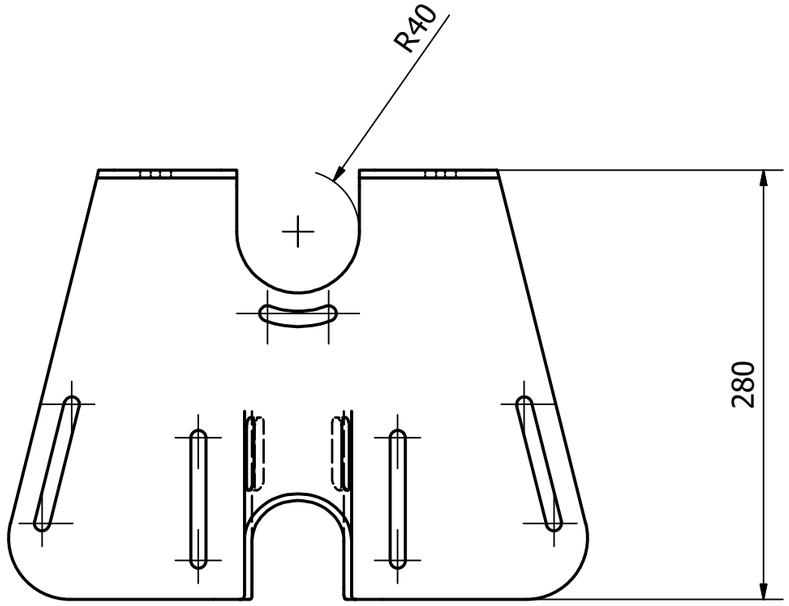

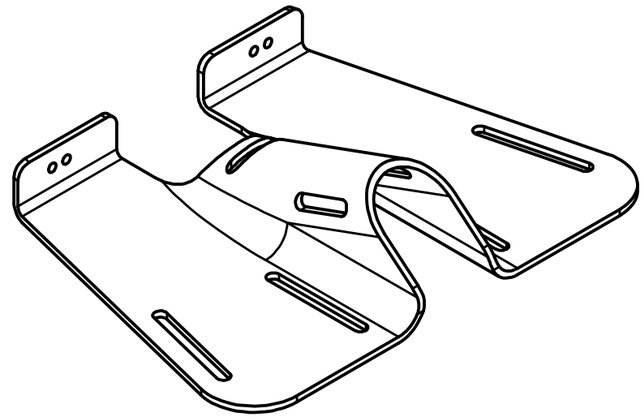

Designed by	Checked by	Approved by	Date		Date	
Ludvig					2019-04-30	

Footpad		Edition	Sheet 1 / 1

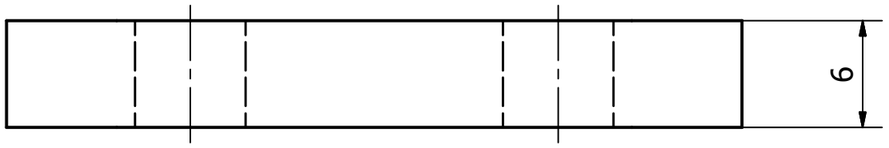

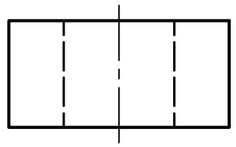

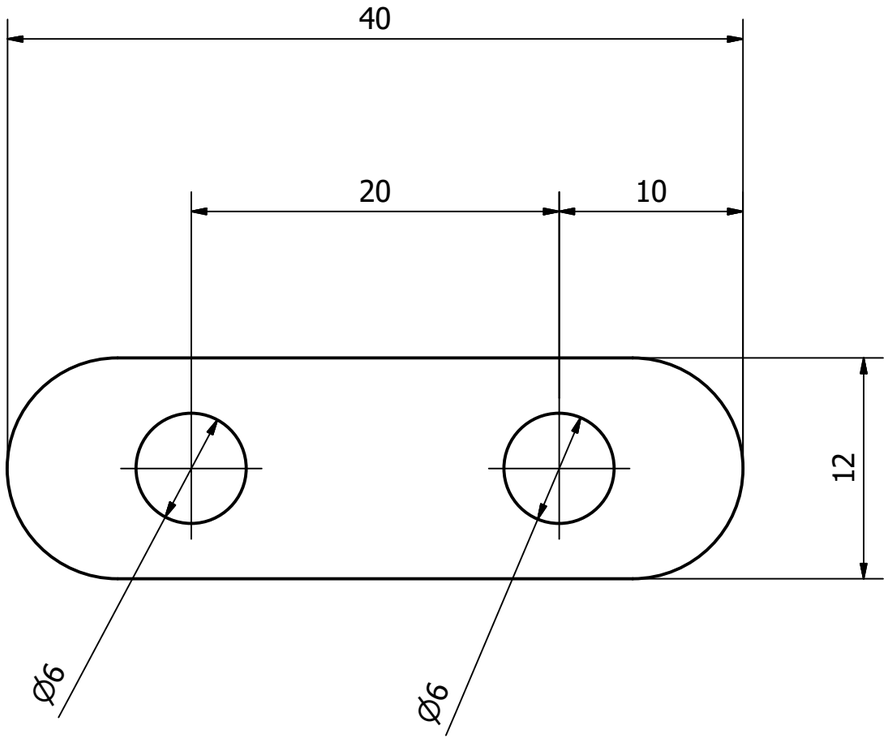

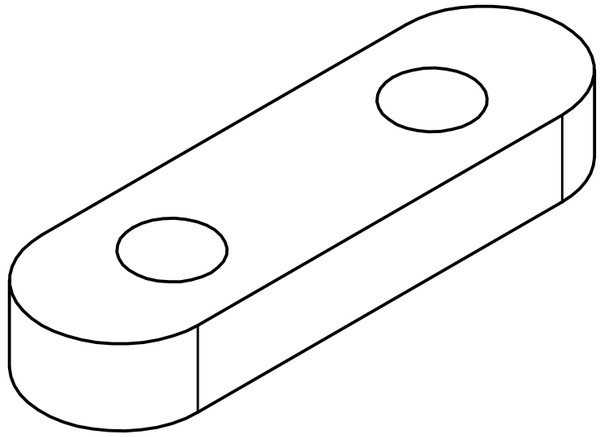

Designed by	Checked by	Approved by	Date		Date	
Ludvig					2019-05-01	

NoseRiser		Edition	Sheet 1 / 1

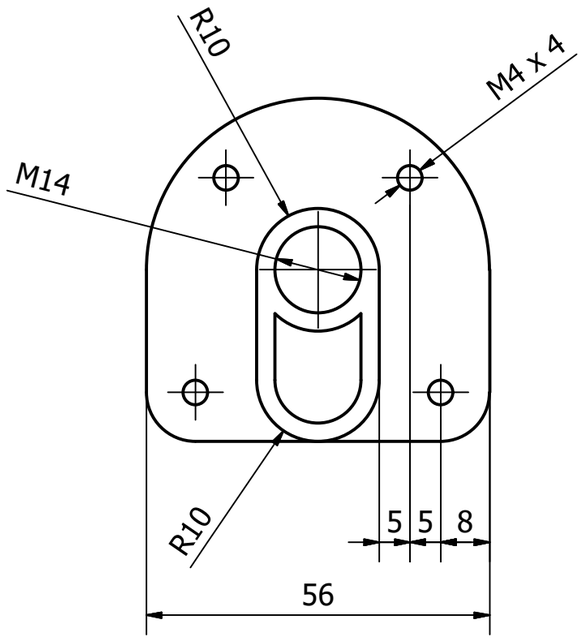

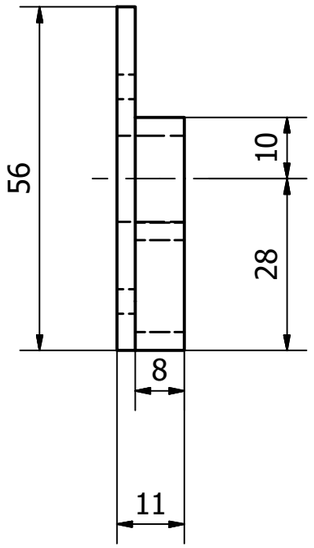

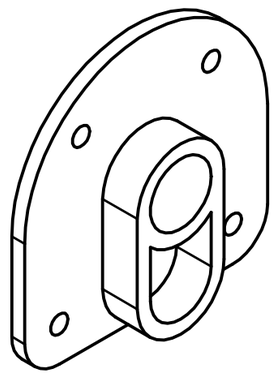

Designed by	Checked by	Approved by	Date		Date	
Ludvig					2019-04-30	

BackrestFastener		Edition	Sheet 1 / 1

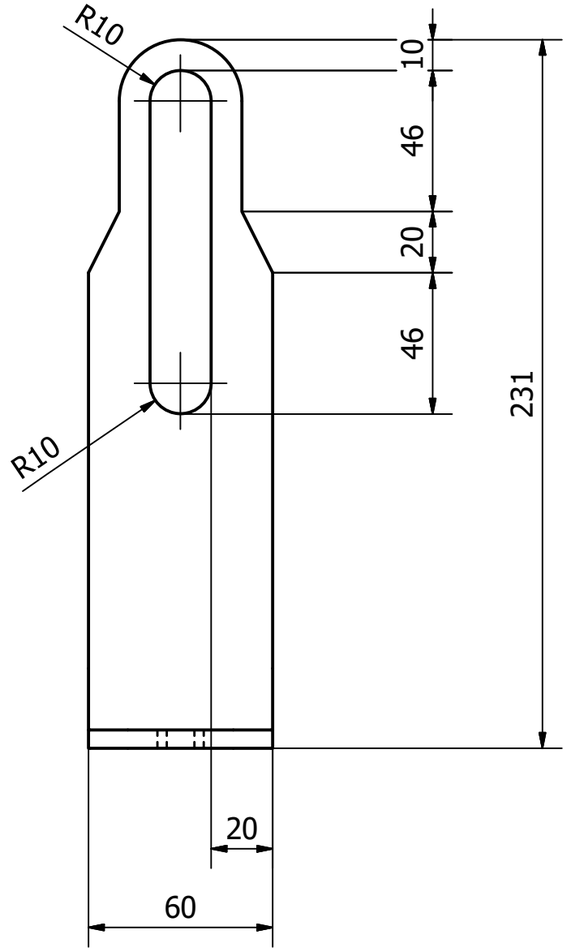

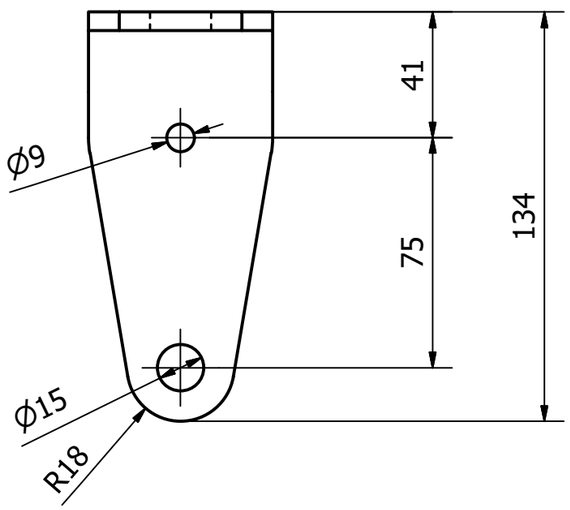

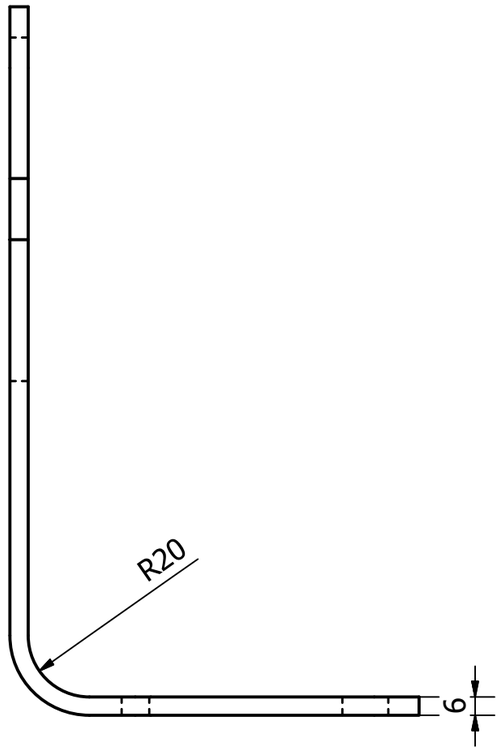

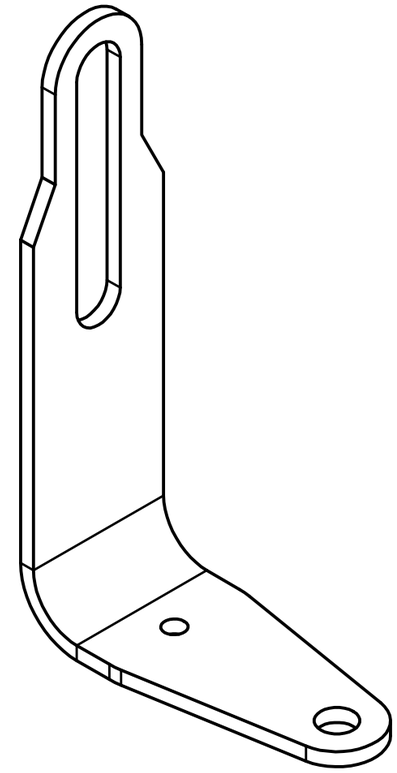

Designed by	Checked by	Approved by	Date		Date	
Ludvig					2019-04-30	

BackrestPost		Edition	Sheet 1 / 2

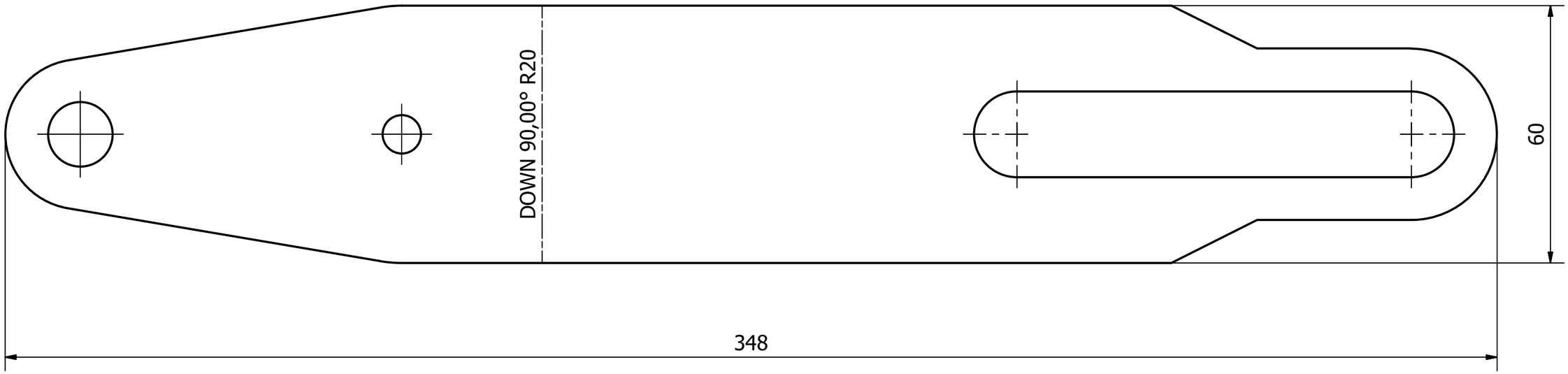

Flat pattern

Designed by	Checked by	Approved by	Date		Date	
Ludvig					2019-04-30	

BackrestPost	Edition	Sheet 2 / 2	

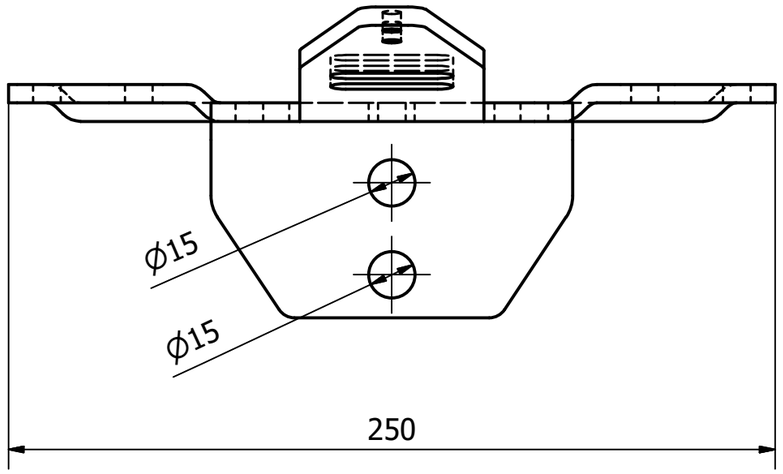

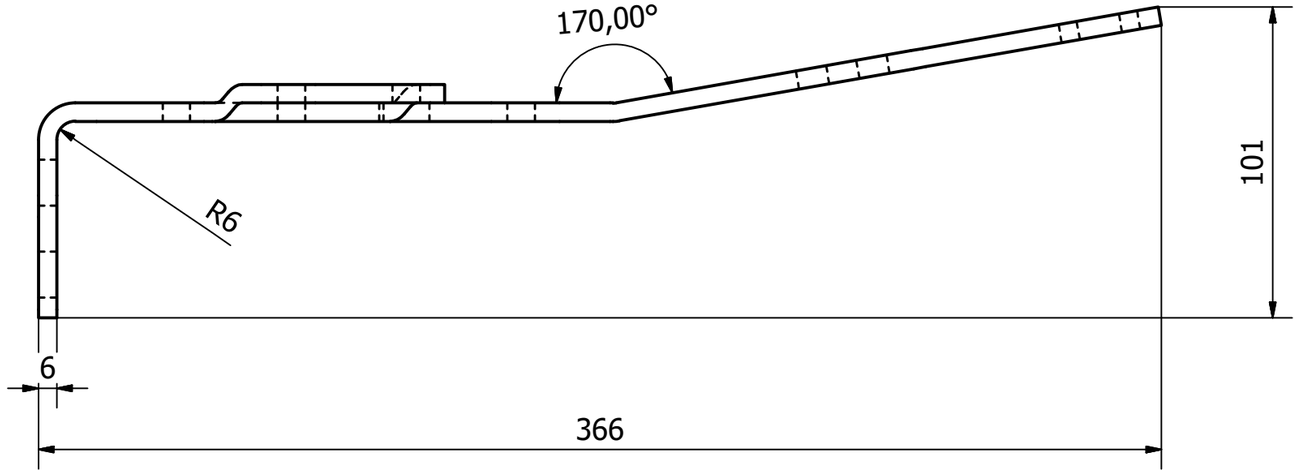

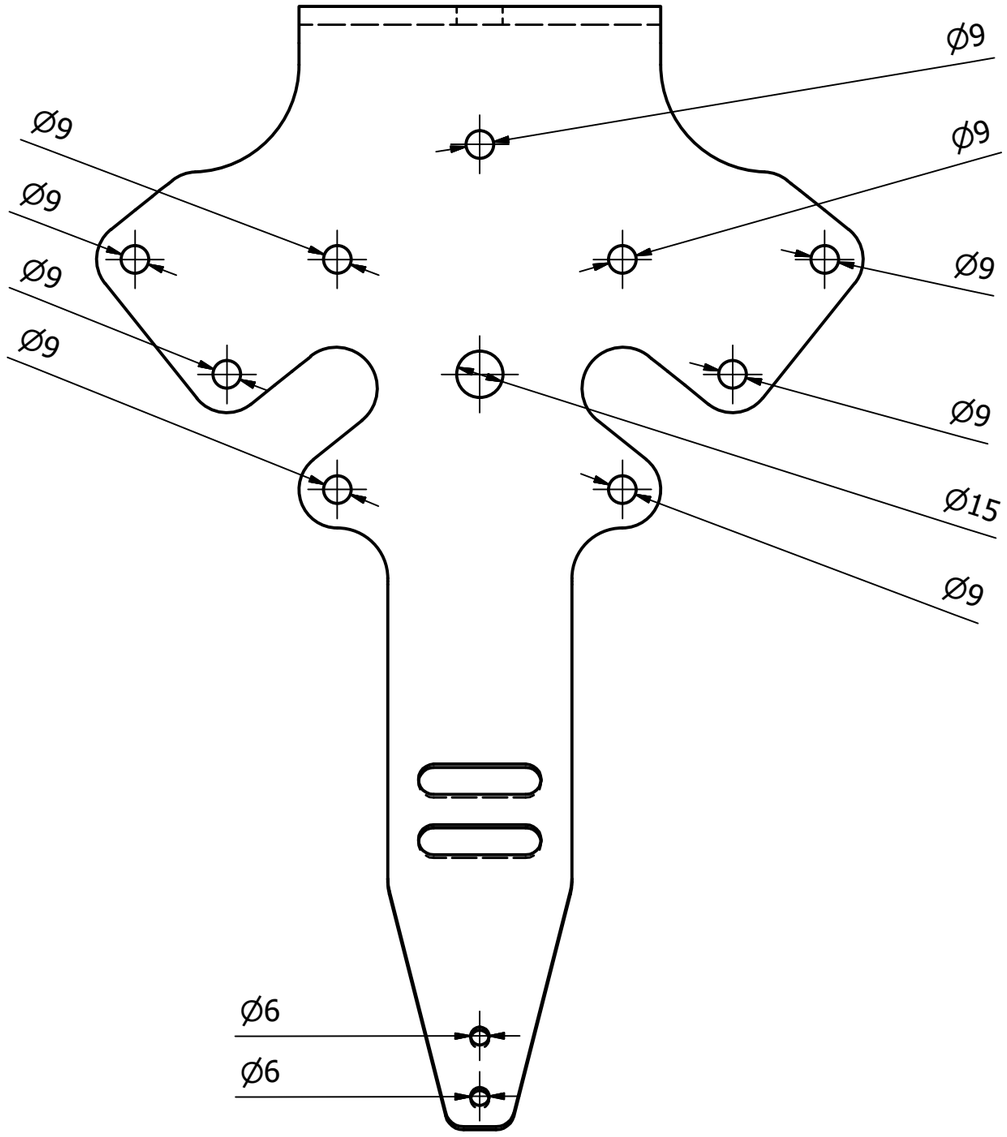

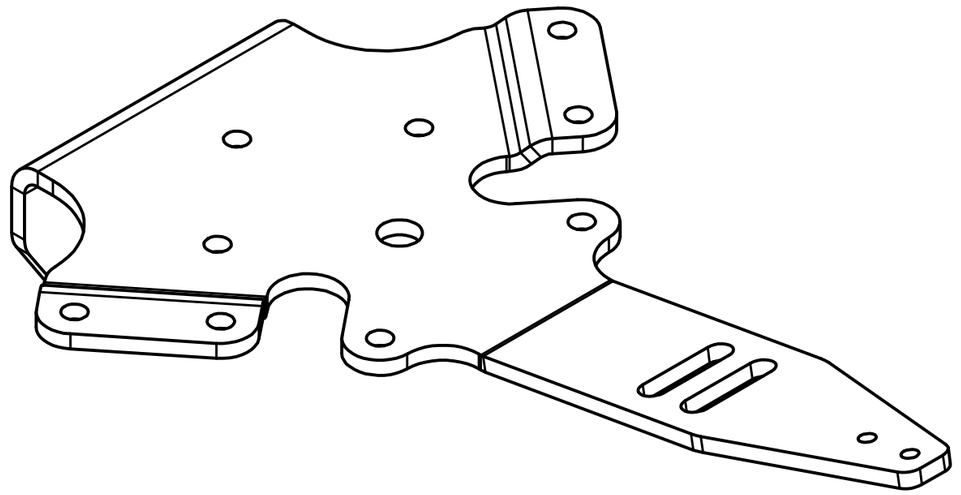

Designed by	Checked by	Approved by	Date		Date	
Ludvig					2019-05-01	
				Hub	Edition	Sheet 1 / 2

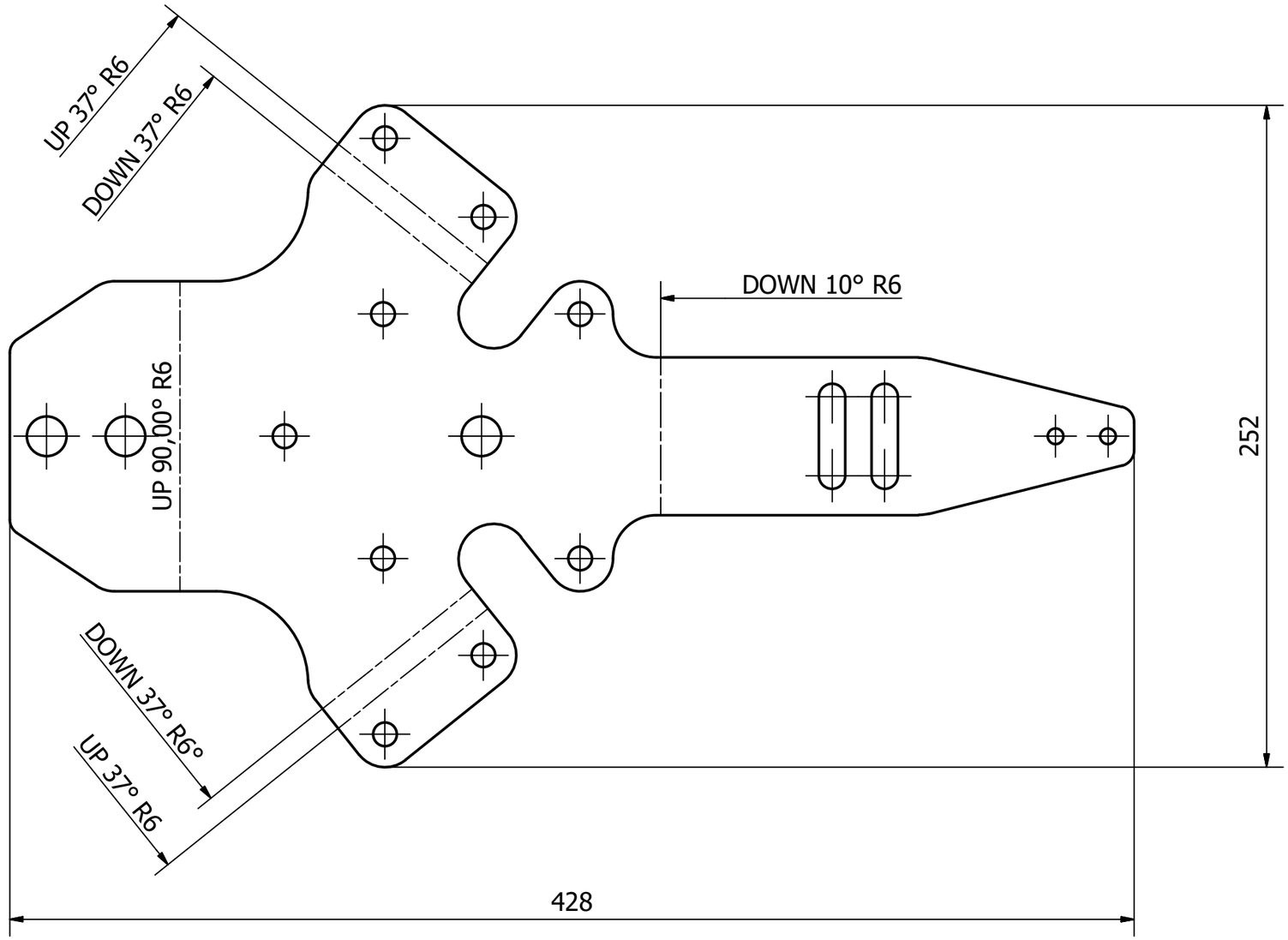

Flat pattern

Designed by	Checked by	Approved by	Date		Date	
Ludvig					2019-05-01	

Hub	Edition	Sheet 2 / 2

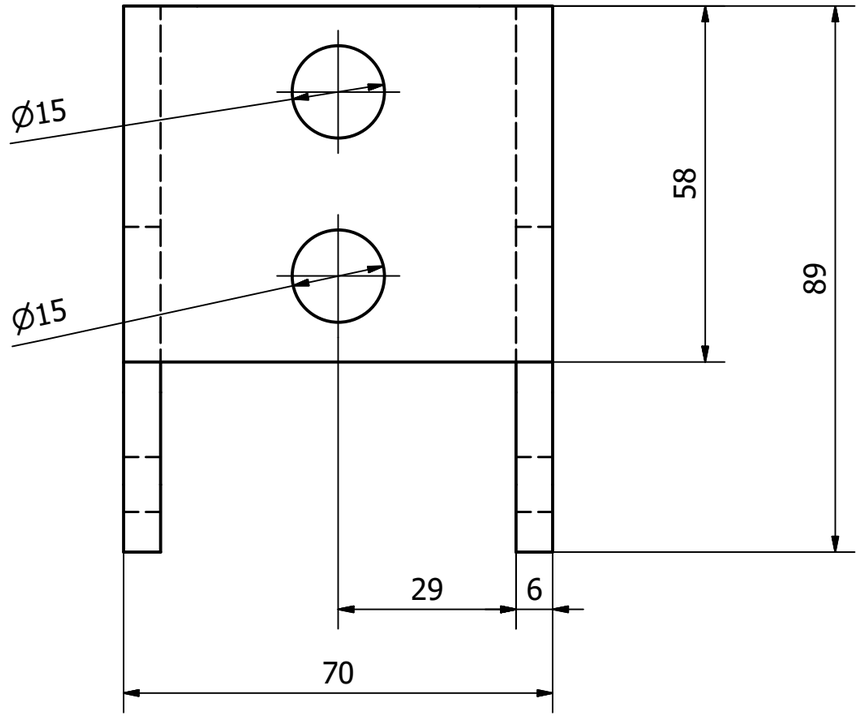

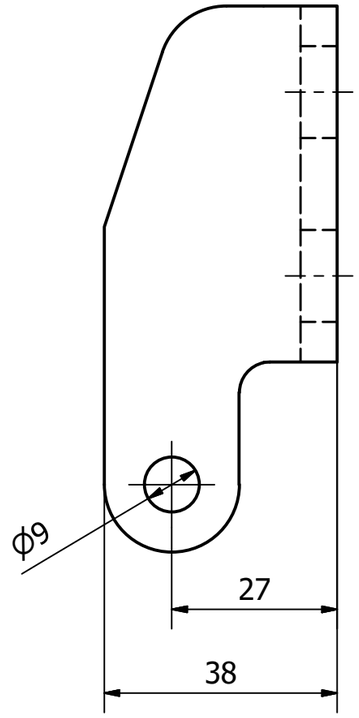

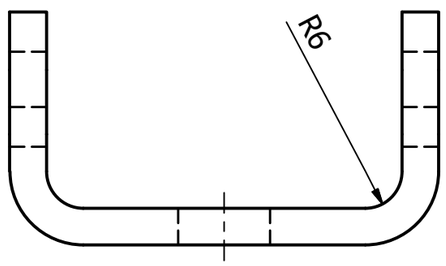

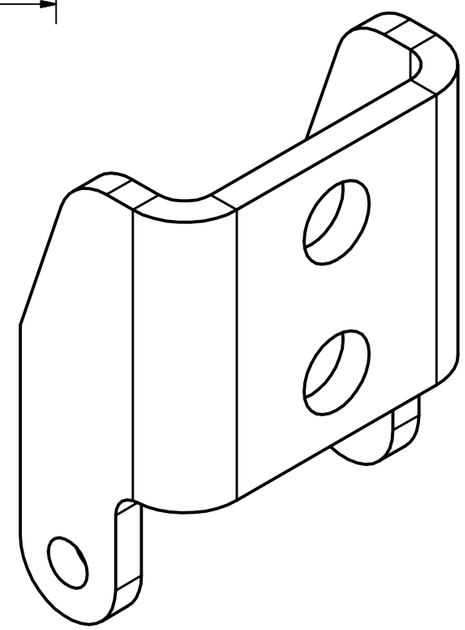

Designed by	Checked by	Approved by	Date		Date	
Ludvig					2019-05-01	

HubHinge		Edition	Sheet 1 / 1

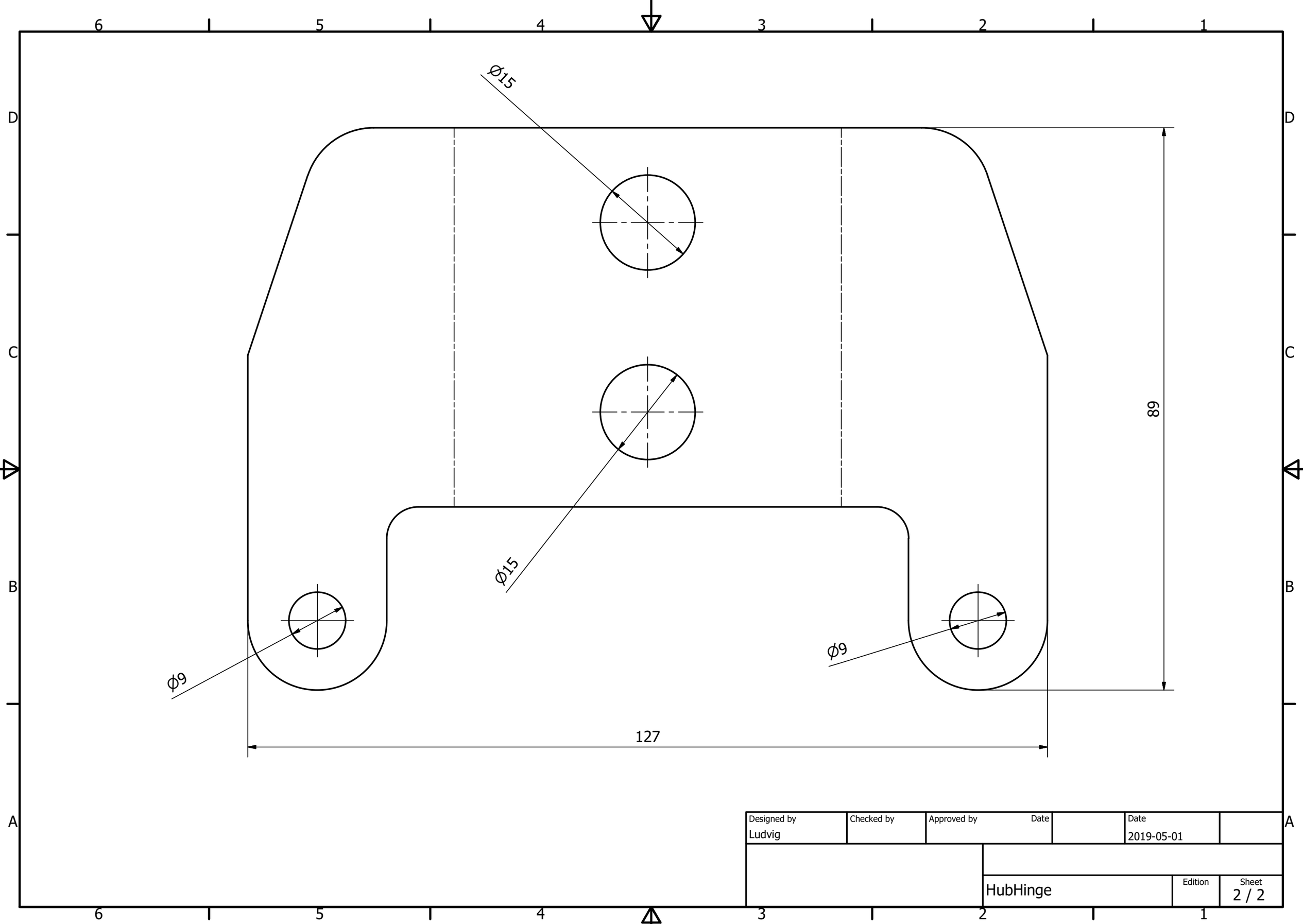

Designed by	Checked by	Approved by	Date		Date	
Ludvig					2019-05-01	

HubHinge		Edition	Sheet 2 / 2

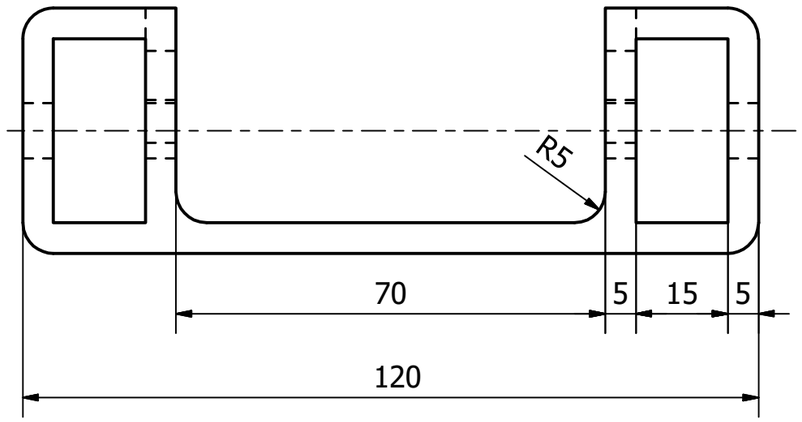

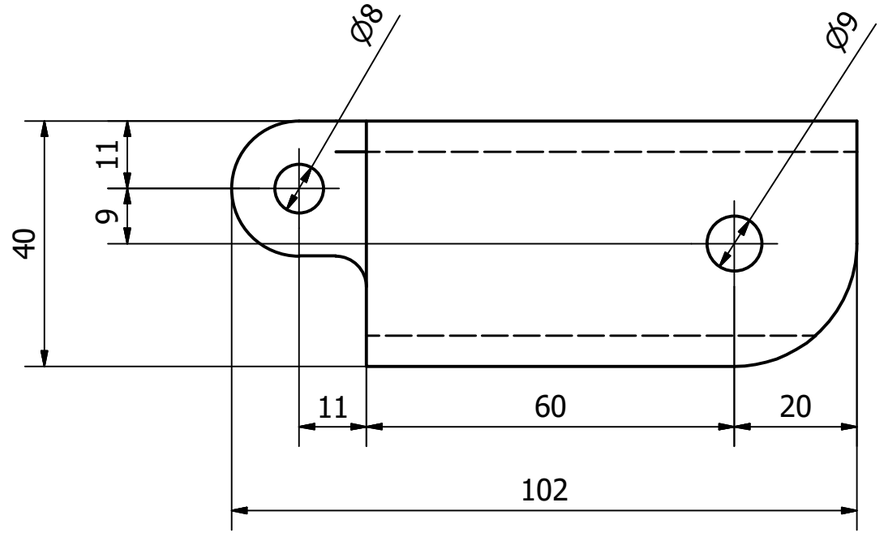

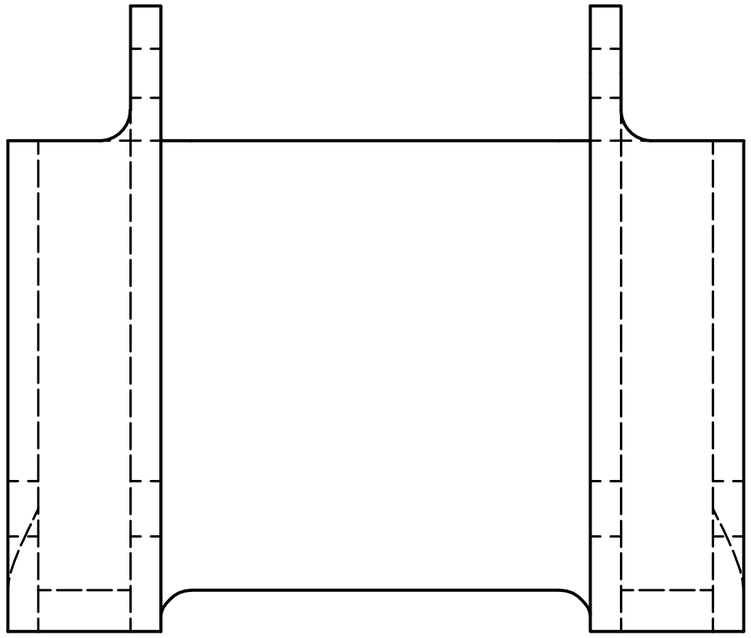

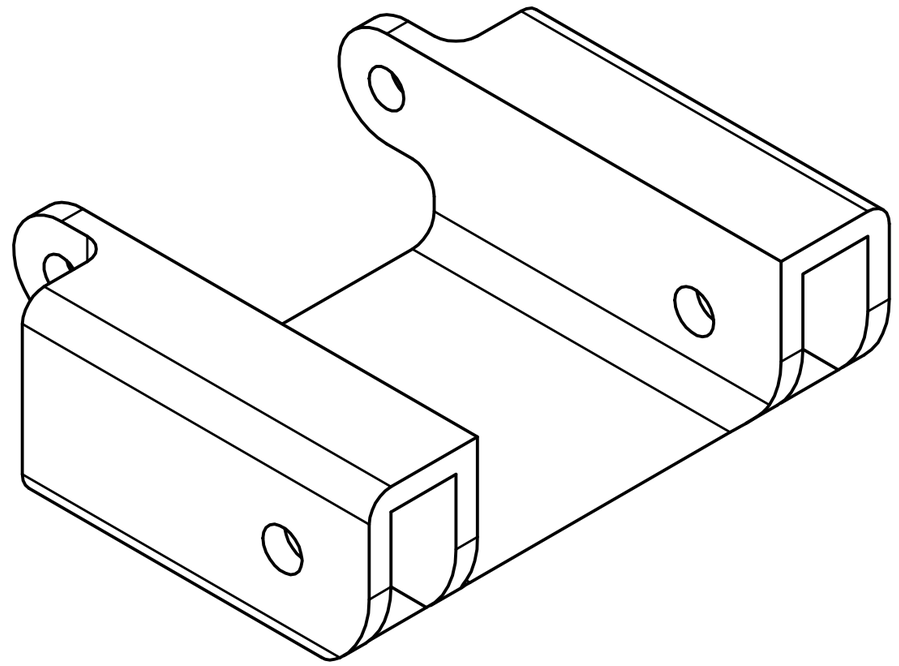

Designed by	Checked by	Approved by	Date		Date	
Ludvig					2019-05-01	

Hinge		Edition	Sheet 1 / 1

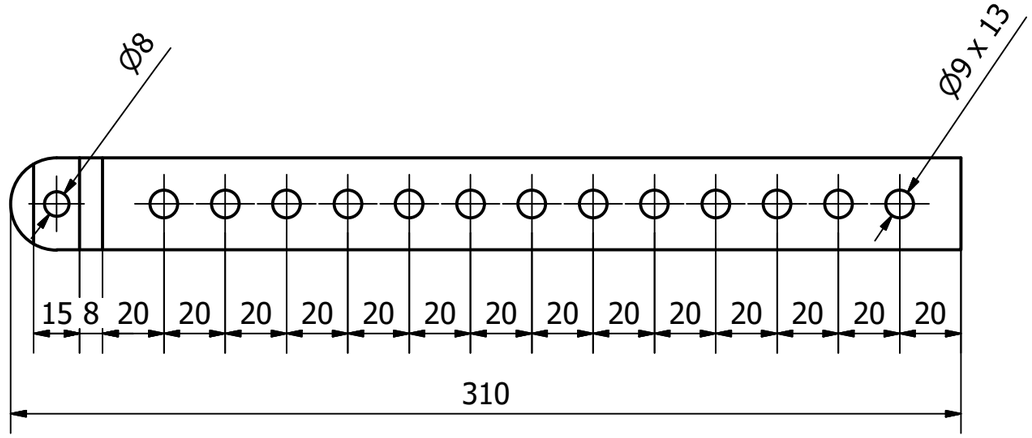

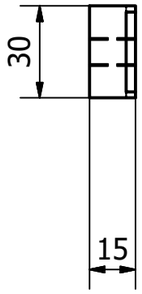

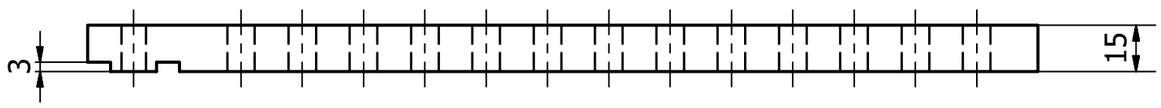

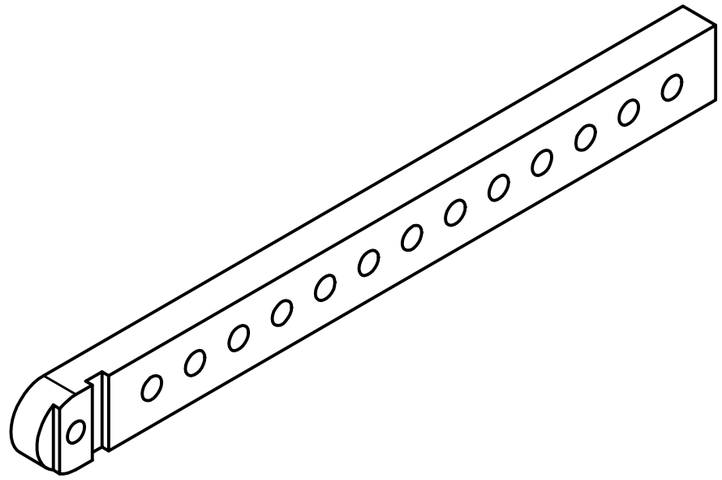

Designed by	Checked by	Approved by	Date		Date	
Ludvig					2019-05-01	

	Lever	Edition	Sheet 1 / 1

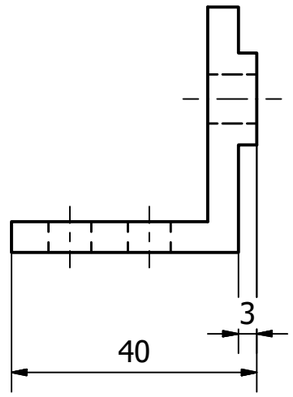

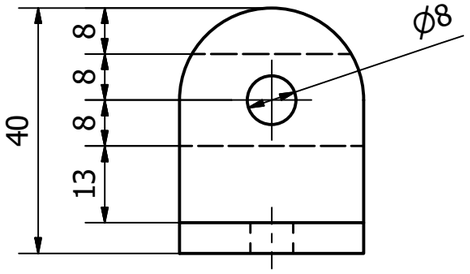

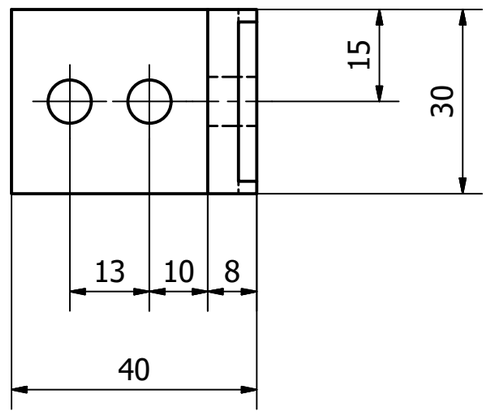

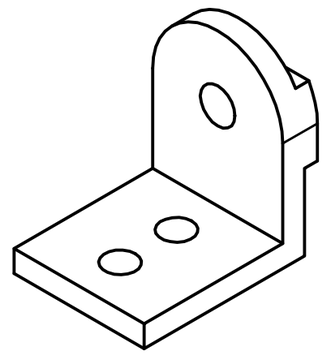

Designed by	Checked by	Approved by	Date		Date	
Ludvig					2019-05-01	

FootpadFastener		Edition	Sheet 1 / 1

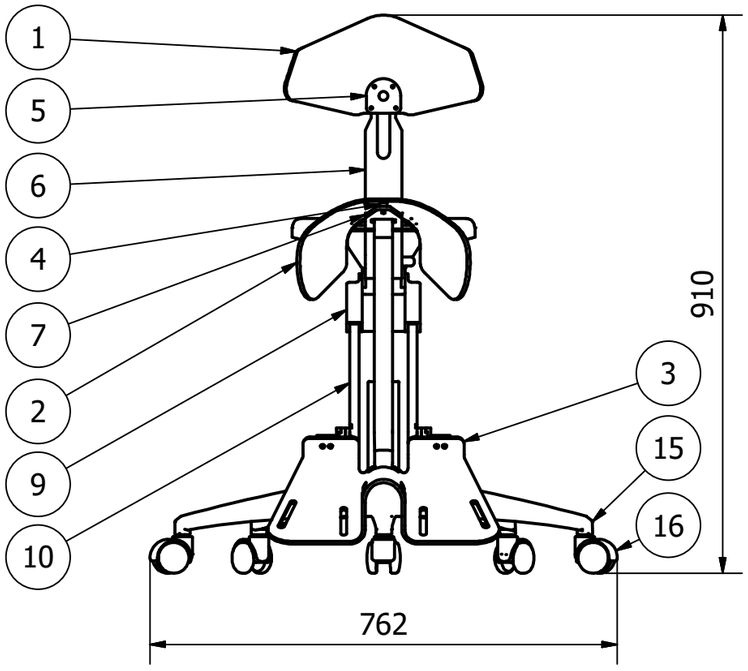

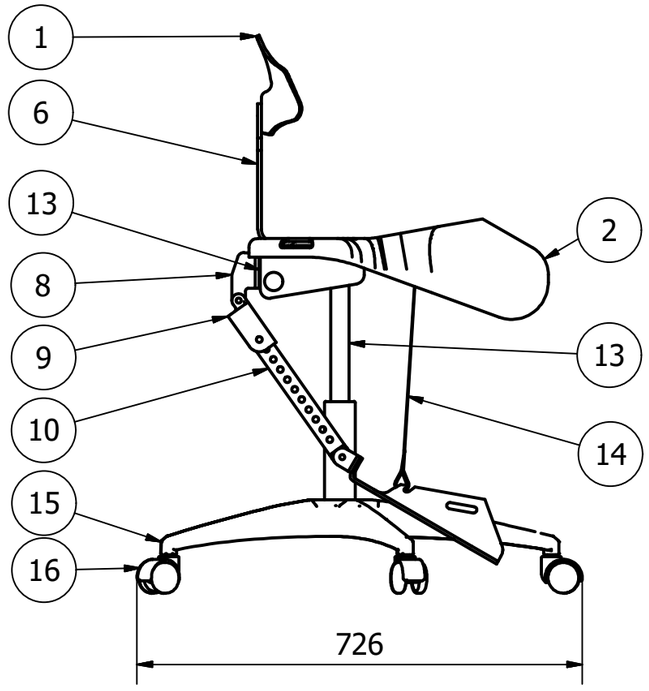

A (1 : 2)

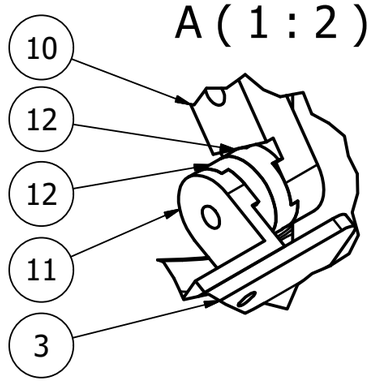

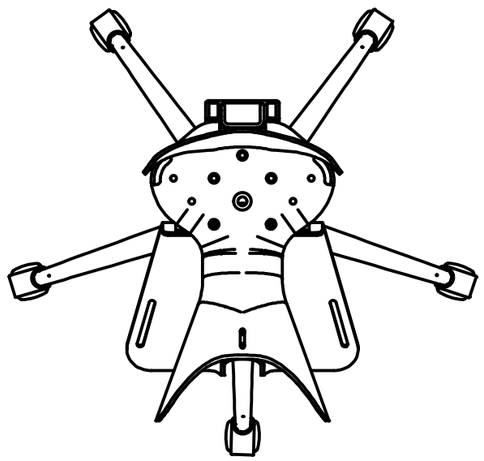

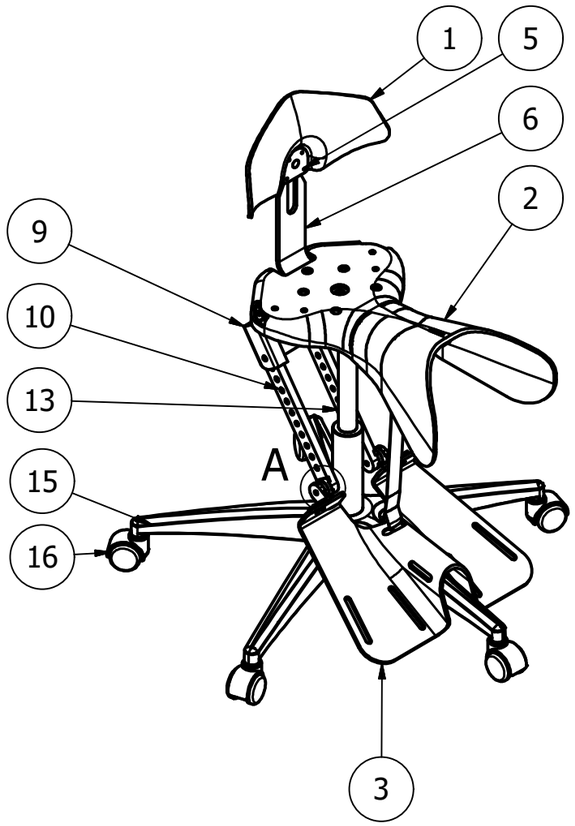

PARTS LIST			
ITEM	QTY	PART NUMBER	DESCRIPTION
1	1	Backrest	
2	1	Seat	
3	1	Footpad	
4	1	Nose Bushing	
5	1	Backrest Fastener	
6	1	Backrest Post	
7	1	Hub	
8	1	HubHinge	
9	1	Hinge	
10	2	Lever	
11	2	Footpad Fastener	
12	4	FrictionJoint	
13	1	Gas Spring & Height Adjustment	
14	1	Strap	
15	1	Legs	STEP AP214
16	5	Wheel 50 mm	STEP AP214

Designed by	Checked by	Approved by	Date	Date	
lla082				5/21/2019	

Working Chair	Edition	Sheet 1 / 1	